SYNCHRONOUS GENERATOR MODELS FOR THE SIMULATION OF ELECTROMAGNETIC TRANSIENTS

by

Vladimir Brandwajn
B.Sc., Technion, Israeli Institute of Technology, 1971
M.Sc., Technion, Israeli Institute of Technology, 1973

A THESIS SUBMITTED IN PARTIAL FULFILMENT OF
THE REQUIREMENT FOR THE DEGREE OF
DOCTOR OF PHILOSOPHY

in the Department
of
Electrical Engineering

We accept this thesis as conforming to
the required standard

THE UNIVERSITY OF BRITISH COLUMBIA
April, 1977

In presenting this thesis in partial fulfilment of the requirements for an advanced degree at the University of British Columbia, I agree that the Library shall make it freely available for reference and study. I further agree that permission for extensive copying of this thesis for scholarly purposes may be granted by the Head of my Department or by his representatives. It is understood that copying or publication of this thesis for financial gain shall not be allowed without my written permission.

Department of Electrical Engineering

The University of British Columbia
2075 Wesbrook Place
Vancouver, Canada
V6T 1W5

Date 16 May June, 1977

ABSTRACT

Techniques for modelling of synchronous generators in the simulation of electromagnetic transients are described. First of all, an adequate mathematical model of the generator is established. It uses the conventional set of generator data only, which are readily available, but it is flexible enough to accommodate additional data, if and when such become available. The resulting differential equations of the generator are then transformed into linear algebraic equations, with a time varying coefficient matrix, by using the numerically stable trapezoidal rule of integration. These equations can be interfaced with the equations of an electromagnetic transients program in one of two ways:

(a) Solve the equations of the generator simultaneously with the equations of a three-phase Thevenin equivalent circuit of the transmission network seen from the generator terminals.

(b) Replace the generator model with a modified Thevenin equivalent circuit and solve the network equations with the generator treated as known voltage sources $\underline{e}_{ph}^{red}(t-\Delta t)$ behind constant resistances $[R_{ph}^{red}]$. After the network solution at each time step, the stator quantities are known and used to solve the equations for the rotor windings.

These two methods cover, in principle, all possible interfacing techniques. They are not tied to the trapezoidal rule of integration, but can be used with any other implicit integration technique. The results obtained with these two techniques are practically identical. Interfacing by method (b), however, is more general since it does not require a Thevenin equivalent circuit of the network seen from the generator

terminals. The numerical examples used in this thesis contain comparisons with field test results in order to verify the adequacy of the generator model as well as the correctness of the numerical procedures.

A short discussion of nonlinear saturation effects is also presented. A method of including these effects into the model of the generator is then proposed.

Typical applications of the developed numerical procedures include dynamic overvoltages, torsional vibrations of the turbine-generator shaft system, resynchronization of the generator after pole slipping and detailed assessment of generator damping terms in transient stability simulations.

TABLE OF CONTENTS

LIST OF ILLUSTRATIONS

LIST OF TABLES

ACKNOWLEDGEMENT

I would like to express my deep appreciation to Dr. H.W. Dommel for his unflagging patience, advice and most importantly faith through all phases of this work.

Thanks are also due to Dr. A.C. Soudack for his cooperation in this project.

The financial support from the National Research Council of Canada and the University of British Columbia is gratefully acknowledged.

1. INTRODUCTION

The importance of general-purpose computer programs for the simulation of electromagnetic transients in power systems is constantly increasing. Some of the elements of power systems can now be represented with a high degree of sophistication, e.g., overhead lines with frequency dependent line parameters [1]. Some other elements, however, are not yet represented in enough detail, including synchronous generators. Normally, sinusoidal voltage sources $E''_{max}\cos(\omega t + \rho)$ behind impedances $R_a + j\omega L''_d$ have been used to represent generators in transient studies. In the derivation of this approximate model, it is assumed that rotor fluxes do not change immediately after the disturbance, and that subtransient saliency of the generator can be ignored. This simple model is quite adequate for certain types of studies during the first cycle or so after the disturbance which initiates the transient phenomena, e.g., switching surge studies, transient recovery voltage studies, and other types of studies involving fast transients [2]. It is also adequate if the generator impedance is only a small part of the total impedance between the generator and the location of the disturbance.

Recent interest in electromagnetic transient phenomena which persist over longer time spans makes it worthwhile to implement more accurate models for synchronous generators into programs for electromagnetic transients [2-4]. Potential applications include studies of subsynchronous resonance [4-5], dynamic overvoltages, accurate assessment of damping terms in transient stability studies (due to d.c. offset, harmonics, and asymmetries in short-circuit currents), and other studies.

This thesis discusses the major problems of interfacing generator models with an electromagnetic transients program and proposes new

solution techniques. Firstly, the choice of an appropriate generator model and the calculation of its parameters are discussed. This discussion and a description of numerical problems in the simultaneous solution of the generator equations and the equations of the connected transmission network provide the necessary background for the introduction of interfacing techniques - around which the major research effort of the thesis was concentrated. The proposed techniques cover in principle all the possible approaches to interface problems. Numerical examples are used to test the validity of the proposed techniques. Some additional problems related to the solution of generator equations, e.g., proposed treatment of saturation effects, are described in the final chapter of this thesis.

The contributions of this thesis to power system analysis consist of:

(a) a critical review of synchronous generator models and selection of a model appropriate for the simulation of electromagnetic transients,

(b) a new method for the calculation of synchronous generator parameters from test data,

(c) a new physical interpretation of the discretization error for the trapezoidal rule of integration applied to series inductances, which shows that the resulting difference equations are exact solutions of equivalent lossless stub lines,

(d) the development of two alternative interfacing techniques for solving the generator and network equations simultaneously, with one being similar to a technique developed in industry concurrently

with the research project of this thesis and the other one being a new technique with less restrictions than the first one, and

(e) an analysis and proposed treatment of saturation effects in the synchronous generator.

2. SYNCHRONOUS GENERATOR MODEL

2.1 General Remarks about Physical Device Modelling

In general, the derivation of a mathematical model of any physical device consists of the following steps [6]:

(1) Selection of a model structure based upon observations and physical knowledge;

(2) fitting of parameters of the chosen model to available data;

(3) verification and testing of the model;

(4) application of the model to its given purpose.

The basic decisions are made at the first stage. It is, for example, necessary to decide whether the physical device can be treated as a linear system. If so, a linear system of equations (differential or algebraic) is used to describe the basic physical phenomena relevant to the device. Therefore, this stage involves some necessary simplifications of the physical reality. At the next stage, relationships between the parameters of the model and the available data have to be established. At this stage, therefore, some additional simplifications may have to be introduced. The last two stages serve as verification of the developed model, and may result in some changes in the model, if necessary. It should, therefore, be remembered that any mathematical model of a physical device always involves simplifications of physical reality.

2.2 Model of the Electric Part

The generator is assumed to be an "ideal synchronous machine" in the sense of Park's definition [7]. The basic assumptions for this ideal generator can be summarized as follows:

(1) Saturation effects are neglected. This allows the application

of the superposition principle, because the model is then linear. Neglecting the saturation effects is a common practice in the theory of alternating-current machines [8-9]. Techniques for including nonlinear effects will be discussed later on.

(2) The magnetic circuit and all rotor windings are assumed to be symmetrical both with respect to the direct axis, which lines up with the center-line through the field poles, and to the quadrature axis 90° behind it (the recommended position of the quadrature axis lagging 90° behind the direct axis is adopted [10]).

(3) A current in any winding is assumed to set up a magneto-motive force sinusoidally distributed in space around the air gap. Any magneto-motive force may be resolved into components along the two axes (direct and quadrature). The sinusoidal distribution does normally imply that only the fundamental component is considered. In connection with this assumption, it should be noticed that the effects of harmonics in the field distribution are small in a well designed machine [11], [12].

(4) It is assumed that a magneto-motive force acting along the direct axis produces a sinusoidally distributed flux wave which also acts along the direct axis. Similarily, a quadrature axis magneto-motive force produces a sinusoidally distributed quadrature axis flux. The factors relating magneto-motive force and flux are, however, different on the two axes in a salient pole machine [11].

(5) It is assumed that the damper bars can be represented as two

concentrated hypothetical windings, one in the direct axis (D) and the other in the quadrature axis (Q) [8]. Another hypothetical winding (g) in the quadrature axis is normally added for round rotor machines to represent the deep flowing eddy currents. Consequently, the machine consist of seven windings: three a.c. stator windings, one field winding for direct axis, one hypothetical winding D for direct axis and two hypothetical windings g, Q for the quadrature axis.

This "ideal machine" is schematically shown in Fig. 1.

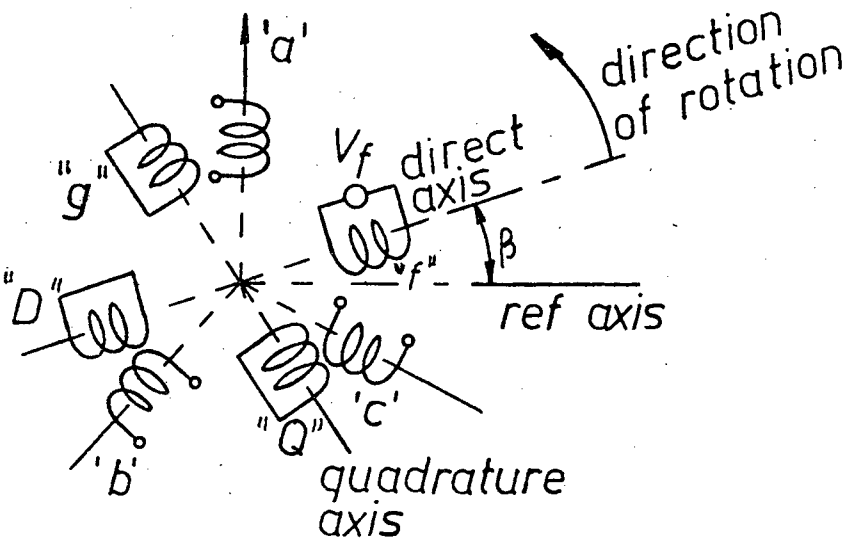

Fig. 1. Schematic representation of a synchronous generator (position of windings is shown in space).

A system of seven linear differential equations describes the relationship between the voltages and the currents in the seven windings of the idealized generator. The voltage equations of the generator, in

phase coordinates*, have the following form**:

$$\underline{v} = -[R]\underline{i} - \frac{d}{dt}\underline{\psi} \tag{1}$$

where the vector of fluxes $\underline{\psi}$ is given in general as:

$$\underline{\psi} = [L]\underline{i} = \begin{bmatrix} L_{aa} & M_{ab} & M_{ac} & M_{af} & M_{aD} & M_{aQ} & M_{ag} \\ M_{ab} & L_{bb} & M_{bc} & M_{bf} & M_{bD} & M_{bQ} & M_{bg} \\ M_{ac} & M_{bc} & L_{cc} & M_{cf} & M_{cD} & M_{cQ} & M_{cg} \\ M_{af} & M_{bf} & M_{cf} & L_{f} & M_{fD} & 0 & 0 \\ M_{aD} & M_{bD} & M_{cD} & M_{fD} & L_{D} & 0 & 0 \\ M_{aQ} & M_{bQ} & M_{cQ} & 0 & 0 & L_{Q} & M_{Qg} \\ M_{ag} & M_{bg} & M_{cg} & 0 & 0 & M_{Qg} & L_{g} \end{bmatrix} \cdot \begin{bmatrix} i_a \\ i_b \\ i_c \\ i_f \\ i_D \\ i_Q \\ i_g \end{bmatrix} \tag{2}$$

The matrix [L] is always symmetrical, irrespective of rotor position β.

The self and mutual inductances of the armature contain even harmonic terms of rotor position β [12], e.g.,

$$\begin{aligned} L_{aa} &= L_{ao} + L_{a2}\cos 2\beta_1 + L_{a4}\cos 4\beta_1 + \ldots \\ L_{bb} &= L_{bo} + L_{b2}\cos 2\beta_2 + L_{b4}\cos 4\beta_2 + \ldots \\ L_{cc} &= L_{co} + L_{c2}\cos 2\beta_3 + L_{c4}\cos 4\beta_3 + \ldots \end{aligned} \tag{3}$$

and

$$\begin{aligned} M_{ab} &= M_{abo} + M_{ab2}\cos 2\beta_3 + M_{ab4}\cos 4\beta_3 + \ldots \\ M_{ac} &= M_{aco} + M_{ac2}\cos 2\beta_2 + M_{ac4}\cos 4\beta_2 + \ldots \\ M_{bc} &= M_{bco} + M_{bc2}\cos 2\beta_1 + M_{bc4}\cos 4\beta_1 + \ldots \end{aligned} \tag{4}$$

---

* Phase coordinates refer to actual currents and voltages in the 3 phases a, b, c of the stator and to actual currents and voltages in the rotor windings.

** Capital letters in square brackets [ ] indicate matrix quantities; straight lines underneath letters indicate vector quantities.

where

$$\beta_1 = \omega t + \delta + \pi/2$$
$$\beta_2 = \beta_1 - 2\pi/3 \qquad (5)$$
$$\beta_3 = \beta_1 + 2\pi/3$$

The self and mutual inductances of the rotor L_f, L_D, L_Q, L_g, M_{fD}, and M_{Qg} are constant. The mutual inductances between armature and rotor contain odd harmonic terms, e.g.,

$$\begin{aligned} M_{af} &= M_{af1}\cos\beta_1 + M_{af3}\cos 3\beta_1 + \ldots \\ M_{aD} &= M_{aD1}\cos\beta_1 + M_{aD3}\cos 3\beta_1 + \ldots \\ M_{aQ} &= M_{aQ1}\sin\beta_1 + M_{aQ3}\sin 3\beta_1 + \ldots \\ M_{ag} &= M_{ag1}\sin\beta_1 + M_{ag3}\sin 3\beta_1 + \ldots \end{aligned} \qquad (6)$$

Similar relationships exist for the other two phases b and c [12]. Practical considerations allow a reduction of the number of parameters appearing in (2)-(6). For example, a properly designed balanced machine implies full symmetry of the phases a, b, and c, e.g.,

$$\begin{aligned} L_{ao} &= L_{bo} = L_{co} = L_s \\ L_{a2} &= L_{b2} = L_{c2} = L_m \\ M_{abo} &= M_{aco} = M_{bco} = M_s \\ M_{ab2} &= M_{ac2} = M_{bc2} = M_2 \end{aligned} \qquad (7)$$

Other simplifying assumptions are made to adjust the complexity of the model to the amount of data which is usually available. Some of these can result in noticeable errors, as demonstrated later. The following list summarizes the most common simplifications:

(1) All harmonic terms of order higher than 2 are neglected [8], [12]. This assumption does not seem to cause any noticeable errors [12].

(2) Mutual inductance M_{fD} (field-to-damper) is assumed to be equal to the mutual inductances M_{af1} and M_{aD1} (armature-to-field and armature-to-damper, respectively), when expressed in p.u. [13], i.e.,

$$M_{af1} = M_{aD1} = M_{fD} = M_f \tag{8}$$

The same assumption is made for the quadrature axis. These assumptions can sometimes cause significant errors in the simulation of rotor quantities [14].

(3) The second harmonic terms in self and mutual inductances of the armature are assumed to be equal, i.e., $M_2 = L_m$. This assumption simplifies the model significantly, since it eliminates the coupling among the direct, quadrature, and the zero axes [15]. This simplification is practically always made and seems to be justified [12], [16], but it should, nevertheless, be remembered as a possible source of errors.

Inclusion of the assumptions mentioned above results in the following, simplified inductance matrix [L]:

$$[L] = \begin{bmatrix} L_{aa} & M_{ab} & M_{ac} & M_{af} & M_{af} & M_{aQ} & M_{aQ} \\ M_{ab} & L_{bb} & M_{bc} & M_{bf} & M_{bf} & M_{bQ} & M_{bQ} \\ M_{ac} & M_{bc} & L_{cc} & M_{cf} & M_{cf} & M_{cQ} & M_{cQ} \\ M_{af} & M_{bf} & M_{cf} & L_f & M_f & 0 & 0 \\ M_{af} & M_{bf} & M_{cf} & M_f & L_D & 0 & 0 \\ M_{aQ} & M_{bQ} & M_{cQ} & 0 & 0 & L_Q & M_q \\ M_{aQ} & M_{bQ} & M_{cQ} & 0 & 0 & M_q & L_g \end{bmatrix} \tag{9}$$

where

$$\begin{aligned} L_{aa} &= L_s + L_m \cos 2\beta_1 \\ L_{bb} &= L_s + L_m \cos 2\beta_2 \\ L_{cc} &= L_s + L_m \cos 2\beta_3 \end{aligned} \tag{10}$$

$$M_{ab} = M_o + L_m \cos 2\beta_3$$
$$M_{ac} = M_o + L_m \cos 2\beta_2 \qquad (11)$$
$$M_{bc} = M_o + L_m \cos 2\beta_1$$

and

$$M_{af} = M_f \cos\beta_1$$
$$M_{bf} = M_f \cos\beta_2 \qquad (12)$$
$$M_{cf} = M_f \cos\beta_3$$

$$M_{aQ} = M_q \sin\beta_1$$
$$M_{bQ} = M_q \sin\beta_2 \qquad (13)$$
$$M_{cQ} = M_q \sin\beta_3$$

The resistance matrix [R] is simply a diagonal matrix, which has the following form for a balanced design:

$$[R] = \begin{bmatrix} R_a & & & 0 & & & \\ & R_a & & & & & \\ & & R_a & & & & \\ 0 & & & R_f & & & \\ & & & & R_D & & \\ & & & & & R_Q & \\ & & & & & & R_g \end{bmatrix} \qquad (14)$$

The model of a synchronous generator derived above is believed to be the best, presently possible compromise between the available amount of test data and the desired accuracy of simulations. Results obtained with this model agree quite well with field tests, which verifies the adequacy of this model [3].

The mathematical model of a synchronous generator in phase-coordinates is fully defined by (1) and (9)-(14). It is, however, common

practice in the power industry to describe the generator in a different reference frame, namely in d,q,0-coordinates [7]. In this reference frame, all inductances defined by (9)-(13) are constant. It should be emphasized, however, that introduction of higher harmonics or unequal second harmonic terms in the armature inductances will result in a time-varying inductance matrix [L] even in d,q,0-coordinates [15].

Before proceeding with transformations to the new reference frame, it is useful to rewrite (1) into the following form:

$$\underline{v} = -[R]\underline{i} - [L]\frac{d\underline{i}}{dt} - \frac{d}{dt}([L])\underline{i} \tag{15}$$

The transformation is defined as follows:

$$\underline{i}_p = [P]\cdot\underline{i} \tag{16}$$

and similarly:

$$\underline{v}_p = [P]\cdot\underline{v} \tag{17}$$

where the subscript "p" denotes Park's d,q,0-quantities.

The transformation matrix [P] has the following general form:

$$[P] = \left[\begin{array}{c|c} W & 0 \\ \hline 0 & I \end{array}\right] \tag{18}$$

where

[I] = identity matrix of dimension 4 x 4;

and the matrix [W] is given as [17]:

$$[W] = \sqrt{\frac{2}{3}}\begin{bmatrix} \cos\beta_1 & \cos\beta_2 & \cos\beta_3 \\ \sin\beta_1 & \sin\beta_2 & \sin\beta_3 \\ \sqrt{\frac{1}{2}} & \sqrt{\frac{1}{2}} & \sqrt{\frac{1}{2}} \end{bmatrix} \tag{19}$$

Park's original transformation matrix and that of many other authors has $\frac{2}{3}$ as a factor, and a negative sign in the second row. The latter is due

to the assumption that the quadrature axis is leading the direct axis by 90°, rather than lagging behind by 90°. The particular choice of the transformation matrix (19) makes the transformation power invariant and its matrix orthogonal, i.e.,

$$[P]^{-1} = [P]^{T} \tag{20}$$

Application of this transformation to (15) yields:

$$\begin{aligned} \underline{v}_p &= -[P][L]([P]^{-1}\frac{d}{dt}\underline{i}_p + \frac{d}{dt}([P]^{-1})\underline{i}_p) - [P]\frac{d}{dt}([L])[P]^{-1}\underline{i}_p - [R]\underline{i}_p \\ &= -[L_p]\frac{d}{dt}\underline{i}_p - [R]\underline{i}_p - [L_p']\underline{i}_p \end{aligned} \tag{21}$$

where

$$[L_p] = [P][L][P]^{-1} = \begin{bmatrix} L_d & 0 & 0 & \sqrt{\frac{3}{2}}M_f & \sqrt{\frac{3}{2}}M_f & 0 & 0 \\ 0 & L_q & 0 & 0 & 0 & \sqrt{\frac{3}{2}}M_q & \sqrt{\frac{3}{2}}M_q \\ 0 & 0 & L_0 & 0 & 0 & 0 & 0 \\ \sqrt{\frac{3}{2}}M_f & 0 & 0 & L_f & M_f & 0 & 0 \\ \sqrt{\frac{3}{2}}M_f & 0 & 0 & M_f & L_D & 0 & 0 \\ 0 & \sqrt{\frac{3}{2}}M_q & 0 & 0 & 0 & L_Q & M_q \\ 0 & \sqrt{\frac{3}{2}}M_q & 0 & 0 & 0 & M_q & L_g \end{bmatrix} \tag{22}$$

and

$$[L_p'] = [P]\frac{d}{dt}([P]^{-1}[P][L][P]^{-1}) = [P]\frac{d}{dt}([P]^{-1}[L_p])$$

$$= \omega \begin{bmatrix} 0 & L_q & 0 & 0 & 0 & \sqrt{\frac{3}{2}}M_q & \sqrt{\frac{3}{2}}M_q \\ -L_d & 0 & 0 & -\sqrt{\frac{3}{2}}M_f & -\sqrt{\frac{3}{2}}M_f & 0 & 0 \\ 0 & 0 & 0 & 0 & 0 & 0 & 0 \\ & 0 & & & 0 & & \end{bmatrix} \tag{23}$$

2.3 Calculation of Parameters for the Model of the Electric Part

As already explained, any mathematical model of a physical device is an approximation of physical reality. Some of the simplifications made in modelling a synchronous generator were discussed in section 2.2. Here, additional simplifications which are often introduced in the calculation of parameters will be discussed, as well as a technique for avoiding them.

The functional relationship between measurable parameters, e.g., R_a, X_d, X_d', X_d'', T_{do}', and T_{do}'' in the direct axis, and the desired set of resistances and self and mutual inductances (or reactances) is partly nonlinear [8], [9]. Approximations are normally made to obtain linearized relationships which are easy to solve [11], [18]. These approximations are based upon the knowledge of machine dimensions, which are normally unknown to the system analyst, and were only justified for hand calculations. There is really no reason any more to introduce them, if data conversion is done by a digital computer.

The model of a synchronous generator was defined in Fig. 1. The inductance matrix $[L_p]$ (in d,q,0-coordinates) was shown in (22) and the matrix of resistances in (14). As shown in Appendix 1, the measured direct axis machine constants are related to the entries in the matrices $[L_p]$ and $[R]$ in the following way

$$L_d' = L_d - \frac{3}{2}\frac{M_f^2}{L_f} \tag{24}$$

$$L_d'' = L_d - \frac{3}{2} M_f^2 \frac{L_f - L_D - 2M_f}{L_f L_D - M_f^2} \tag{25}$$

$$\left.\begin{matrix} T_{do}' \\ T_{do}'' \end{matrix}\right\} = \frac{1}{2}\left(\frac{L_f}{R_f} + \frac{L_D}{R_D}\right) \pm \frac{1}{2}\sqrt{\left(\frac{L_f}{R_f} - \frac{L_D}{R_D}\right)^2 + 4\frac{M_f^2}{R_f R_D}} \tag{26}$$

(positive sign of root for T_{do}', negative sign for T_{do}'')

The above equations are nonlinear and their solution by hand is difficult. Introduction of approximations based on the knowledge of machine dimensions leads to a well known, simplified set of equations [11], [19].

The equations (24)-(26) may be solved directly as a system of nonlinear equations by means of Newton's method. First, (24)-(26) are rearranged to the following form:

$$\underline{G}(\underline{x}) = \underline{0} \tag{27}$$

where $\underline{G} = [g_1, g_2, g_3, g_4]^T$ represents the vectors of functional relationships, $\underline{x} = [R_f, L_f, L_D, R_D]^T$ represents the unknown machine parameters, assuming M_f in p.u. is found from:

$$X_d = X_\ell + \omega \cdot M_f \tag{28}$$

Sometimes, the field resistance R_f in p.u. is given by the manufacturer. In this case, the vector $\underline{x}$ is given as:

$$\underline{x} = [M_f, L_f, L_D, R_D]^T \tag{29}$$

The following relationship is obtained by taking the first term in Taylor's series expansion and equating it to zero:

$$\underline{G}(\underline{x}) = \underline{G}(\underline{x}^*) + [G'(\underline{x}^*)] \cdot (\underline{x} - \underline{x}^*) = \underline{0} \tag{30}$$

where $\underline{x}$ represents the approximate solution point of the newest iteration step and $\underline{x}^*$ the approximate solution of the preceding iteration step (or the original guess). From (30) it follows that

$$\underline{x} = \underline{x}^* - [G'(\underline{x}^*)]^{-1} \cdot \underline{G}(\underline{x}^*) \tag{31}$$

Eq. (31) is used iteratively until convergence is reached. The initial guesses are found with the approximate linear relationships, as normally used before. This procedure converges quite fast. Typically, only 2 iteration steps are required.

A set of equations analogous to (24)-(26) may be obtained for the quadrature axis, which are again solved with Newton's method to obtain the model parameters from the test data. Quite often, the set of data for the quadrature axis is incomplete. In many cases, neither X_q' nor T_{qo}' are given. It is then necessary to reduce the complexity of the model by omitting the g-winding. Equations (24)-(26) are then replaced by the following set of equations [11] (for details see Appendix 1):

$$L_q'' = L_q - \frac{3}{2}\frac{M_q^2}{L_Q} \tag{32}$$

$$T_{do}'' = \frac{L_Q}{R_Q} \tag{33}$$

Quite often, the manufacturer's data sheets show that $T_{qo}' \neq T_{qo}''$, but $X_q' = X_q$. The program would fail in this case because the two assumptions contradict each other (the first implies the existence of a g-winding, whereas the second implies that there is no g-winding). The following equation:

$$L_q - L_q' = M_q\left(1 - \frac{L_g - M_q}{L_g}\right) = 0 \tag{34}$$

would then not have a real solution except for $M_q = 0$, which implies no g- and Q-winding. This special case can be solved without program modifications, however, by setting X_q' nearly equal to X_q, for example, $X_q' = 0.99\, X_q$ (X_q' must always be less than X_q). Since measurement accuracy is typically ±5%, this assumption is acceptable.

To illustrate the impact of linearization on the calculation of parameters, a 30 MVA machine was considered with the following data [11]:

X_d = 1.443 p.u. X_q = 0.707 p.u.

X_d' = 0.214 p.u. X_q'' = 0.1524 p.u.

X_d'' = 0.149 p.u. (calculated from other data)

T_{do}' = 7.8 s T_{qo}'' = 0.3412 s

T_{do}'' = 0.0701 s ω = 314 rad/s

R_f = 0.00064 p.u. (no g-winding)

The results calculated in three different ways are compared in Table I.

Table I. Comparison of data conversion with different methods.

Conversion method	X_{ad} (p.u.)	X_{aq} (p.u.)	X_ℓ (p.u.)	X_f (p.u.)	X_D (p.u.)	X_q (p.u.)	R_D (p.u.)	R_Q (p.u.)
a) approximate conversion	1.3879	0.6520	0.0550	0.1795	0.2298	0.1145	0.01766	0.00715
b) exact conversion (with Newton's method)	1.3533	0.6173	0.0897	0.1368	0.1133	0.0698	0.01026	0.00641
c) Kilgore's method	1.338	0.602	0.105	0.13	0.0678	.0.0515	0.0079	0.0061

While the differences between parameters found from the exact and approximate data conversion methods are not great, the differences in the simulation results of rotor quantities can be significant. The simulated field current i_f in case of a single line-to-ground fault for the generator used in Table I is shown in Fig. 2 for approximate and exact data conversion. The initial conditions for this case are given in Chapter 3. As pointed out by others [12-14], the results with approximately calculated parameters have significantly lower amplitudes of oscillations of rotor quantities, but the possible improvements with exact parameter conversion has not been recognized. The simulated stator quantities,

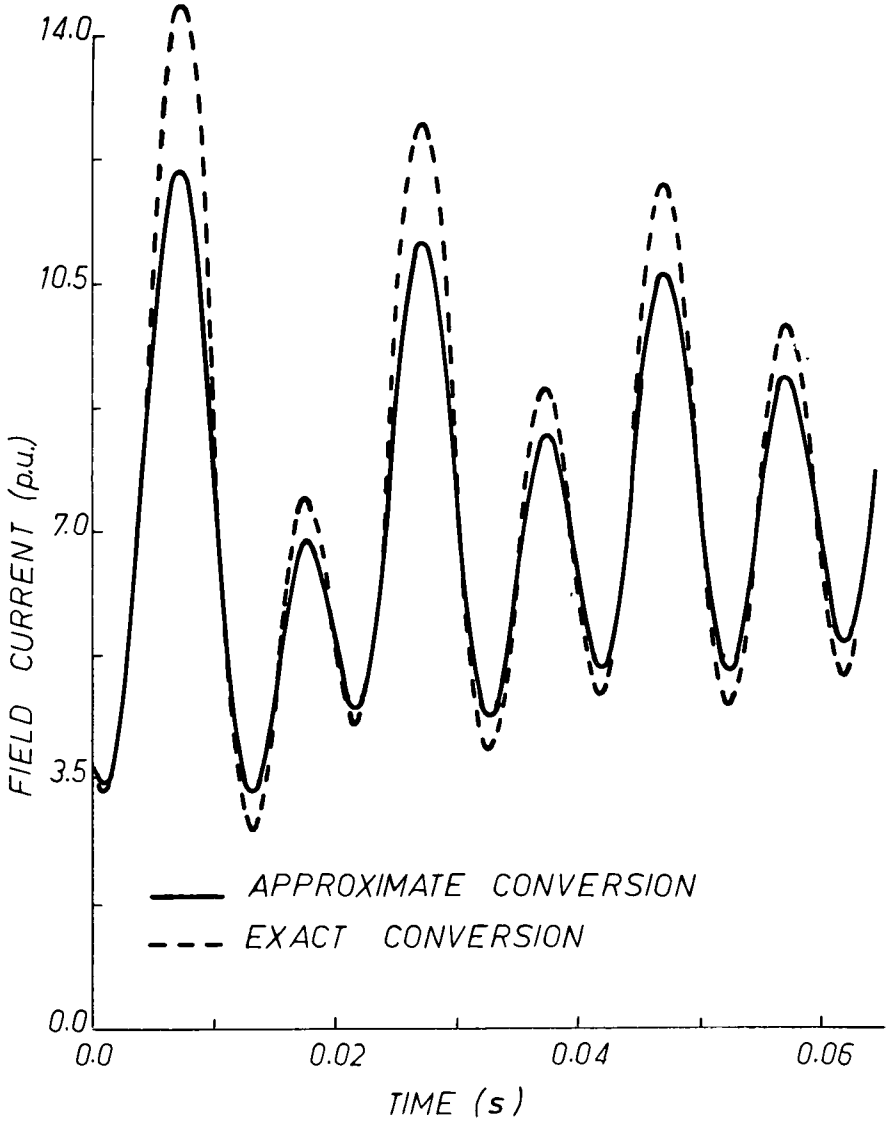

Fig. 2. Comparison of the simulated field currents i_f.

on the other hand, were identical for approximate and exact parameters. This agrees with results published by others [13], [14]. Fig. 3 shows the simulated current i_c in the faulted phase for the single line-to-ground fault with approximate and exact parameters (indistinguishable from each other).

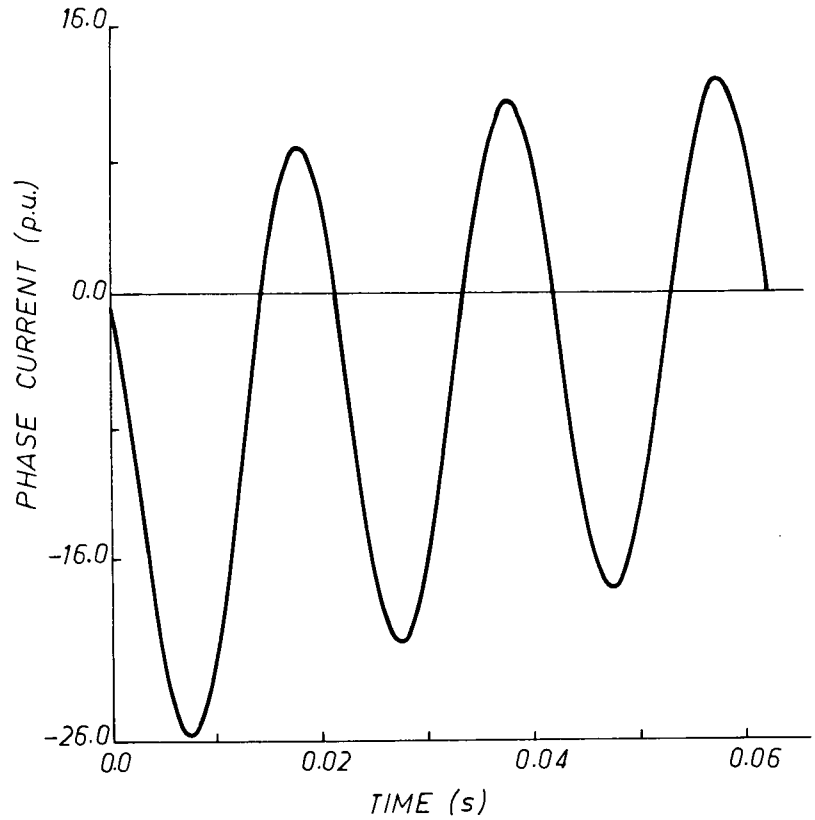

Fig. 3. Identical results for current i_c in the faulted phase with approximate and accurate parameter conversion.

2.4 Recent Proposals for Improvements in Parameter Accuracy

Additional improvements in the model of a synchronous generator are not possible without introduction of additional test data. New testing procedures require, however, a long time to become accepted as new standards. Model improvements occur, therefore, very slowly, but the data conversion algorithm described above can easily be changed to accommodate additional test data if and when they become available.

The first improvement is made if unequal mutual inductances $M_{fd} \neq M_{fD} \neq M_{Dd}$ are permitted. This was done by a number of researchers. In 1969, Canay [14] explained some of the causes of discrepancies between

field measurements and simulation results of rotor quantities. He proposed an improved equivalent circuit of the generator, but he required the knowledge of generator dimensions for obtaining its parameters. In 1971, Yu and Moussa [20] suggested another improved model of a generator. They required introduction of an extra test (time constant T_D of damper winding) to determine the parameters of their model. In 1974, Takeda and Adkins [13] suggested to obtain additional data from the measurement of the unidirectional field current. In the same year, Shackshaft [21] came up with a similar, but slightly more complicated approach. In all cases, the additional data can easily be incorporated into the data conversion algorithm, independent of the way in which it was obtained. It is believed that the data conversion algorithm will reduce the discrepancies between simulation and field tests even more, since it avoids the commonly used linearization of the functional relationships.

Some researchers have suggested measuring the parameters directly in phase coordinates [15], [22]. Such methods will not completely solve the problems, since some windings are inaccessible. They may, however, be very useful for improving the accuracy of the model. A different approach has evolved in the last few years. It is based upon parameter estimation either in the time domain [12] or in the frequency domain [23], [24]. It is this author's opinion that the parameter estimation method will eventually replace all the other approaches. It may, however, be a long time before this happens. It was, therefore, believed to be important to develop a simple method making efficient use of the easily available, conventional set of test data.

2.5 Model of the Mechanical Part of the Generator

It is common practice in transient stability studies to represent the rotating part of the turbine-generator unit (its shaft, generator and turbine rotors) as one lumped mass. This approach is, however, unacceptable in some studies of transient performance of the generator, where the rotational vibrations of different parts of the shaft system are important [3], [4]. As in the case of the electrical part of the generator, the complexity of the model depends on the amount of available data. The actual number of lumped masses may, therefore, vary from case to case. The techniques for modelling mechanical systems of rotating lumped masses are relatively well developed. The description of the mechanical part will, therefore, be relatively short. It should be noted, however, that some of the mechanical parameters are very difficult to obtain, not unlike some of the electrical parameters.

Fig. 4 shows a typical example of a turbine-generator unit with seven lumped masses, which is based upon an actual case [3].

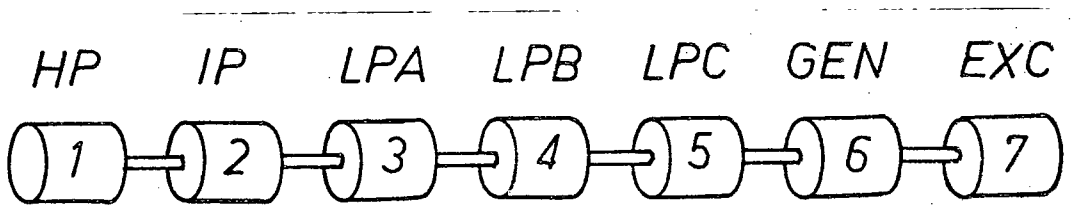

Fig. 4. Torsional model of a turbine-generator unit. (HP - high pressure turbine, IP - intermediate pressure, LPA, LPB - low pressure units, GEN - generator, EXC - exciter).

The dynamic equations of a rotating mechanical system can be derived from Newton's second law [25]. The following general equation can be written for each rotating mass:

$$J \frac{d^2\theta}{dt^2} = \sum_i T_i(t) \tag{35}$$

where

J = moment of inertia

θ = angle (rotational displacement)

$\sum_i T_i$ = sum of all torques acting on the rotating mass

To illustrate the use of eq. (35), the three-mass system of Fig. 5 will be used. Assume that

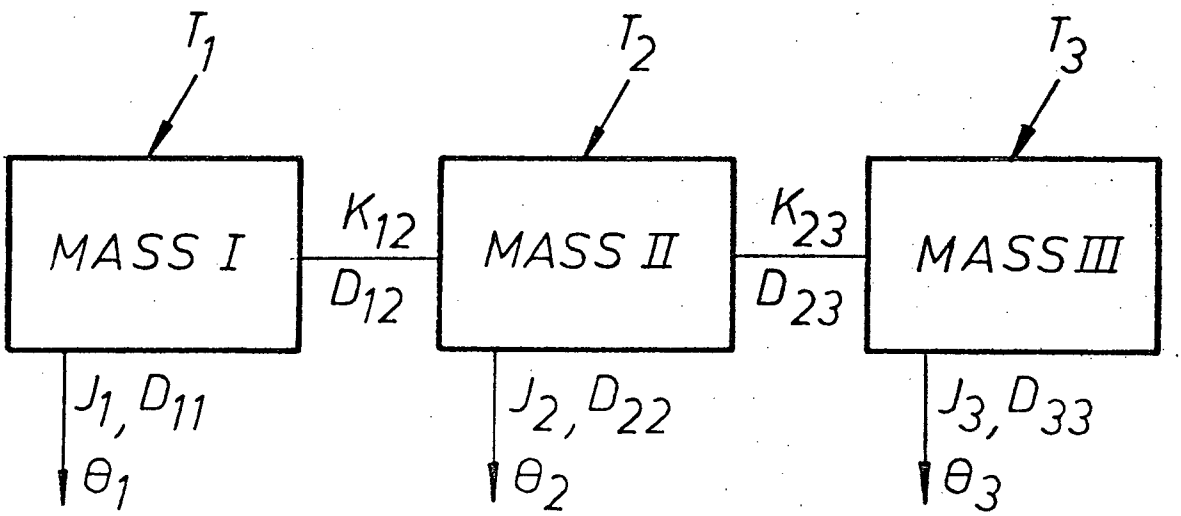

Fig. 5. Schematic representation of a three rotating masses system.

$K_{i,i+1}$ = shaft stiffness coefficient (between masses i and i+1);

D_{ii} = viscous self damping coefficient (of the mass i);

$D_{i,i+1}$ = viscous mutual damping-coefficient (between masses i and i+1);

J_i = moment of inertia (of the mass i);

θ_i = angle (of the mass i);

T_i = external torque (applied to mass i).

Starting with mass 1, the following three equations can be written: for mass 1,

$$J_1\frac{d^2\theta_1}{dt^2} + D_{11}\frac{d\theta_1}{dt} + D_{12}\frac{d}{dt}(\theta_1-\theta_2) + K_{12}(\theta_1-\theta_2) = T_1 \tag{36}$$

for mass 2,

$$J_2\frac{d^2\theta_2}{dt^2} + D_{22}\frac{d\theta_2}{dt} + D_{12}\frac{d}{dt}(\theta_2-\theta_1) + D_{23}\frac{d}{dt}(\theta_2-\theta_3) + K_{12}(\theta_2-\theta_1) + K_{23}(\theta_2-\theta_3) = T_2 \tag{37}$$

and for mass 3,

$$J_3\frac{d^2\theta_3}{dt^2} + D_{33}\frac{d\theta_3}{dt} + D_{23}\frac{d}{dt}(\theta_3-\theta_2) + K_{23}(\theta_3-\theta_2) = T_3 \tag{38}$$

Equations (36)-(38) assume that the system is linear, which is an acceptable simplification for rotational vibrations of small amplitude.

A three-mass system has all the characteristic features of an n-mass system. Therefore, equations (36)-(38) can be generalized to obtain the following system of equations for any system of n rotating masses:

$$[J]\frac{d^2}{dt^2}\underline{\theta} + [D]\frac{d}{dt}\underline{\theta} + [K]\underline{\theta} = \underline{T} \tag{39}$$

where

[J] = diagonal matrix of moments of inertia;

$\underline{T}$ = vector of external torques applied to the system;

$\underline{\theta}$ = vector of angular displacements;

[D] = matrix of damping coefficients, which has the following form for the case of Fig. 5,

$$[D] = \begin{bmatrix} D_{11}+D_{12} & -D_{12} & 0 \\ -D_{12} & D_{22}+D_{12}+D_{23} & -D_{23} \\ 0 & -D_{23} & D_{33}+D_{23} \end{bmatrix} \tag{40}$$

[K] = matrix of stiffness coefficients, which has the following form for the case of Fig. 5,

$$[K] = \begin{bmatrix} K_{12} & -K_{12} & 0 \\ -K_{12} & K_{12}+K_{23} & -K_{23} \\ 0 & -K_{23} & K_{23} \end{bmatrix} \tag{41}$$

In the case of turbine-generator units, the external torques are of two types:

(1) mechanical in the turbine stages;

(2) electromagnetic in the generator and exciter rotors.

The calculation of mechanical torques in transient stability studies can be simple or very complicated. In the former case, it is assumed that mechanical torque or power remains constant after the disturbance. In the latter case, the dynamics of the speed governor and associated control systems must also be modelled [26], [27]. In electromagnetic transient studies, which is the subject of this thesis, the issue is less complicated due to much shorter time spans involved (normally, cases are only simulated up to 1 sec. after the disturbance). It is then possible to assume constant mechanical power input and calculate the torque from the following relationship:

$$T = \frac{P}{\omega_m} \tag{42}$$

where

P = mechanical power prior to disturbance,

ω_m = angular speed of the mechanical system.

It has been shown that the assumption of constant mechanical torque produces satisfactory results [4], but constant mechanical power seems to be a more reasonable assumption than constant mechanical torque.

The electromagnetic torque developed in the rotor of a synchronous generator is equal to the air gap torque produced by the rotating electromagnetic field [9] and may be described by the following formulas:

(a) in Park's d,q,0-coordinates [9]:

$$T_e = (\psi_d i_q - \psi_q i_d) \cdot \frac{n}{2} \tag{43}$$

(b) in phase-coordinates [28]:

$$T_e = \frac{n}{2\sqrt{3}} [\psi_a(i_b - i_c) + \psi_b(i_c - i_a) + \psi_c(i_a - i_b)] \tag{44}$$

where

n = number of poles of the generator.

The torque in the exciter (if it is a d.c. generator directly coupled to the turbine-generator shaft; not modelled in other cases such as motor-driven generators or rectifiers) is determined by the amount of electric energy produced by the generator and is given as:

$$T_{ex} = \frac{n}{2 \cdot \omega_m} (v_f \cdot i_f + R_{ex} i_f^2) \tag{45}$$

where

ω_m = angular speed of the exciter;

v_f = voltage at exciter terminals;

i_f = excitation current;

R_{ex} = armature resistance of the exciter.

The electromagnetic torque carries a sign opposite to that of the mechanical torque, since it represents a load to the mechanical system.

2.6 Conclusions

An idealized, linear model of a synchronous generator, which is described by relatively simple equations, has been presented in sections

2.2 and 2.5. The model of the mechanical part was only included for completeness, since the rest of the thesis is primarily concerned with the electric part of the synchronous generator.

This model of a synchronous generator has been shown to be adequate even for such complex problems as subsynchronous resonance [3], [4]. It should be understood, however, that the rotor quantities are not always reproduced accurately [13], [14]. The problem lies in obtaining enough and sufficiently accurate data. The numerical calculations, on the other hand, can be carried out with very high accuracy. The complexity of calculations should, therefore, be related to the accuracy of measurements [29], since there is not much sense in creating a very complex model for inaccurate data. Lack of reliable data often forces the analyst to use simplifications in the model.

Saturation effects have been neglected in the development of this model. However, as shown later, in section 5.5, it is possible to include them without sacrificing the simplicity of the model.

The electric part of a synchronous generator was described in two systems of coordinates. These two descriptions are equivalent for theoretical considerations. For numerical solutions, however, one system of coordinates may offer advantages over the other system. This problem will be discussed in section 3.3.

3. NUMERICAL SOLUTION OF THE GENERATOR EQUATIONS

3.1 Choice of Integration Method

The dynamic behaviour of a synchronous generator is described by two sets of differential equations, one set for the electric part, and another set for the mechanical part. It is important to bear in mind that no digital computer solution of differential equations can give a continuous history of the transient phenomena. It can only give a sequence of "snapshot pictures" at discrete time intervals Δt. Such discretization causes truncation errors, which can lead to numerical instability [30]. The stepsize Δt should, therefore, be small enough to avoid build-up of truncation errors, but not too small to avoid unnecessary computer time.

It is important to consider the structural properties of the generator equations in connection with the choice of the stepsize Δt. The system of equations for the electric part of the generator and for the electric network, to which it is connected, is stiff, i.e. the time constants of the system are widely separated [31]. In typical transient stability studies, the ratio of the largest to the smallest time constant may be in the order of 10^3 or 10^4 [32]. The ratios in studies of electromagnetic transients, with which this thesis is concerned, are similar. Even the time constants of the generator equations alone may, in this case, have a ratio in the order of 10^2 or 10^3, e.g., $\frac{T_{do}'}{T_{do}''} = 1.12 \cdot 10^2$ for the generator from section 2.3. In order to avoid numerical instability (due to build-up of truncation errors), most integration methods, especially those which are explicit, require an integration stepsize Δt which is smaller than the smallest time constant. For instance, fourth-order

Runge-Kutta methods require a stepsize which is approximately less than 1/5 of the smallest time constant. Such a small stepsize is required in spite of the fact that in stiff systems the components associated with the smallest time constants are normally negligible for most of the simulation time span. The overall behaviour of the system, which is of primary interest, is determined by the largest time constants. The time span of the simulation is, therefore, determined by the largest time constant. A very small stepsize Δt is, therefore, very expensive in simulating stiff systems.

Round-off errors create additional problems in the numerical solution of differential equations. They may become worse for a solution with a very small stepsize Δt than for a solution with a larger one. Round-off and truncation error problems are interrelated and are normally considered together as one problem of numerical stability of the solution.

Any practical method of numerical integration should not only be numerically stable, but also reasonably accurate and efficient. Therefore, the numerical integration method needed in the case of electromagnetic transients should provide a compromise between:

(a) numerical stability;

(b) accuracy;

(c) numerical efficiency.

The implicit trapezoidal rule of integration seems to be the best compromise for these sometimes contradictory requirements [31], [33]. This method does not suffer from the smallest time constant barrier, i.e., the stepsize Δt is not controlled by it. The stepsize Δt is restricted mainly by accuracy of the solution, and not by its numerical stability [34]. A fundamental theorem due to Dahlquist [35] states:

Theorem: Let a method be called A-stable, if, when it is applied to the problem $\frac{dy}{dt} = \lambda y$, $\lambda < 0$, it is stable for all $\Delta t > 0$. Then:

(1) No explicit linear multistep method is A-stable;

(2) no implicit linear multistep method of order greater than two is A-stable;

(3) the most accurate A-stable linear multistep method of order two is the trapezoidal rule:

$$y(t+\Delta t) - y(t) = \frac{\Delta t}{2}\{f(t,y(t)) + f(t+\Delta t, y(t+\Delta t))\} \quad (46)$$

for an equation $$\frac{dy}{dt} = f(t,y) \quad (47)$$

The A-stability property was the main reason for the choice of this particular integration method.

Some additional, important facts speak in favour of the trapezoidal rule. First of all, it is very simple to program, and does not require past history points except for those of the immediately preceding time step. It is, therefore, self-starting. It is also important to note that the trapezoidal rule with a constant stepsize Δt creates constant state transition matrices for linear systems with constant coefficients. This property reduces significantly the amount of calculations involved in the solution process. Finally, it is worth mentioning that the use of this integration method assures consistency with the Transient Program [34], which uses the same solution method.

A number of different solution techniques were suggested in the literature, but none of them seems to have clear advantages over the trapezoidal rule [3], [32], [36-39].

Two cases were run to compare the trapezoidal rule with the fourth-order Runge-Kutta method for generator equations. The generator described in section 2.3 was used in both cases. First, a three-phase short-circuit was simulated as shown in Fig. 6. The voltage of the infinite busbar was $2.0\angle 0°$ p.u., and the initial conditions of the generator were $1.734\angle -5.2°$ p.u. stator current and 3.56 p.u. field current. The network parameters were R_e = 1.0 p.u.

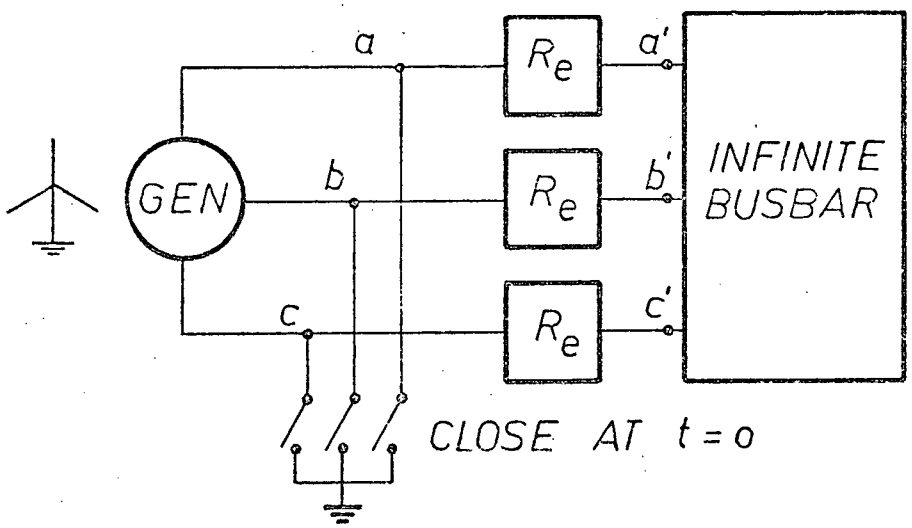

Fig. 6. Three phase-to-ground fault at generator terminals.

The simulation results for a time step of Δt = 100 μs were practically identical for the fourth-order Runge-Kutta method and the trapezoidal rule of integration, but some differences were visible for Δt = 1 ms. Fig. 7 compares the results for the field current i_f.

As a second test case, a line-to-ground fault of an unloaded generator was chosen, with the same generator data as for the first case. The fourth-order Runge-Kutta method became numerically unstable in this case, even for Δt = 100 μs. The reason may have been the way in which the external network was simulated, namely as a very large resistance R_e

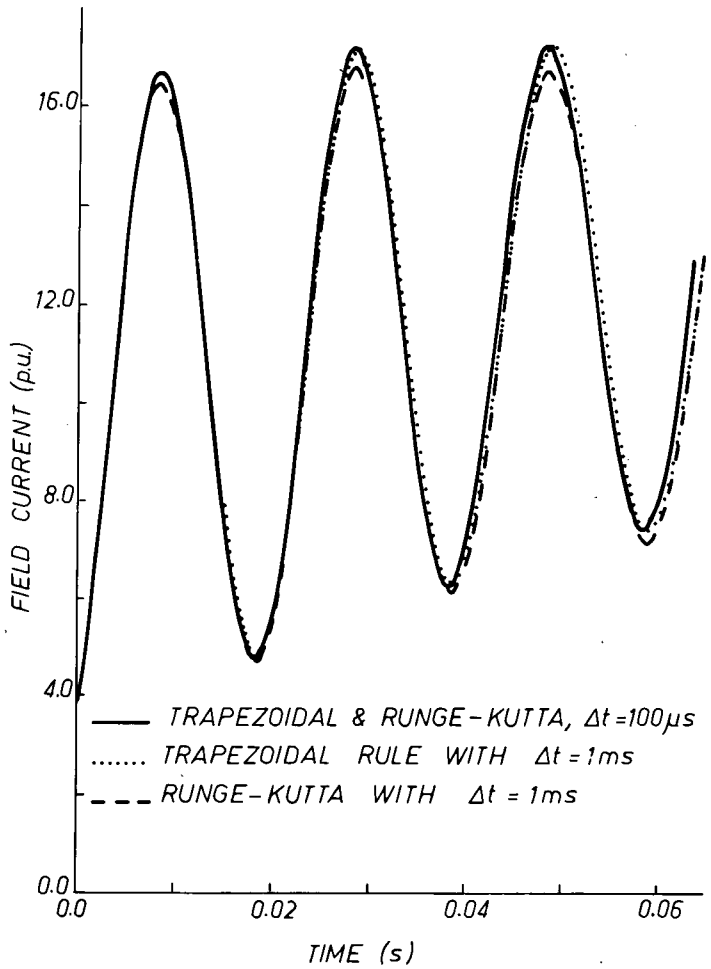

Fig. 7. Comparison of simulation results for the field current in case of a three-phase fault.

in the two unfaulted phases and zero resistance in the faulted phase. The comparison of the results for two different stepsizes Δt is shown in Fig. 8.

Figs. 7 and 8 show that an increase in the stepsize Δt results in decreased accuracy of the solution with the trapezoidal rule, but not in numerical instability. Stepsizes greater than 1 ms were not considered, since the time step for the simulation of realistic cases is dictated by the solution of electromagnetic transients in the external network, where stepsizes are typically in the order of 50 to 100 μs.

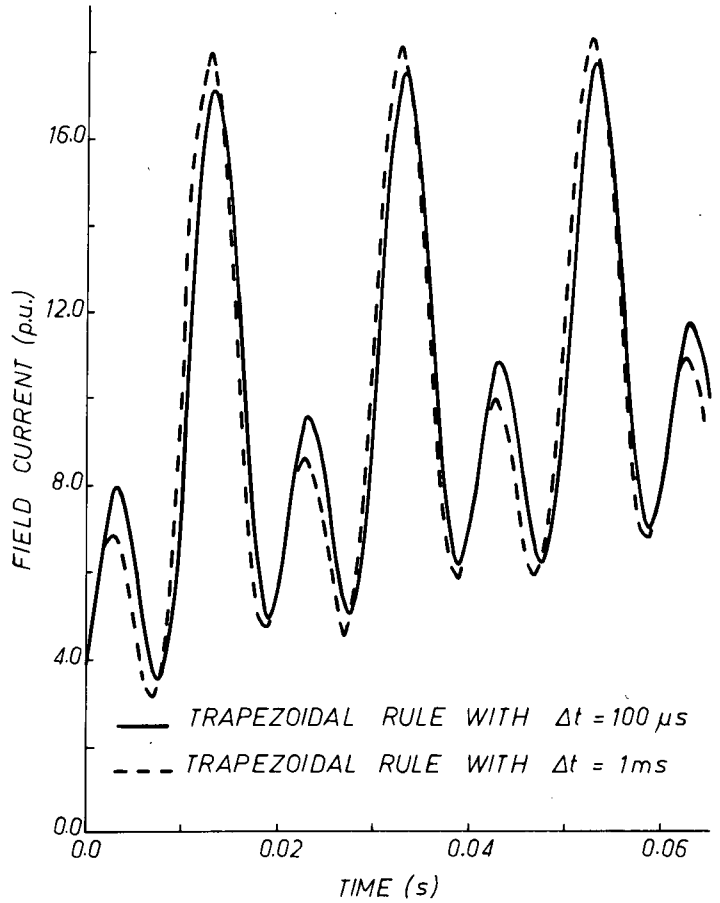

Fig. 8. Comparison of simulation results for the field current in case of a line-to-ground fault.

3.2 Physical Interpretation of the Trapezoidal Rule of Integration for a Lumped Inductance

It is very important to understand the build-up of discretization errors when the differential equations of the generator are replaced by difference equations*. As shown earlier, the generator model consists of lumped inductances and resistances. The resistance part does not

* The trapezoidal rule of integration applied to $v = L\frac{di}{dt}$ is identical with replacement of the derivative by a central difference quotient.

cause discretization errors, since the functional relationship

$$v = -Ri \tag{48}$$

is solved accurately (except for round-off errors) as a linear algebraic equation. Discretization errors must only be considered for the inductance part. To keep the explanation simple, consider a single inductance L between two nodes "k" and "m" as shown in Fig. 9:

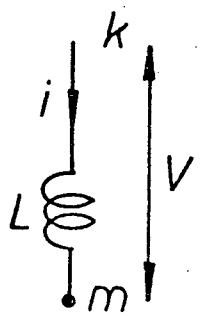

Fig. 9. Inductance between nodes k and m.

Application of the trapezoidal rule to

$$v = L \frac{di}{dt} \tag{49}$$

yields:

$$i(t+\Delta t) = i(t) + \frac{\Delta t}{2L}\{v(t+\Delta t) + v(t)\} \tag{50}$$

It will now be shown that replacing the differential equation (49) by the difference equation (50) is identical to replacing the lumped inductance L by a short-circuited, lossless transmission line of travel time $\tau = \frac{\Delta t}{2}$ and characteristic impedance $Z = \frac{2L}{\Delta t}$. This line, which replaces L, has (unavoidable) shunt capacitance C' per unit length which goes to zero as Δt goes to zero, and a series inductance L' per unit length which, when multiplied with line length, is equal to the value L of the lumped inductance. It is schematically shown in Fig. 10. The equations of the lossless line can be solved exactly with Bergeron's method* [34]. With this method, the following equation can be derived

* Method of characteristics in mathematical references.

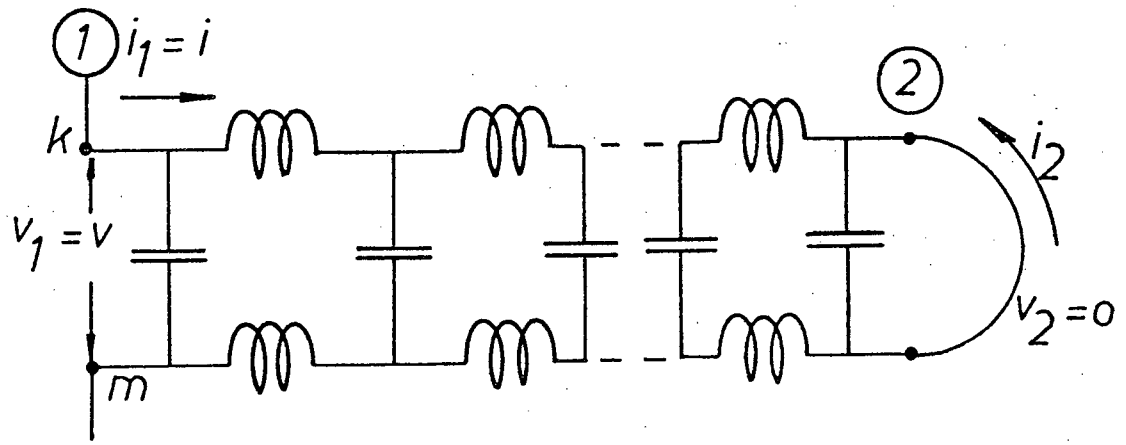

Fig. 10. Schematic representation of a lossless, short-circuited transmission line.

for a ficticious observer travelling from terminal "1" to "2" if he leaves terminal "1" at $t-\Delta t$,

$$v_1(t-\Delta t) + Zi_1(t-\Delta t) = -Zi_2(t-\frac{\Delta t}{2}), \tag{51}$$

and for an observer leaving terminal "2" towards "1" at $t - \frac{\Delta t}{2}$,

$$Zi_2(t - \frac{\Delta t}{2}) = v_1(t) - Zi_1(t) \tag{52}$$

Summation of (51) and (52) yields

$$v_1(t-\Delta t) + Zi_1(t-\Delta t) + v_1(t) - Zi_1(t) = 0 \tag{53}$$

which can be rewritten as

$$i_1(t) = i_1(t-\Delta t) + \frac{1}{Z}(v_1(t) + v_1(t-\Delta t)) \tag{54}$$

Equation (54) is identical with (50), when

$$Z = \frac{2L}{\Delta t} \tag{55}$$

where Z is defined as follows:

$$Z = \sqrt{\frac{L'}{C'}} \tag{56}$$

Equation (54) is an exact solution for a lossless transmission line [40]. Therefore, the application of the trapezoidal rule to a lumped inductance L is equivalent to replacing the lumped inductance with a short-circuited, lossless "stub" line with distributed inductance L' = L/length and travel time $\tau = \frac{\Delta t}{2}$, which is then solved accurately.

The error committed by this replacement can be evaluated quite easily by calculating the input impedance of a short-circuited lossless line. The steady-state behaviour of a single-phase transmission line can be described by the following general equations [41]:

$$V_1 = \cosh(\gamma\ell)V_2 + \sinh(\gamma\ell)\cdot I_2 Z \tag{57}$$

and

$$I_1 = \sinh(\gamma\ell)\frac{V_2}{Z} + \cosh(\gamma\ell)\cdot I_2 \tag{58}$$

with V and I being phasor values.

For a short-circuit at terminal "2" ($V_2 = 0$), the input impedance seen from "1" can be described as follows:

$$Z_{IN} = \frac{V_1}{I_1} = Z \tanh(\gamma\ell) \tag{59}$$

For the lossless line, the characteristic impedance is:

$$Z = \sqrt{\frac{L'}{C'}} \tag{60}$$

and the propagation constant is

$$\gamma = \sqrt{j\omega L' j\omega C'} = j\omega\sqrt{L'C'} \tag{61}$$

This leads to the following relationship:

$$Z_{IN} = j\omega L \cdot \frac{2}{\Delta t\cdot\omega} \cdot \tan\left(\frac{\Delta t\cdot\omega}{2}\right) \tag{62}$$

The error in the frequency domain can now be assessed by calculating the ratio of the known true value $Z_{lumped} = j\omega L$ to the computed value Z_{IN} given by (62):

$$H(\omega) = \frac{Z_{lumped}}{Z_{IN}} = \frac{\Delta t \cdot \omega}{2} \cot\left(\frac{\Delta t \cdot \omega}{2}\right) \tag{63}$$

Equation (63) is the ratio of the impedance resulting from the application of the trapezoidal rule of integration to the impedance of the lumped inductance. It is probably more illustrative to consider the relative error

$$G(\omega) = H(\omega) - 1.0 \tag{64}$$

instead of the absolute error $H(\omega)$. The relative amplitude error $|G(\omega)|$ is plotted in Fig. 11 as a function of $\frac{\omega \cdot \Delta t}{2}$, and the phase error $\arg G(\omega)$ is plotted in Fig. 12 as a function of the same variable.

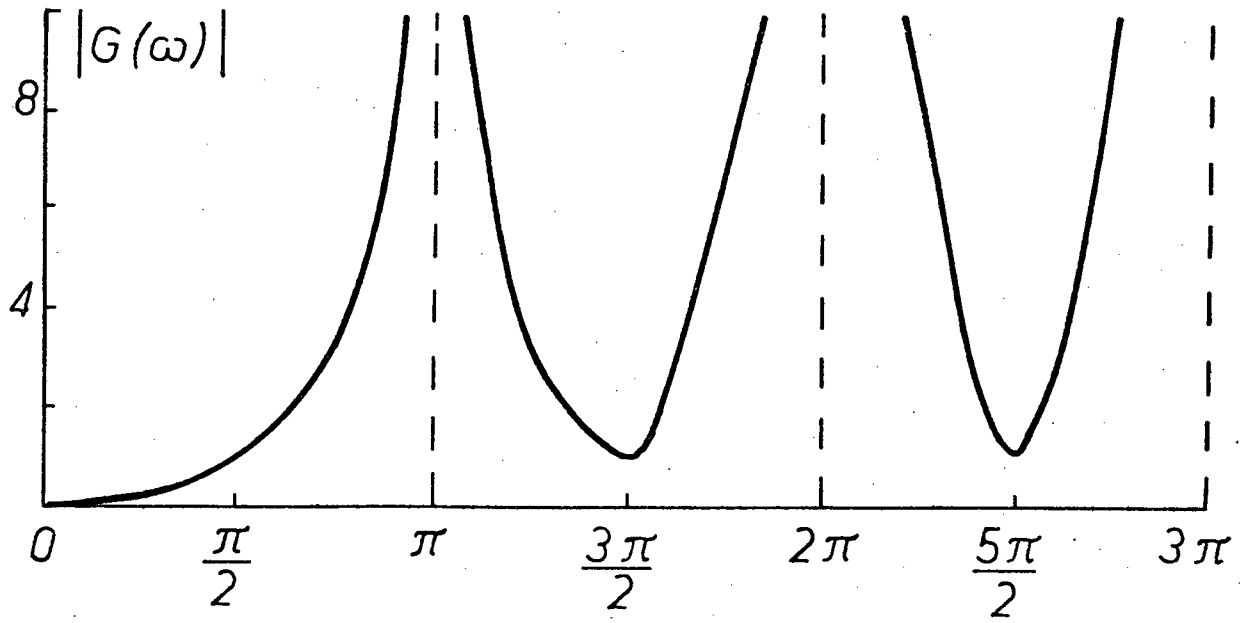

Fig. 11. Relative amplitude error of the trapezoidal rule of integration.

Figs. 11 and 12 give a simple physical explanation of the error for any given stepsize Δt. Low frequencies are reproduced practically without any error, since

$$\lim_{x \to 0} \left(|x \cdot \cot x - 1|\right) = 0 \tag{65}$$

where

$$x = \frac{\omega \Delta t}{2} \tag{66}$$

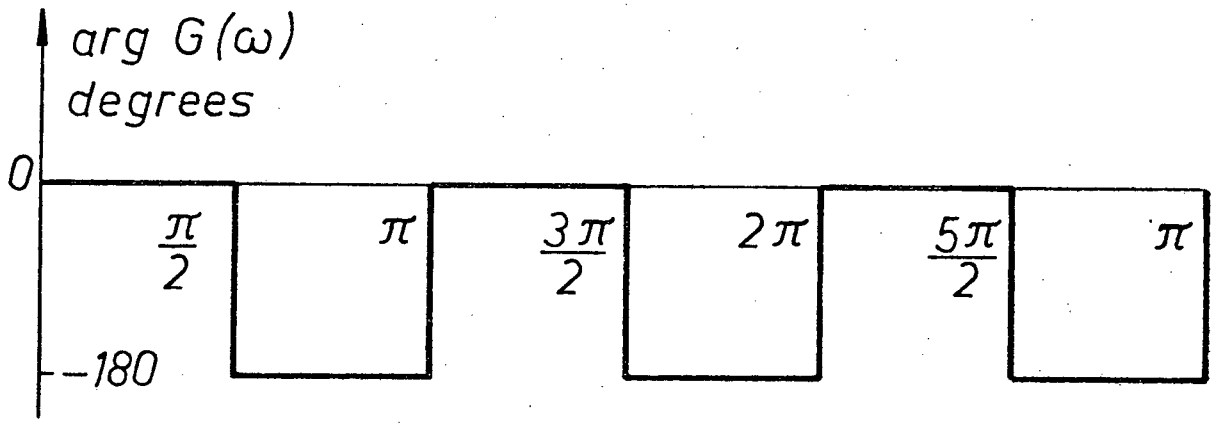

Fig. 12. Phase error of the trapezoidal rule of integration.

The error increases with frequency until an absolute blocking (H = 0) is reached for

$$f_1 = \frac{1}{2\Delta t} \tag{67}$$

For Δt = 100 μs, a typical stepsize used in studies of electromagnetic transients, the first blocking frequency is equal to f_1 = 5 kHz. If the frequency is increased beyond f_1, then the element is seen by the solution algorithm as if it were capacitive up to $2f_1$, at which point the element is seen as a short-circuit, reversing to inductive afterwards. The next blocking point is reached at

$$f_2 = \frac{3}{2\Delta t} \tag{68}$$

From there on, the situation repeats itself periodically.

Similar analysis conducted for a lumped capacitance shows that application of the trapezoidal rule to its differential equation is equivalent to replacing the lumped capacitance by an open-ended lossless line.

In this case, the ratio becomes:

$$H(\omega) = \frac{2}{\Delta t \cdot \omega} \tan\left(\frac{\omega \Delta t}{2}\right) \tag{69}$$

Identical results can be achieved with "the transfer function" approach [42].

The above facts explain the sometimes large local error of the solution. The overall numerical stability of the solution, however, is unaffected [35], [43]. The trapezoidal rule of integration can thus be regarded as a procedure which changes impedance values differently for different frequencies, but solves the system accurately with these modified impedances. The solution is obviously stable, but more or less inaccurate.

3.3 Choice of Coordinate System

In studying electromagnetic transients it is not clear a priori which system of coordinates is more advantageous for integrating the differential equations of the electric part. It is clear, however, that general-purpose computer programs must interface the resulting difference equations of the generator with those of the network in phase coordinates. Otherwise the ability to simulate any general type of electric network would be lost, thus eliminating the generality of the program. The integration of the generator equations directly in phase coordinates would seem, therefore, to be the best choice. It must be realized, however, that the trapezoidal rule will then produce discretization errors even for balanced steady-state conditions, since the flux and the currents in the phases change sinusoidally at fundamental frequency. Integration in d,q,0-coordinates, on the other hand, would be exact for balanced steady-state conditions with the trapezoidal rule, since flux and currents in

d,q,0-coordinates are constant in this case. If the latter approach is used, then the resulting difference equations must be transformed back to phase coordinates before they are interfaced with the difference equations of the network.

For general transient conditions, the choice is not at all clear. As an example, a single line-to-ground fault at the generator terminals has phase currents varying at 60 Hz, if the harmonics and dc-offset are ignored. Currents in d,q,0-coordinates, on the other hand, will vary at 60 Hz and 120 Hz, with the latter caused by negative sequence components.

The final choice was made after considering the numerical efficiency. The amount of calculations in d,q,0-coordinates is significantly smaller, since the inductance matrix $[L_p]$ is constant in this case [44]. Preliminary experiments showed that integration in d,q,0-coordinates gives very satisfactory answers, and d,q,0-coordinates were finally chosen for the work in this thesis.

As shown in Appendix 2, the trapezoidal rule of integration in both systems of coordinates leads to the same form of linear relationships between voltages and currents, and only the discretization errors are different. The choice of system of coordinates, therefore, does not change the general approach outlined in this thesis.

If space harmonics in the magnetic field distribution are taken into account, then integration in phase coordinates will probably be more advantageous. Self and mutual inductances could then be defined directly in phase coordinates. The inductance matrix $[L_p]$ in d,q,0-coordinates would no longer be constant, in this case anyhow, thus diminishing the main advantage of this system of coordinates.

3.4 Multiphase Equivalent Networks

The analysis of connected subnetworks becomes simpler if each subnetwork has already been reduced to a multiphase equivalent circuit in which only terminals at the connection points are retained and all other terminals are eliminated. Such a situation exists when generators are connected to a transmission system. On the generator side, only the stator windings are directly connected to the transmission network, i.e., only three pairs of its terminals must be retained if the generator equations are to be solved simultaneously with the network equations. This assumes, of course, that the generator equations can in fact be reduced to equations containing the retained terminals, only. This is indeed possible, as explained in chapter 3.5. All other pairs of terminals on the rotor are then concealed. The situation is similar in the transmission network. Again, only three pairs of its terminals are connected to each generator, thus making all the rest of them concealed, provided that the network can be reduced to the retained terminals only. Since the interface between the electromagnetic transients, which solves the network, and the generator model is performed only through the retained pairs of terminals, it seems appropriate to discuss in some detail the idea of a multiphase equivalent network.

Multiphase equivalent networks have not been used for a very long time. Since a number of good references are available [45], [46], only a short outline will be given here to aid in the understanding of interface techniques. The theory will first be explained for steady state, with voltages and currents being phasors, and then extended to the solution of electromagnetic transients in section 3.5. This extension becomes straightforward with the concept of resistive companion models [47].

The generator or the network can either be described by a set of independent node equations with an admittance matrix, $[Y]\underline{V} = \underline{I}$, or with an impedance matrix, $\underline{V} = [Z]\underline{I}$ where $[Z] = [Y]^{-1}$. Retained terminal pairs are generally located across only a few independent node pairs. The node impedance or admittance matrix of the reduced network, which contains only the retained terminal pairs, can be obtained from the full impedance or admittance matrix by elimination of the concealed variables.

Consider a general network with N independent node pairs and with R terminal pairs to be retained. Such a network may be described by the following nodal equations with an admittance matrix:

$$\begin{bmatrix} \underline{I}_R \\ \underline{I}_E \end{bmatrix} = \left[\begin{array}{c|c} Y_{RR} & Y_{RE} \\ \hline Y_{ER} & Y_{EE} \end{array}\right] \cdot \begin{bmatrix} \underline{V}_R \\ \underline{V}_E \end{bmatrix} \tag{70}$$

or by an inverse relationship with an impedance matrix.

$$\begin{bmatrix} \underline{V}_R \\ \underline{V}_E \end{bmatrix} = \left[\begin{array}{c|c} Z_{RR} & Z_{RE} \\ \hline Z_{ER} & Z_{EE} \end{array}\right] \cdot \begin{bmatrix} \underline{I}_R \\ \underline{I}_E \end{bmatrix} \tag{71}$$

where subscript "R" denotes the retained variables, and subscript "E" denotes the concealed variables, which are to be eliminated. Elimination of the concealed variables results in the following relationships:

$$\underline{I}_R = ([Y_{RR}] - [Y_{RE}][Y_{EE}]^{-1}[Y_{ER}])\underline{V}_R + [Y_{RE}][Y_{EE}]^{-1} \cdot \underline{I}_E \tag{72}$$

and

$$\underline{V}_R = ([Z_{RR}] - [Z_{RE}][Z_{EE}]^{-1}[Z_{ER}])\underline{I}_R + [Z_{RE}][Z_{EE}]^{-1} \cdot \underline{V}_E \tag{73}$$

Equations (72) and (73) may be interpreted as generalized forms of Norton's or Thevenin's theorem. Equation (73) will be considered closer. It can be rewritten as follows:

$$\underline{V}_R = [Z_R]\underline{I}_R + \underline{V}_{RO} \tag{74}$$

Setting $\underline{I}_R = \underline{0}$ gives the open-circuit terminal voltages as:

$$\underline{V}_R = [Z_{RE}][Z_{EE}]^{-1}\underline{V}_E \tag{75}$$

The equivalent impedance $[Z_R]$ is defined as follows:

$$[Z_R] = [Z_{RR}] - [Z_{RE}][Z_{EE}]^{-1}[Z_{ER}] \tag{76}$$

Equation (74) describes, therefore, the multiphase Thevenin equivalent circuit of a network. It is a reduced network with concealed terminals eliminated. Analysis is simplified if the impedance matrix $[Z_R]$ behind the voltage sources $\underline{V}_{RO}$ is constant. The Thevenin equivalent circuit of (73) is only useful if the voltages $\underline{V}_E$ across the concealed node pairs are known, and (72) is only useful if the currents $\underline{I}_E$ across the concealed node pairs are known. A three-phase Thevenin equivalent circuit is shown schematically in Fig. 13.

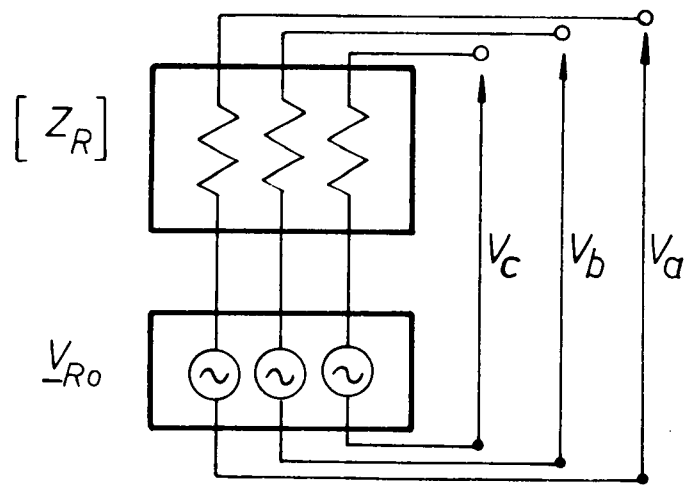

Fig. 13. Schematic representation of a three-phase Thevenin equivalent circuit.

The multiphase equivalent circuit was derived from nodal equations, but it can also be derived from other forms of network description, e.g., from branch equations or mesh equations.

The concept of multiphase Thevenin equivalent circuits, which was derived for steady state above, can also be used for transient conditions. The efficient calculation of a Thevenin equivalent circuit for the transmission network has already been explained in Appendix 3 for transient conditions. Therefore, only the Thevenin equivalent circuit of the generator must still be derived for transient conditions, which is done in the following section.

3.5 Three-Phase Equivalent Circuit of the Generator

After the application of the trapezoidal rule, the nodal voltage equations of a generator in d,q,0-coordinates have the following form (for details see Appendix 2):

$$\underline{v}_p(t) = [R^{comp}]\underline{i}_p(t) + \underline{e}_p(t-\Delta t) \qquad (77)$$

Equation (77) can be visualized as voltage sources $\underline{e}_p(t-\Delta t)$ behind resistances $[R^{comp}]$. Such equivalent resistive networks, which result from the implicit integration of differential equations, are called "resistive companion network models" in network theory [47]. They have been used in power systems analysis for more than 10 years [48]. The resistive matrix $[R^{comp}]$ is constant in d,q,0-coordinates, and the voltage sources $\underline{e}_p(t-\Delta t)$ are calculated from the known "past-history terms" of the preceding time step $t-\Delta t$. The ability to create such "resistive companion network models" is not limited to the trapezoidal rule of integration only, but works for any implicit integration as shown in Appendix 4.

Equation (77) represents a system of seven equations. The first three of them describe the stator windings, and the rest describe the rotor windings. Therefore, (77) can be rewritten as follows

(subscript "p" and superscript "comp" dropped to simplify notation):

$$\underline{v}_s(t) = [R_{ss}]\underline{i}_s(t) + [R_{sr}]\underline{i}_r(t) + \underline{e}_s(t-\Delta t) \qquad (78a)$$

$$\underline{v}_r(t) = [R_{rs}]\underline{i}_s(t) + [R_{rr}]\underline{i}_r(t) + \underline{e}_r(t-\Delta t) \qquad (78b)$$

where subscript "s" denotes stator quantities, and "r" rotor quantities. Elimination of rotor currents $\underline{i}_r(t)$ (rotor terminals are concealed) results in the following relationship:

$$\underline{v}_s(t) = ([R_{ss}] - [R_{sr}][R_{rr}]^{-1}[R_{rs}])\underline{i}_s(t) + \underline{e}_s(t-\Delta t) + [R_{sr}][R_{rr}]^{-1}\cdot(\underline{e}_r(t-\Delta t) - \underline{v}_r(t)) \qquad (79)$$

As mentioned in section 3.4, the equivalent circuit of (79) is really only useful if concealed variables are known, which is $\underline{v}_r(t)$ here. Since all damper windings are permanently short-circuited, the voltages across these windings are always equal to zero, and therefore known. Only the field winding requires special attention. Depending on the type of study, three approaches can be used:

(a) For many studies t_{max} is so short that the exciter output does not change within that time span. The voltage across the field winding $v_f(t)$ is then constant and equal to the pre-disturbance value.

(b) For studies over longer time spans, the response of the excitation system may have to be taken into account. Differential equations are then used to describe relationships between terminal voltage, voltage output v_f of the exciter, and possibly supplementary variables such as shaft speed, acceleration, electric power, etc. If implicit integration is applied to these differential equations (linear or linearized over one

time step), then linear algebraic relationships among these quantities are obtained. With a typical time constant of 30 ms for a fast excitation system with rectifiers, it should be permissible to calculate the excitation system output at time t from the known input values at time t-Δt, and $v_f(t)$ would then again be known in the solution of the generator equations. This approach was used successfully for practical cases [49]. Standard IEEE excitation system models define the terminal voltage as an RMS-value. Therefore, the problem arises in transient studies how to define RMS-values from instantaneous values under transient conditions. This could, for example, be done by including a model for the transient behaviour of the transducer. This issue may require further research.

(c) If the time delay of one time step introduced in method (b) above is unacceptable, then it becomes necessary to retain the field winding in the equivalent circuit, which leads to a four-phase equivalent circuit of the generator. The fourth equation must then be interfaced with the equations which describes the excitation system dynamics. This will not affect the interface procedures described in this thesis (for details see Appendix 5).

Equation (79) can now be rewritten as follows:

$$\underline{v}_s(t) = [R_{ss}^{red}]\underline{i}_s(t) + \underline{e}_s^{red}(t-\Delta t) \tag{80}$$

with

$$[R_{ss}^{red}] = \begin{bmatrix} a_{11} & a_{12} & 0 \\ a_{21} & a_{22} & 0 \\ 0 & 0 & a_{33} \end{bmatrix} \tag{81}$$

where all nonzero elements are constant if Δt and ω are constant (for details see Appendix 5), and where $\underline{e}_s^{red}(t-\Delta t)$ is known at time t from known past history at $t-\Delta t$ and $v_f(t)$.

Equation (80), after transformation to phase-coordinates, describes the three-phase equivalent circuit of the generator in those coordinates. The resulting resistive companion matrix $[R_{ph}^{comp}]$ is time dependent:

$$[R_{ph}^{comp}] = \begin{bmatrix} b_{11}(t) & b_{12}(t) & b_{13}(t) \\ b_{21}(t) & b_{22}(t) & b_{33}(t) \\ b_{31}(t) & b_{32}(t) & b_{33}(t) \end{bmatrix} \qquad (82)$$

Calculation of the matrix $[R_{ss}^{red}]$ according to (79) is numerically very inefficient and is better done in practice with a Gauss-Jordan elimination scheme [50], as briefly explained in Appendix 6.

4. INTERFACING THE GENERATOR MODELS WITH THE TRANSIENTS PROGRAM

4.1 Problem Formulation

The generators and the network to which they are connected, can in principle be solved as one system of equations. However, it is then not easy to write general-purpose computer programs which can handle any network configuration [51]. It is, therefore, necessary to devise interfacing procedures which preserve the generality of the network representation in the Transients Program.

When electric networks are connected together, then certain boundary conditions must be satisfied for voltages and currents at the connection points. The situation for two three-phase networks is shown in Fig. 14. The conditions, which must be satisfied at any time t, are based upon Kirchhoff's laws, in this case:

$$v_1 = v_6, \quad v_2 = v_5, \quad v_3 = v_4 \qquad \text{and}$$

$$i_1 + i_4 = 0, \quad i_2 + i_5 = 0, \quad i_3 + i_6 = 0.$$

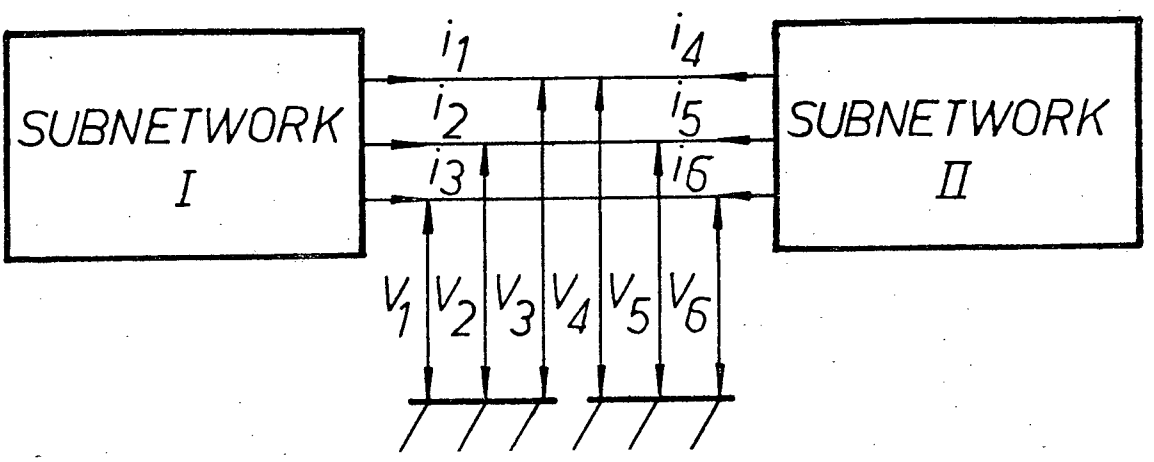

Fig. 14. Schematic representation of two connected networks.

These conditions must also be satisfied when two computer programs are interfaced, when each of them describes the behaviour of one subnetwork only. Subnetwork I could be the generator, and subnetwork II the transmission system in a particular case. The generator is connected to the transmission network through three pairs of terminals, i.e., all the other pairs of terminals of the transmission system are, from the generator's point of view, concealed. Similarly, looking from the transmission system into the generator, only the three stator pairs of generator terminals are visible, and the rotor windings are concealed. There are, therefore, two possible ways of interfacing a generator program with a network transients program. The first one is based upon the calculation of a three-phase Thevenin equivalent circuit of the transmission network, as seen from the generator's stator terminals, and solving it together with the full set of generator equations or with the reduced set of generator equations, in which only stator terminals are retained. The final solution in the transmission network is obtained by superimposing the voltage changes which results from the generator currents on the solution obtained without generator currents [2]. The second approach is based upon the development of a three-phase Thevenin equivalent circuit for the generator in the form of a voltage source behind a time-invariant, symmetrical matrix $[R_{ph}^{red}]$. The complete solution is then obtained by solving the transmission network with the generator treated as voltage sources behind $[R_{ph}^{red}]$ in one step. This approach results in a significantly simpler interface code.

4.2 Method I - Interface by Means of a Thevenin Equivalent Circuit of the Transmission Network

The Transients Program was modified to produce a three-phase Thevenin equivalent circuit of the transmission network seen from the generator terminals (in its original form it could only produce single-phase equivalent circuits). The equivalent circuit can be described by the following equation:

$$\underline{v}_N(t) = [R_N^{terminal}]\underline{i}_N(t) + \underline{v}_{NO}(t) \qquad (83)$$

where the subscript "N" denotes network quantities, and the subscript "O" denotes open-circuit quantities.

The 3 x 3 matrix $[R_N^{terminal}]$ is precomputed before entering the time step loop, and must only be recomputed when the network configuration changes due to switching actions or when the program moves into a new segment in the piecewise linear representation of nonlinear elements [45]. A practical way of calculating this matrix, as done in the Transients Program, is briefly described in Appendix 6. The voltage vector $\underline{v}_{NO}(t)$ contains the three-phase voltages of the Transients Program solution without the generator.

The generator is represented by its three-phase equivalent circuit:

$$\underline{v}_{ph}(t) = [R_{ph}^{comp}]\underline{i}_{ph}(t) + \underline{e}_{ph}(t-\Delta t) \qquad (84)$$

where the subscript "ph" denotes generator quantities in phase coordinates, and where

$$\underline{v}_{ph}(t) = \underline{v}_N(t) \quad \text{and} \quad \underline{i}_{ph}(t) = -\underline{i}_N(t) \qquad (85)$$

With (85), equations (83) and (84) can be solved for the unknown voltages

and currents. After subtracting (84) from (83), the following relationship is obtained:

$$\underline{i}_N(t) = [[R_N^{terminal}] + [R_{ph}^{comp}]]^{-1}(\underline{v}_{NO}(t) - \underline{e}_{ph}(t-\Delta t)) \qquad (86)$$

The final network solution is found by superimposing the voltage changes

$$\underline{\Delta v}(t) = [R_N^{network}] \cdot \underline{i}_N(t) \qquad (87)$$

on the previous solution without the generator. $\underline{\Delta v}(t)$ is the vector of all voltages on nodes without voltage sources in the transmission network, and $[R_N^{network}]$ is a precomputed n x 3 matrix from which $[R_N^{terminal}]$ was extracted for (84).

The final solution of the generator is found by solving for the concealed variables which were eliminated in reducing the equations to a three-phase Thevenin equivalent circuit. After transformation of the stator currents to d,q,0-coordinates, the rotor currents are found as follows:

$$\underline{i}_r(t) = -[R_{rr}]^{-1}[R_{rs}]\underline{i}_s(t) - [R_{rr}]^{-1}(\underline{v}_r(t) + \underline{e}_r(t-\Delta t) \qquad (88)$$

where the matrices $[R_{rr}]^{-1}$ and $[R_{rr}]^{-1}[R_{rs}]$ were found as by-products of the reduction process, as explained in Appendix 6.

A flow chart for this solution algorithm, with the mechanical part of the turbine-generator included, is shown in Fig. 15.

The prediction part of the solution algorithm is only needed if the mechanical part is included for modelling the relative rotor oscillations around synchronous speed. Since the interfacing is done in phase coordinates, it is necessary to know both the angular position θ and the speed ω_m of the rotor at the new time step in order to calculate the matrix $[R_{ph}^{comp}]$ and the vector $\underline{e}_{ph}(t-\Delta t)$. A similar situation exists

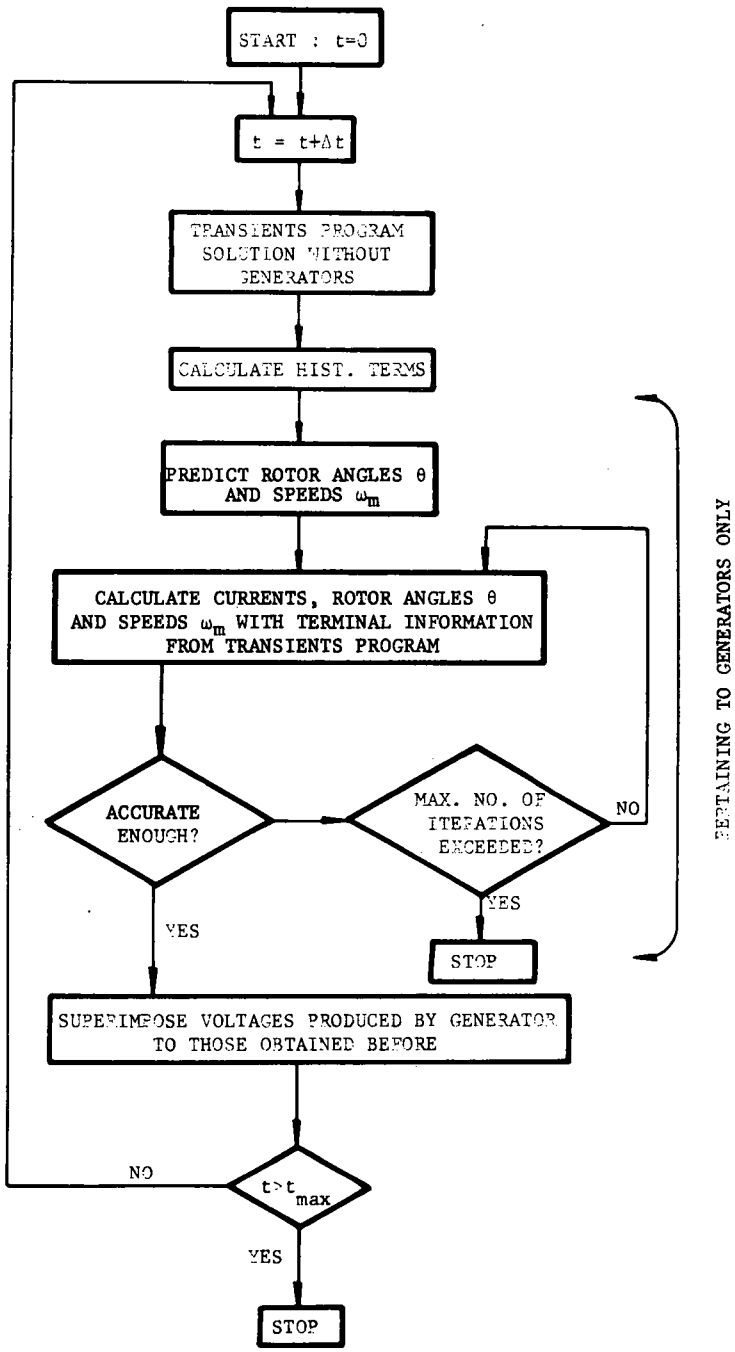

Fig. 15. Flow chart of solution with method I.

when the interfacing is done in d,q,0-coordinates. It is then necessary to know θ and ω_m in order to calculate the matrix $[R_p^{comp}]$ and the three-phase Thevenin equivalent circuit of the transmission system in Park's coordinates. After the generator currents have been calculated, it is possible to calculate the electromagnetic torque $T_{e\ell}$. With this value, the equations of the mechanical part can be solved to get updated value of the speed ω_m. If these values differ too much from the predicted values, then the solution is repeated until the differences are negligible. This solution algorithm performed satisfactorily [4]. Corrections are not much of a problem in this solution algorithm, anyhow.

4.3 Limitations of Method I

The solution method described in chapter 4.2 is quite straightforward and numerically stable if only one generator is connected to the transmission network. If there are more generators connected to the network, as is usually the case, then the method works without further modifications only if the generators are separated through distributed-parameter lines, i.e., if three-phase equivalent circuits of the network exist independently for each generator because distributed-parameter lines disconnect the network [2], [44]. The Transients Program checks this condition automatically when it calculates three-phase equivalent circuits at generator terminals. The program could be changed to calculate 6-phase equivalent circuits if two generators are connected to the network without separation through distributed-parameter lines, or 9-phase equivalent circuits for three generators, etc. For the general case of m generators, however, the programming would become too complicated and the execution time would probably become too big.

A number of alternative methods are possible to overcome this limitation. The generators could be separated by short distributed-parameter transmission lines. This may, however, require a significant reduction of the stepsize Δt in order to keep the length of such artificial lines short, since Δt must be less than the travel time [48]. A slightly different approach has been used successfully by Southern California Edison Company, whereby transformer leakage inductances of step-up transformers are approximated as stub-lines [44]. If a group of generators not separated by transmission lines feeds into the same busbar, then the possibility exists of creating one equivalent circuit for this group of generators, which would be relatively easy. This method can be extended to groups of generators which feed through unit transformers into the same busbar. In this case, the generator equation would have to be expanded to include the transformer equations as well.

The limitations mentioned above do not significantly degrade the practical value of method I. They simply imply that certain precautions are needed when special cases are simulated.

4.4 Method II - Interface with a Modified Thevenin Equivalent Circuit of the Generator

It is common practice in the power industry to represent generators by sinusoidal voltage sources of the form $E''_{max}\cos(\omega t+\rho)$ behind subtransient impedances $R_a + j\omega L''_d$ in quasi-steady-state fault studies and in some types of transient studies. In the derivation of this model it is assumed that flux changes in the rotor windings immediately after the distrubance can be ignored, and that subtransient saliency can also be ignored. This simple model is quite adequate for the first cycle or so

after the disturbance which initiates the transient phenomena. Good results have been obtained with this model in switching surge studies, transient recovery voltage studies, and other types of studies involving fast transients. The relatively accurate results obtained with this simple model motivated the research effort described in this chapter. The idea was to find a way to account for the changes in fluxes and to include the subtransient saliency without losing the simplicity of the model.

Before proceeding with the discussion, it may be useful to recall some of the results of section 3.5 where the retained stator variables of the generator were described in d,q,0-coordinates by the equation

$$\underline{v}_s(t) = [R_{ss}^{red}]\underline{i}_s(t) + \underline{e}_s^{red}(t-\Delta t) \tag{89}$$

and where the matrix $[R_{ss}^{red}]$ was given as follows:

$$[R_{ss}^{red}] = \begin{bmatrix} a_{11} & a_{12} & 0 \\ a_{21} & a_{22} & 0 \\ 0 & 0 & a_{33} \end{bmatrix} \tag{90}$$

As mentioned in section 3.5, the matrix $[R_{ss}^{red}]$ becomes time-dependent when it is transformed directly to phase-coordinates. While nodal network solutions, such as in [34], can in principle be modified to accept time-dependent resistances, program execution would be slowed down significantly if the network conductance matrix had to be retriangularized in each time step. Also, the conductance matrix becomes asymmetric in this case, which means that the upper as well as the lower triangular matrices would have to be stored. This would increase storage requirements as well as computation time compared with the present

method based upon symmetry where only the upper triangular matrix is stored.

A number of ways were tried out to approximate (89) in such a way that the resistance matrix becomes constant and symmetric in phase coordinates. The following scheme seemed to work best:

(1) Split the matrix $[R_{ss}^{red}]$ into the sum of two terms,

$$[R_{ss}^{red}] = [R_{const}^{red}] + [R_{var}^{red}] \tag{91}$$

where the matrix $[R_{const}^{red}]$ is given as:

$$[R_{const}^{red}] = \begin{bmatrix} \frac{a_{11}+a_{22}}{2} & 0 & 0 \\ 0 & \frac{a_{11}+a_{22}}{2} & 0 \\ 0 & 0 & a_{33} \end{bmatrix} \tag{92}$$

with coefficients a_{ik} as defined in Appendix 5.

(2) Transform the matrix $[R_{const}^{red}]$ to phase coordinates. The result is a constant symmetric matrix $[R_{ph}^{red}]$ of the following form:

$$[R_{ph}^{red}] = \begin{bmatrix} a & b & b \\ b & a & b \\ b & b & a \end{bmatrix} \tag{93}$$

The elements of the matrix $[R_{var}^{red}]$ are normally much smaller than those of $[R_{const}^{red}]$, and their influence in (89) can be accounted for by multiplying them with the predicted values of stator currents rather than with actual, yet unknown, values and adding these terms to the voltage sources. Therefore, the following relationship in d,q,0-coordinates is obtained:

$$\underline{v}_s(t) = [R_{const}^{red}]\underline{i}_s(t) + \{\underline{e}_s^{red}(t-\Delta t) + [R_{var}^{red}]\underline{i}_s^{pred}(t)\} \tag{94}$$

where $\underline{i}_s^{pred}(t)$ is the vector of the predicted d,q,0-stator currents at time t.

Transformation of (94) to phase-coordinates yields the desired Thevenin equivalent circuit of the generator:

$$\underline{v}_{ph}(t) = [R_{ph}^{red}]\underline{i}(t) + \underline{e}_{ph}^{red}(t-\Delta t) \qquad (95)$$

Since the matrix $[R_{ph}^{red}]$ is symmetric and time-independent, the generator can be represented in the Transients Program simply as a set of voltage sources $\underline{e}_{ph}^{red}(t-\Delta t)$ behind resistances $[R_{ph}^{red}]$. The inverse of $[R_{ph}^{red}]$ enters into the nodal conductance matrix of the transmission network as any other resistive branch, as described in [48].

After the network solution has been found in the new time step at time t, the stator quantities will be known, and the rotor currents can then be found from (88). Therefore, the solution of the transmission network together with the generators proceeds at each time step as follows:

(1) Solve the network equations together with the Thevenin equivalent circuits of the generators reduced to the stator windings as given by (95);

(2) Solve equation (88) of rotor windings, using the stator currents found in the previous step.

There is a need to predict the angular position θ and the speed ω_m of the rotor, just as in method I. The problem of iterative corrections is, more complex in this case, however, since iterations with the complete network solution would be quite costly. Fortunately, it has already been shown that the angular position θ can be predicted accurately enough without need for corrections [4], [32]. A reasonably accurate prediction for the angular speed ω_m can probably be obtained from the

integration of the mechanical equations, with linear extrapolation of the electrical torque because of the relatively small stepsize Δt used in integration of the electric part in comparison with the relatively big time constants of the mechanical part. Furthermore, the terms containing the angular speed ω_m are only a small part of $\underline{e}_{ph}^{red}(t-\Delta t)$ in (95). It is, therefore, reasonable to expect that ω_m can be predicted with sufficient accuracy. It is also possible to introduce some sort of iteration loop to improve the solution such as the one shown in Fig. 16.

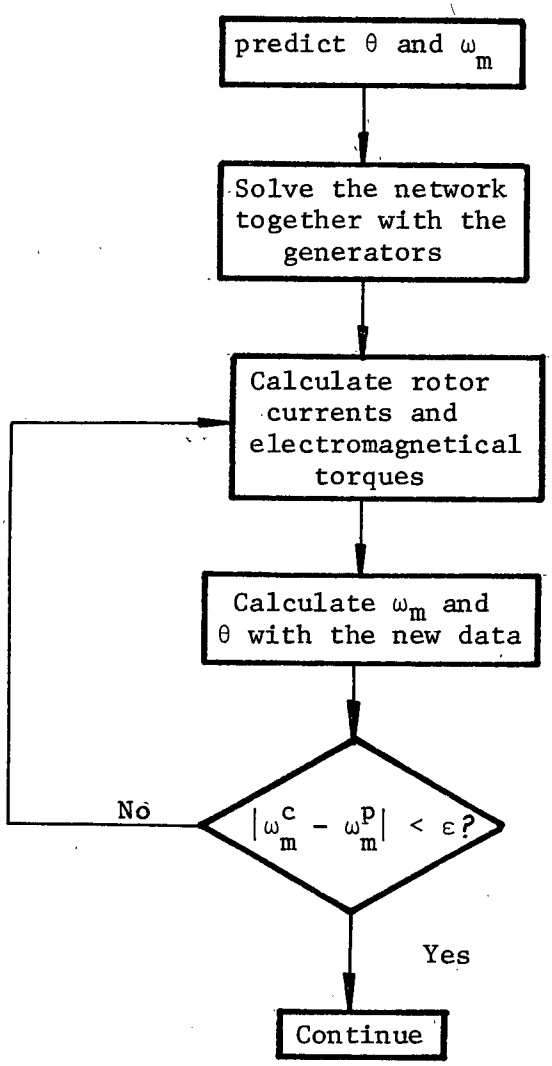

Fig. 16. Flow chart of the iteration scheme.

No serious problems are expected. Experience gained by the General Electric Company seems to prove this statement [3]. A computer program developed by this company and the results obtained with it seem to indicate that no significant errors are introduced when using the predicted values of the angular speed ω_m.

4.5 Remarks about Method II

As already mentioned, the elements of the resistance matrix $[R^{red}_{var}]$ are normally much smaller than the elements of the matrix $[R^{red}_{const}]$. This is true of typical generators where subtransient saliency is very small. If X''_d differs significantly from X''_q, the elements of the matrix $[R^{red}_{var}]$ may become large. This would increase the relative weight of the inaccuracies resulting from the prediction of the stator currents, which in turn could result in inaccurate solutions. Although such a case seems to be highly improbable for any practical generator equipped with damper windings, it should, nevertheless, be mentioned as a possible problem.

Experience has shown that for stepsizes Δt in the order of 10^{-4}s, method II works remarkably well. It does not suffer from the limitations typical of method I, since the generators are simply modelled as voltage sources behind resistances. In the network solution it is possible, therefore, to have any number of generators connected to the network, either at the same busbar or at different busbars, without loss of generality.

The prediction of the d,q,0-stator currents $\underline{i}^{pred}_s(t)$ does influence the accuracy, of course, and can be performed in a number of ways:

(1) Assume that the voltages at the generator terminals are constant over the next time step, and use the new currents found

from (89) as predicted values.

(2) Use straight-line extrapolation of the currents. Information for two preceding time steps at $t-2\Delta t$ and $t-\Delta t$ must then be stored.

(3) Use parabolic extrapolation of the currents. Information for three preceding time steps must then be stored.

(4) Use any combination of the three previous methods, e.g., straight-line extrapolation of the voltages combined with approach 1.

In all the tests conducted for this thesis, there were no visible differences between the results obtained with different prediction methods as long as some type of prediction of the stator currents was used. Simply setting $\underline{i}_s^{pred}(t) = \underline{0}$ is too inaccurate. Fig. 17 compares the field current from the example of section 2.3, calculated in three different ways:

(a) The predicted currents are obtained by assuming that the voltages at the generator terminals are constant over the next time step, with stepsize $\Delta t = 100$ μs.

(b) The currents from the previous time step are used as predicted values, i.e., $\underline{i}_s^{pred}(t) = \underline{i}_s(t-\Delta t)$, ($\Delta t = 100$ μs).

(c) The influence of the term $[R_{var}^{red}]\underline{i}_s(t)$ is neglected, i.e., $\underline{i}_s^{pred}(t) = \underline{0}$, ($\Delta t = 100$ μs). This amounts to neglecting the subtransient saliency and speed terms in the generator model.

The differences are larger for the stator currents, as shown in Fig. 18 for one of the unfaulted phases (phase a).

Using current values from the previous time step $t-\Delta t$ can only be justified for a small stepsize Δt. With increasing Δt, the error introduced by this simple prediction may become intolerable, and possibly lead to numerical instability.

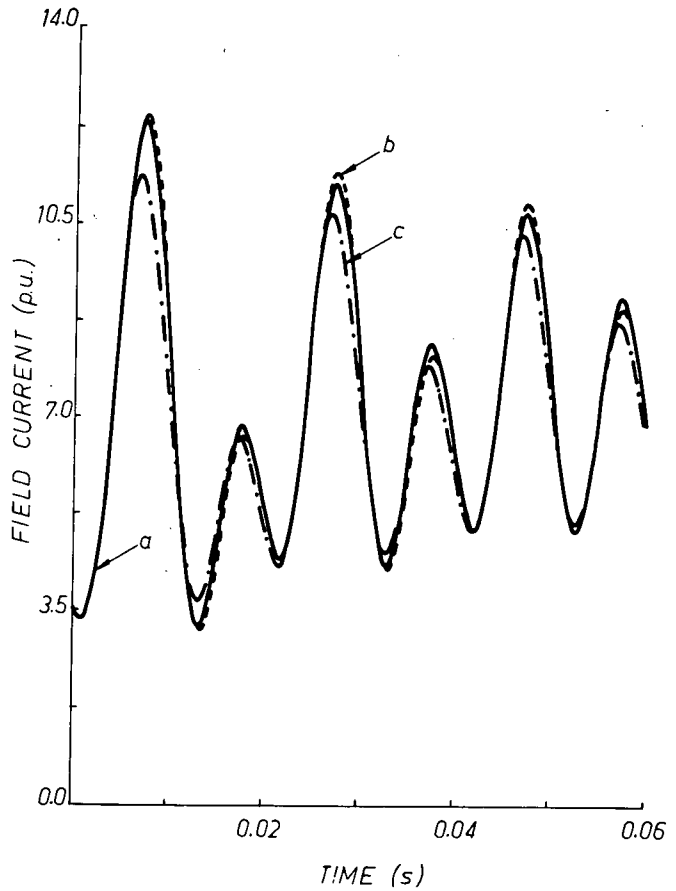

Fig. 17. Comparison of field current with various prediction techniques.

The low sensitivity to the accuracy of prediction of the stator currents may serve as an indication of the behaviour of the solution for inaccurately predicted angular speed ω_m. It is possible to interpret the error in prediction of ω_m as an additional error in the predicted stator currents. It is, therefore, believed that no serious problems will arise with the introduction of the mechanical part of the generator.

The elements of the matrix $[R_{ph}^{red}]$ can be precalculated before entering the time step loop. Simple matrix multiplication (transformation from one coordinate system to another) and basic algebra show that:

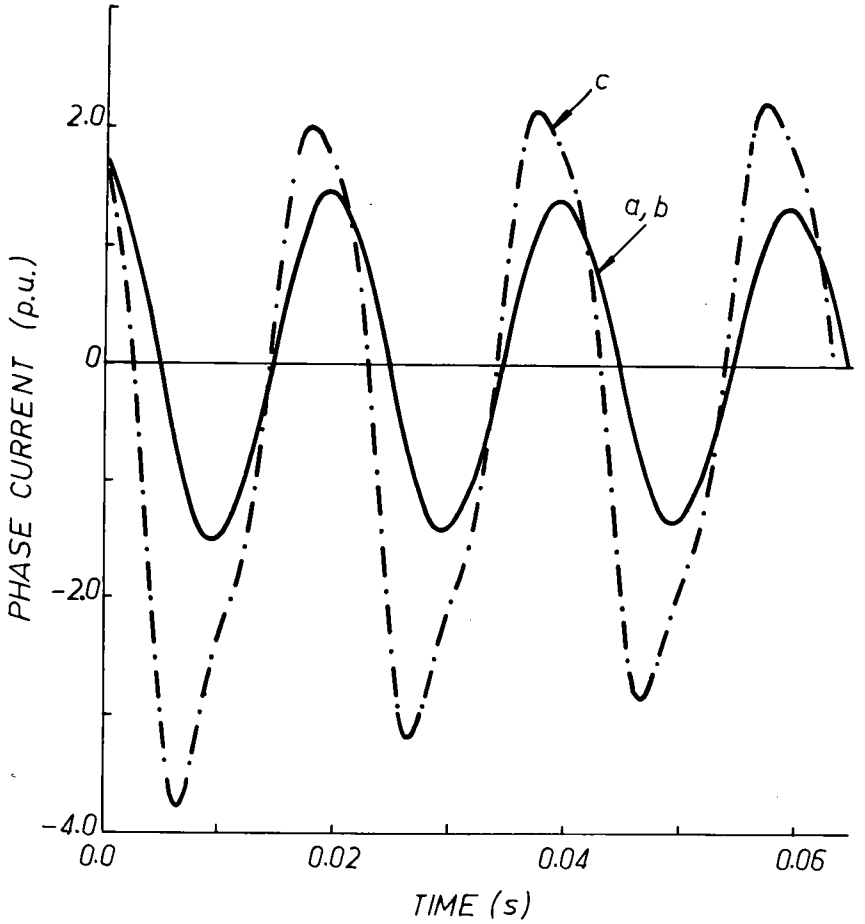

Fig. 18. Comparison of stator current in phase "a" with various prediction techniques.

$$a = \frac{a_{11} + a_{22} + a_{33}}{3} \tag{96}$$

and

$$b = \frac{2a_{33} - a_{11} - a_{22}}{6} \tag{97}$$

where a and b are elements of the matrix $[R_{ph}^{const}]$ defined in (93). These elements remain constant as long as the stepsize Δt does not change and as long as nonlinear saturation effects are ignored.

It is worth mentioning that neither method I nor method II are tied to the trapezoidal rule of integration. The ability to create

resistive companion network models, and to develop reduced three-phase equivalent circuits from them, is a general property of any implicit integration scheme, as shown in Appendix 4. The trapezoidal rule of integration, however, makes the numerical procedure simple. This fact, and the stability properties of this particular integration as discussed in section 3.1 fully justify its use.

4.6 Numerical Examples

It is very easy to set up hypothetical generator and network cases for testing the simulation methods of this thesis. While this is satisfactory for comparing various approaches, it does not answer the question of how closely such simulations agree with field tests. Every effort was, therefore, made to duplicate published field test results, even though not too many such cases could be found. In this connection, it should be remembered that the generator model alone does basically not need verification, since this was already done by others [4], [11-14]. The test examples are, therefore, mainly used to verify the various numerical procedures and interfacing techniques. This was done in stages:

(1) Preliminary Tests

In the preliminary testing of the methods, the interface with the general-purpose Transients Program was replaced by a simple three-phase Thevenin equivalent circuit (voltage source behind external resistance and inductance). This simplification made it easier to test the simulation techniques before interfacing the generator subroutine with the large Transients Program. The program performance was checked for a number of examples. A simulation program using a fourth-order Runge-Kutta integration routine was also run in parallel as a check on the

solution with the trapezoidal rule. Some of these results were already presented in section 3.1 (Fig. 7 and Fig. 8).

(2) Example 1 for Testing Method I

The results of the preliminary tests were compared with the results obtained with method I. This provided a check on both the calculation of the three-phase Thevenin equivalent of the transmission network and on method I itself. Only one example will be shown, since there were no visible differences. The generator described in section 2.3 was used with a line-to-ground fault applied to one of its terminals. The system was simulated as shown in Fig. 19. The network parameters were R_e = 1.0 p.u., $R_{e1} + R_{e2} = R_e$, and R_{e1} = 0.01 p.u. The voltage of the infinite busbar was $2.0\angle 0°$ p.u., and the initial conditions of the generator were $1.734\angle -5.2°$ p.u. stator current and 3.56 p.u. field current. Both the stator currents and the rotor currents were identical for the two different solutions (without and with the calculation of the Thevenin equivalent circuit). The stator current in the unfaulted phase "b" is shown in Fig. 20.

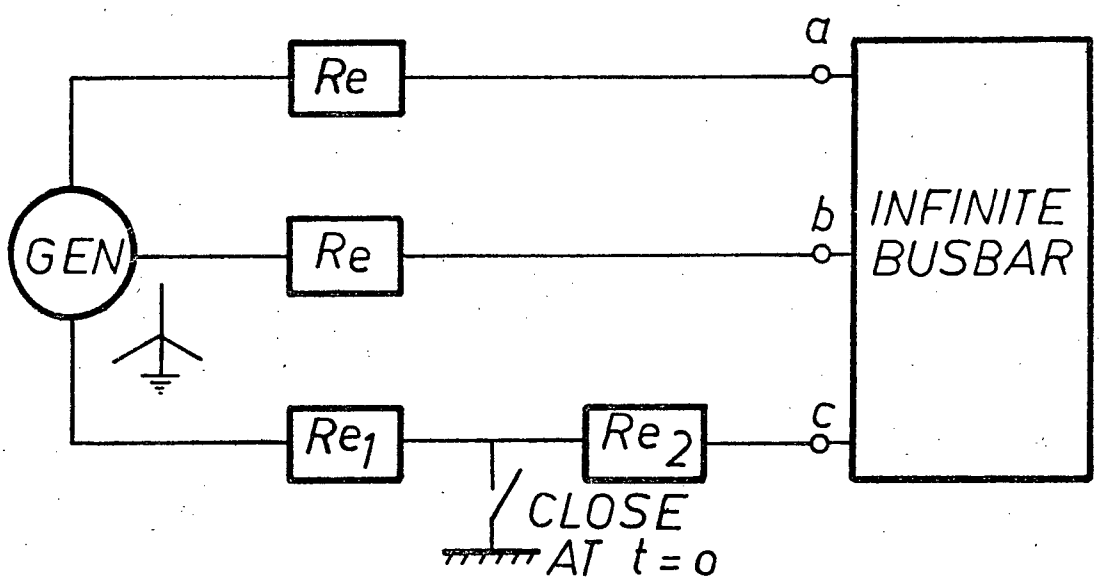

Fig. 19. Line-to-ground fault at generator terminal.

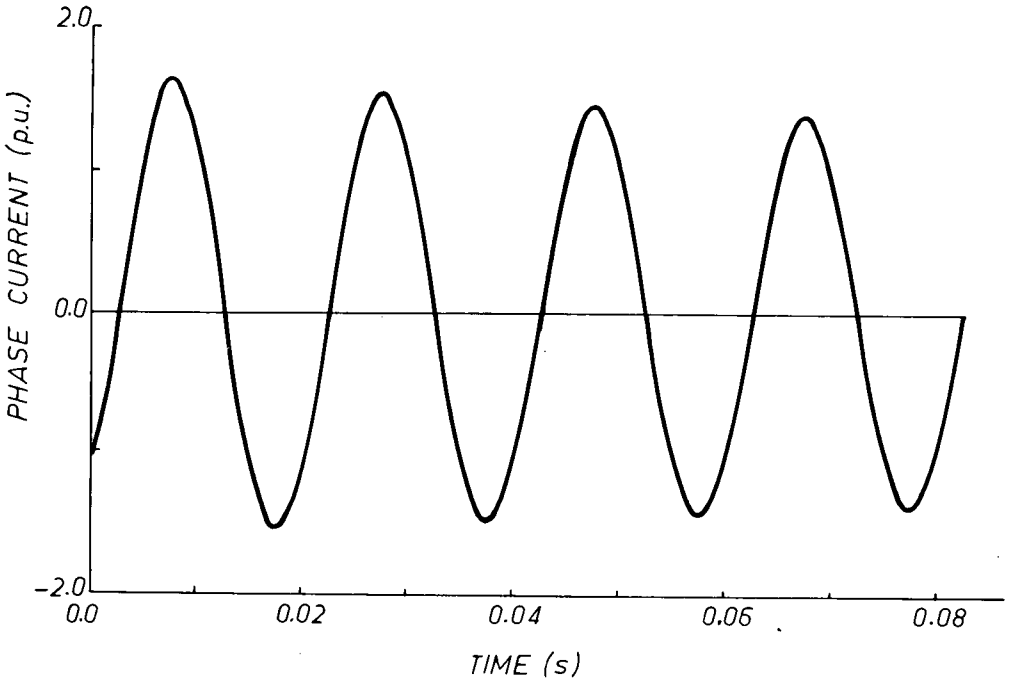

Fig. 20. Simulated current I_b in the unfaulted phase "b".

The simulated field current was already shown in Fig. 2 and the fault current I_c was already shown in Fig. 3.

(3) Example 2 for Method I

This is a test case with an external network for which field test results were available, and which could no longer be solved with the program used for the preliminary tests. The generator had the following data (based on 150 MVA and 13.8 kV, RMS, line-to-line) [53]:

X_d = 1.85 p.u. X_q = 1.76 p.u.

X_d' = 0.2575 p.u. X_q'' = 0.29 p.u. (assumed according to [53])

X_d'' = 0.18 p.u. T_q'' = 0.04 s (assumed according to [53])

X_ℓ = 0.175 p.u. X_o = 0.198 p.u.

T_d' = 0.85 s (no g-winding)

T_d'' = 0.385 s

The data conversion to [R] and [L_p] was done with the formulas published in [11]. The generator was connected to a transmission system, as shown in Fig. 21.

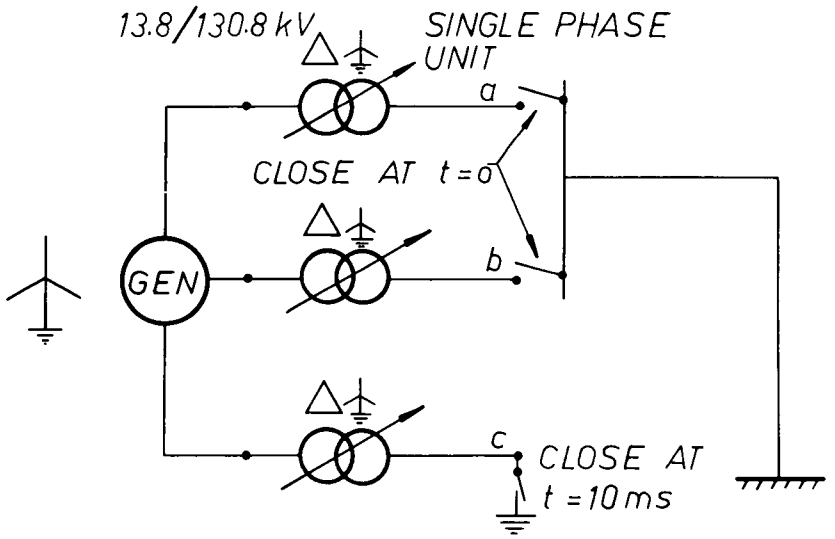

Fig. 21. System diagram.

The system was initially unloaded and the voltage at its terminals was 13.8 kV $\angle -10°$ kV (RMS, line-to-line). A three-phase fault on the high side of the delta/wye connected step-up transformer was studied, with the closing sequence as shown in Fig. 21. The simulated stator currents are compared with the field test results, as given in [54], in Fig. 22. The field current was unavailable for comparison.

The differences in the initial values of the currents result from uncertainty in the generator data, e.g., the values for X_q'' and T_q'' were assumed rather than measured and may be unrealistic, and lack of sufficient information about the initial conditions, e.g., about the instant at which the fault was applied. Because of the latter reason, the initial conditions had to be varied until the results came reasonably

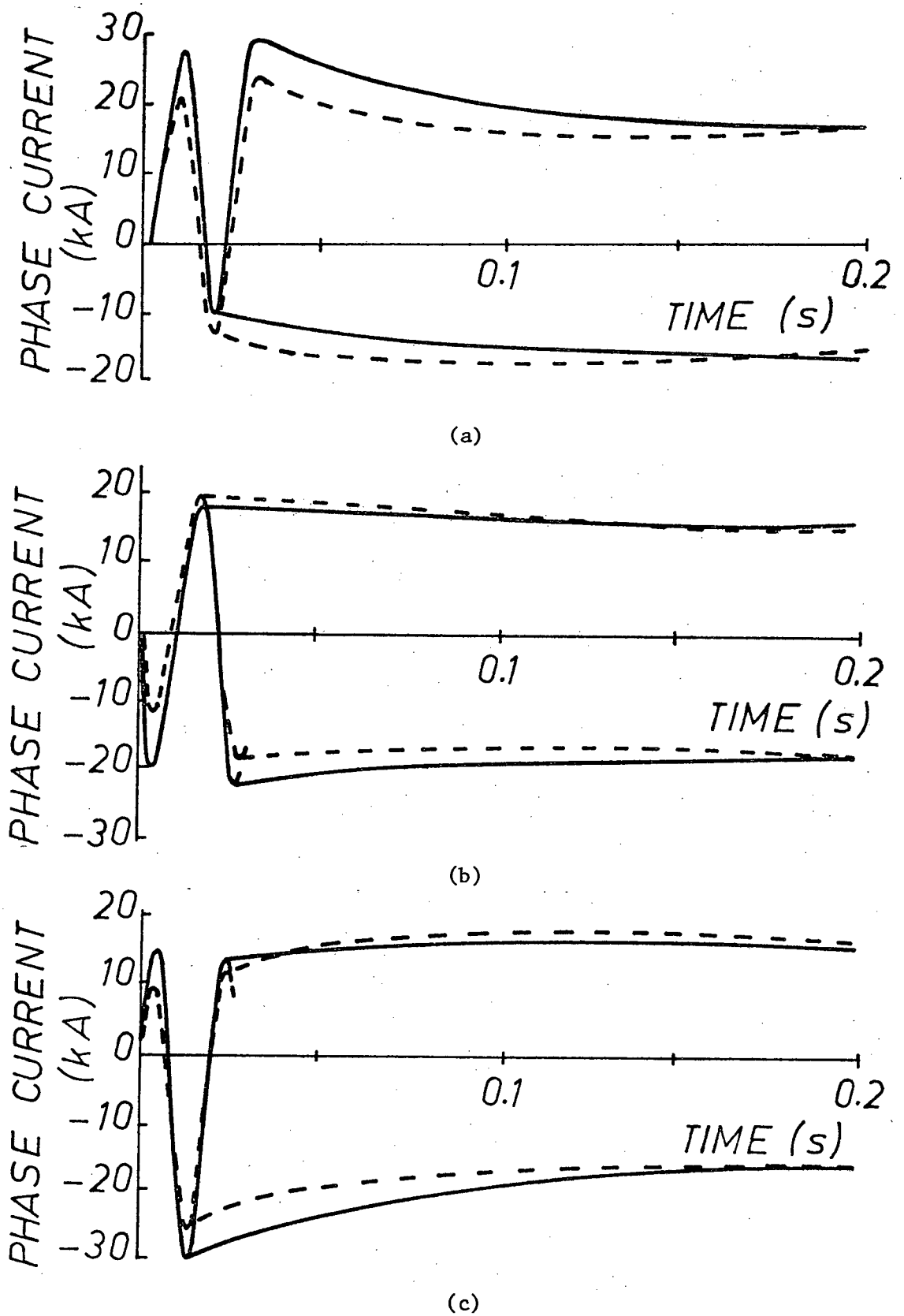

Fig. 22. Comparison of stator currents between simulation and field test for a three-phase fault. (a) = phase "a", (b) = phase "b", (c) = phase "c", — field test, -- simulation.

close to those of the field tests. It should also be remembered that saturation effects were ignored. In view of all these limitations the agreement is reasonably good.

(4) Example 3 for Testing Method I

It was found by a number of researchers that the correct reproduction of stator currents is not much of a problem [13], [14]. It is often difficult, however, to reproduce rotor quantities correctly. To illustrate the accuracy of the simulation of the field current, an attempt was made to duplicate a field test [54]. In this test, the generator described in example 2 was connected to a system as shown in Fig. 23, and a three-phase fault was applied to the high side of the step-up transformer. The network was simulated as coupled inductances with the following parameters given in [54]:

zero sequence inductance $L_0 = 0.22$ H,

positive sequence inductance $L_1 = 0.096$ H.

The initial voltage at the generator terminals was $13.8\angle -30°$ kV (RMS, line-to-line), and the initial field current was 620 A. The switching sequence was as follows [54]:

Phase "b" at t = 0 s, phase "c" at t = 6 ms, and phase "a" at t = 20 ms.

The simulated field current is compared with the measured field current in Fig. 24. (a - field test, b--- simulation)

Examples 2 and 3 verify that the generator model as well as the numerical approach of method I give reasonably accurate results. It is, therefore, possible to proceed to a comparison of method II with method I.

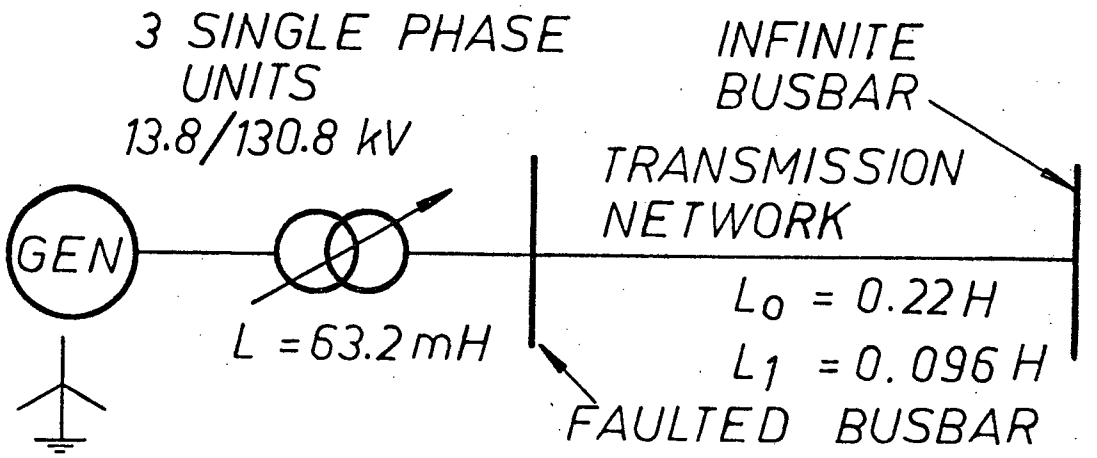

Fig. 23. System diagram.

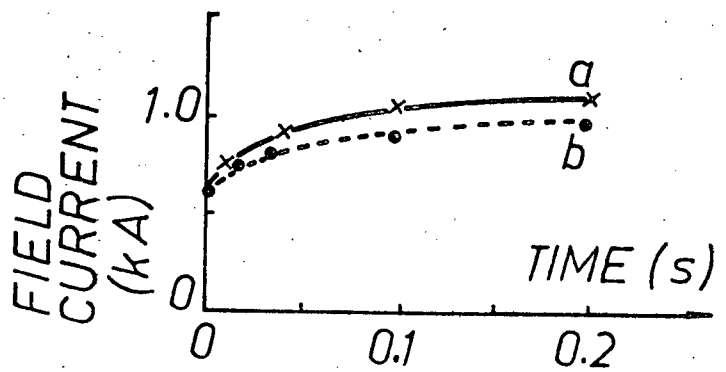

Fig. 24. Comparison of the simulated and measured field current.

(5) Example 4 for Testing Method II

In this example, a single line-to-ground fault was studied. The system was simulated as shown in Fig. 23. However, some changes were introduced. The infinite busbar voltage was increased to $137.23\angle -20$ kV (RMS, line-to-line) and the parameter X_q'' was changed from 0.29 p.u. to 0.18 p.u., which is a more realistic value for a generator with damper windings, than the previous one given in [53]. The results were obtained in three different ways:

(a) Simplified generator model (voltage source $E''_{max}\cos(\omega t+\rho)$ behind

an impedance $R_a + j\omega L_d''$);

(b) Detailed generator model interfaced with method I (simultaneous solution);

(c) Detailed generator model interfaced with method II (new technique).

Fig. 25 compares the simulated current in the faulted phase "a", and Fig. 26 compares the simulated field current.

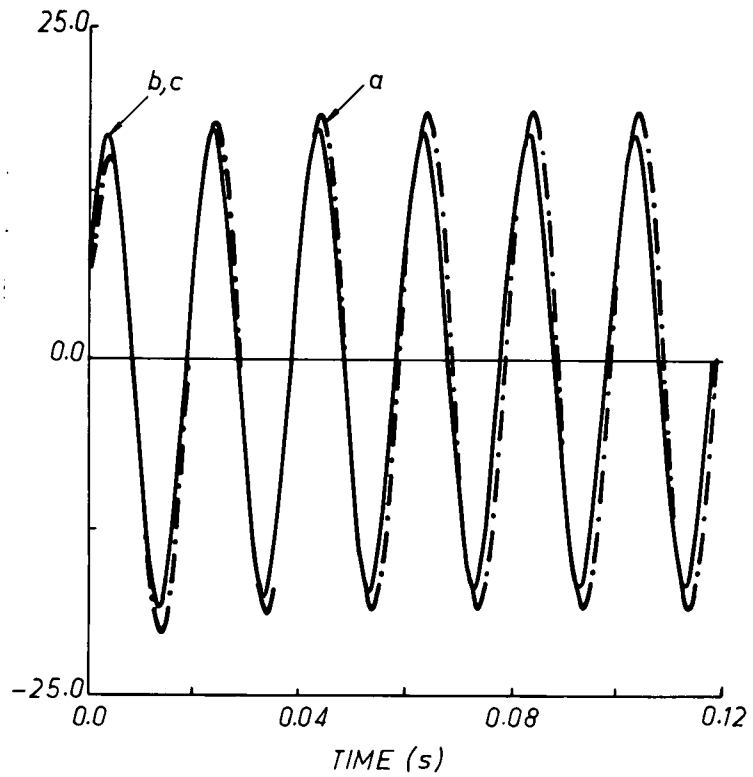

Fig. 25. Comparison of the simulated current in the faulted phase "a".

Figures 25 and 26 imply that the simplified generator model is reasonably accurate for short time studies, but no information can be obtained on

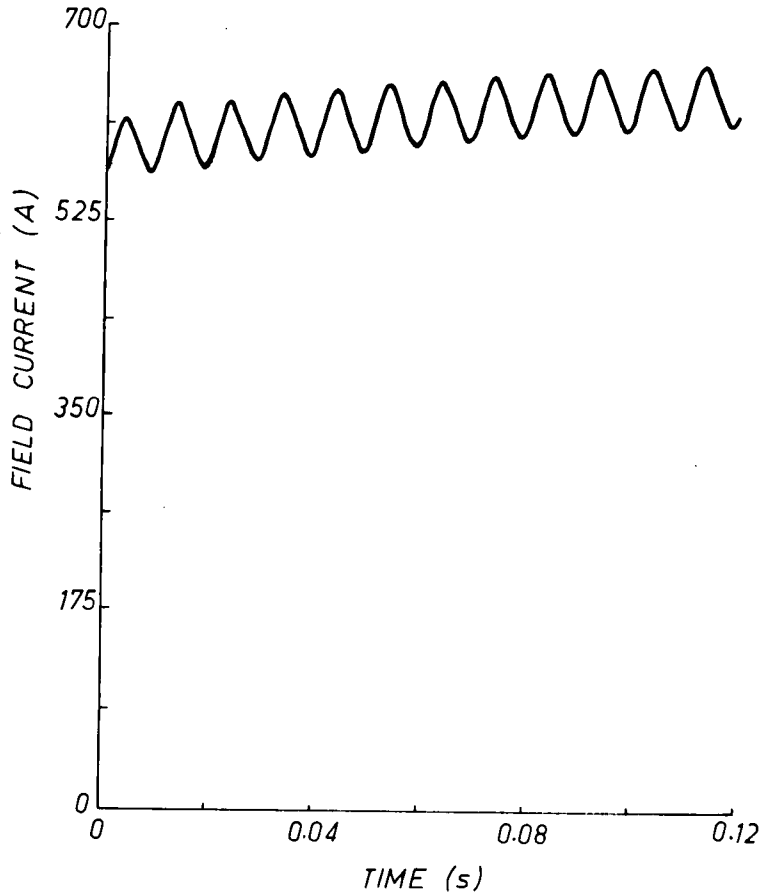

Fig. 26. Identical results for field current.

rotor circuit quantities. The results obtained with method II are indistinguishable from the results obtained with model I.

(6) Example 5 for Testing Method II

This example should provide a more severe test for method II, because it also includes travelling wave effects. The generator from example 4 was connected to a system, as shown in Fig. 27.

The transmission line had the following parameters ("0" = zero sequence, "1" = positive sequence):

R_o = 0.2026 Ω/km , L_o = 2.749 mH/km , C_o = 6.326 μF/km

R_1 = 0.0886 Ω/km , L_1 = 1.005 mH/km , C_1 = 11.408 μF/km

and a length of 96.72 km. The length of the line was chosen in such a way as to match the positive sequence inductance of the transmission network from example 4.

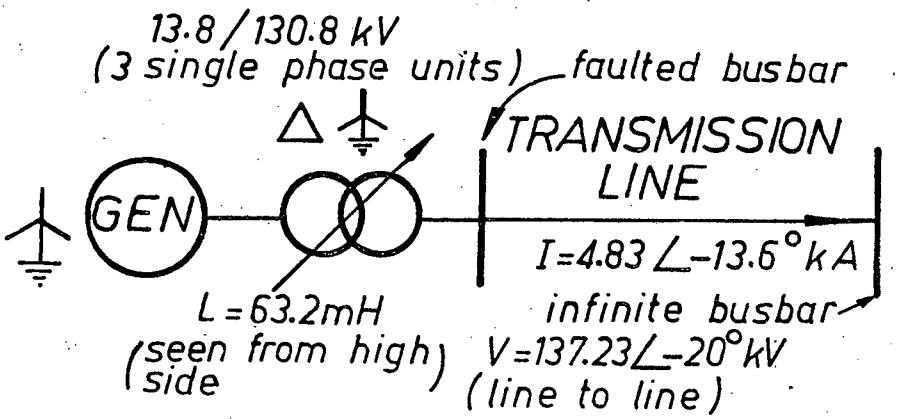

Fig. 27. System diagram.

Once more a single line-to-ground fault on the high side of the step-up transformer was studied. Fig. 28 compares the generator current in the faulted phase "a", calculated in three different ways:

(a) Simplified generator model;

(b) Detailed generator model interfaced with method I (simultaneous solution);

(c) Detailed generator model interfaced with method II (new technique).

Again, the results from methods I and II are practically indistinguishable.

Fig. 28 may lead to the conclusion that the simple generator model is as good as the detailed model. This is only true, however, for

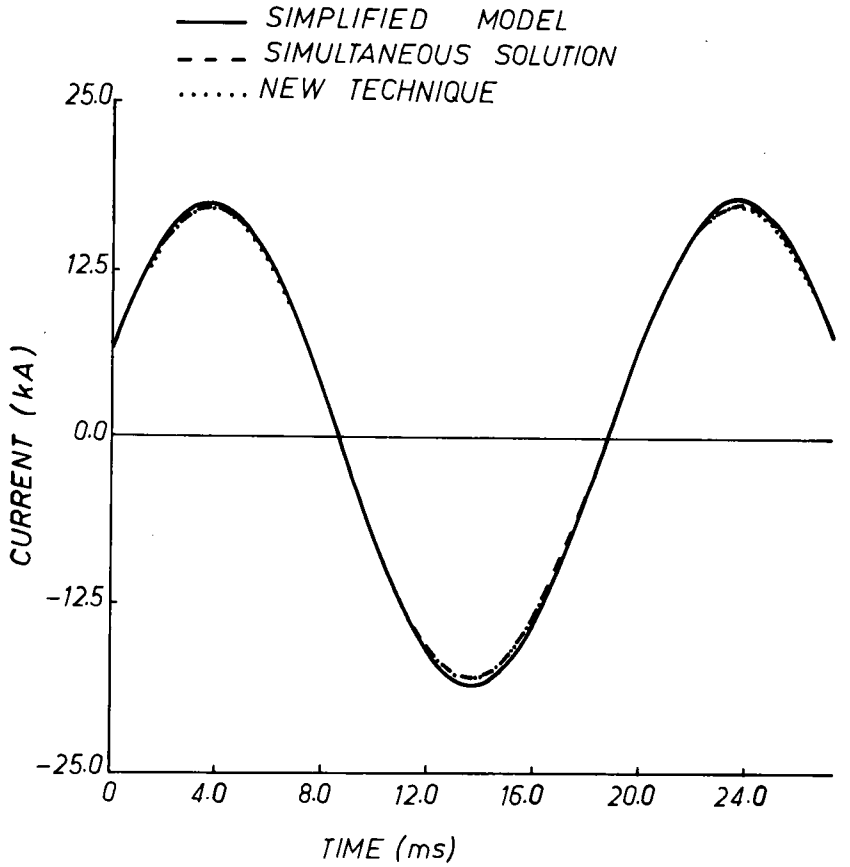

Fig. 28. Comparison of the simulated current for faulted phase "a".

some studies conducted over a very short time span where the flux decay does not play an important role. Fig. 29 compares the three-phase instantaneous power at the generator terminals for the same case and shows that the simple model is much less adequate when power is measured.

Finally, Fig. 30 shows the field current calculated with the two different interface techniques. As for the stator current, methods I and II give again results which are practically identical.

The last two examples prove that the results obtained with method II agree to a high degree with results obtained with method I. This in turn proves the adequacy of method II.

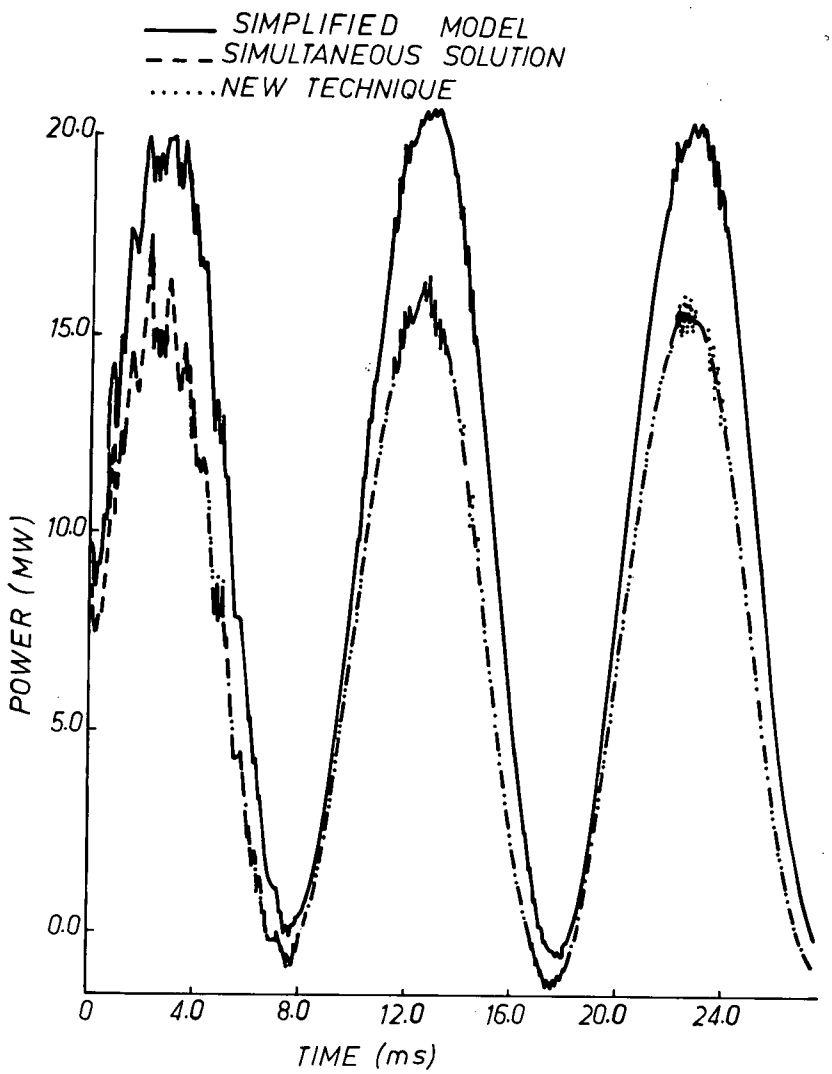

Fig. 29. Comparison of the simulated three-phase instantaneous power.

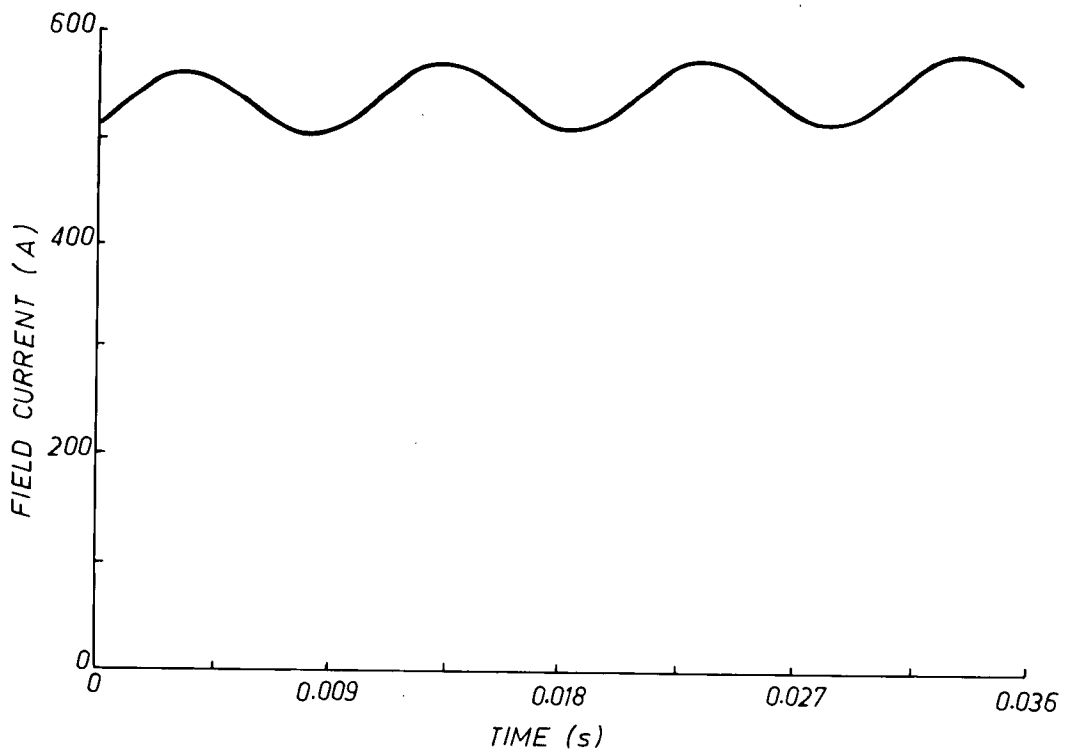

Fig. 30. Identical results for field current.

The set of numerical examples would not be complete without a presentation of a case with a multi-mass mechanical system. A benchmark test case for such a system became available after completion of the thesis. It is, therefore, not included in the main body of the text, but is added as Appendix 8.

5. INITIAL CONDITIONS, DATA SCALING AND SATURATION

5.1 Calculation of the Initial Conditions for a Synchronous Generator

The state of a synchronous generator is fully described by the following variables:

(1) all currents and voltages;

(2) all angular displacements and speeds of the shaft system.

The stator currents and voltages are normally obtained from a phasor solution of the entire system in which the generator is represented as sinusoidal voltage or current sources. This solution usually considers the fundamental frequency only. The rotor circuit variables have to be found from the generator equations, which is straightforward for the case of balanced steady-state operation, but more complicated for the unbalanced case. In the latter case, harmonics exist not only in the rotor circuits but also in the stator circuits [8], [9], which leads to contradictions if the total system was solved at fundamental frequency only. It is common practice, therefore, to assume a balanced steady-state operation for the generator. In this case, the damper currents are zero and the field current is constant. The currents and voltages will vary sinusoidally in phase coordinates, but are constant in d,q,0-coordinates. It is, therefore, easier to use d,q,0-coordinates for the calculation of the initial conditions.

The general voltage equations of the generator were defined in section 2.1 (eq. 21). They are shown again to aid understanding:

$$\underline{v}_p = -[L_p]\frac{d}{dt}\underline{i}_p - [R]\underline{i}_p - [L'_p]\underline{i}_p \qquad (96)$$

For the special case of balanced, steady-state conditions, where $\frac{d}{dt}\underline{i}_p = \underline{0}$,

they can be rewritten as follows:

$$\underline{v}_p = -[R]\underline{i}_p - [L_p']\underline{i}_p \tag{96a}$$

With damper currents and zero sequence voltage and current being zero, (96a) can be reduced to the following set of three voltage equations:

$$v_d = -R_a i_d - \omega L_q i_q \tag{97}$$

$$v_q = -R_a i_q + \omega L_d i_d + \omega\sqrt{\frac{3}{2}}\, M_f i_f \tag{98}$$

and

$$v_f = -R_f i_f \tag{99}$$

The coefficient $\sqrt{\frac{3}{2}}$ in front of M_f in (98) results from the normalized form of Park's transformation matrix [P] as shown in (19). To find the current i_f and the rotor angular position $\beta(0)$ or $\delta(0)$, it is necessary to relate (97-99) in d,q,0-coordinates to the phasor diagram of the machine shown in Fig. 31.

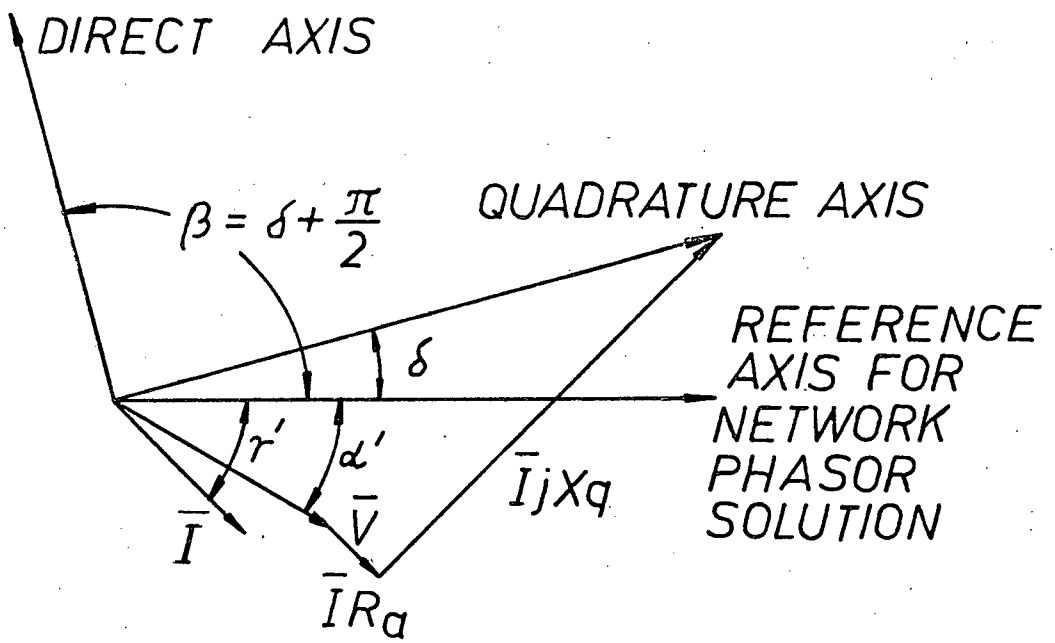

Fig. 31. Phasor diagram of a synchronous generator for balanced, steady-state operation (R_a and X_d, X_q not to scale).

From (97) and (98) it follows that:

$$v_q + jv_d = -R_a(i_q + ji_d) - jX_q(i_q + ji_d) + (X_d - X_q)i_d + e_q \quad (100)$$

where

$$e_q = \omega\sqrt{\frac{3}{2}}\, M_f i_f \quad (101)$$

For a balanced steady-state operation, d,q,0-coordinates are related to phasor values by:

$$i_q + ji_d = \sqrt{3}\cdot\bar{I}\, e^{-j\delta} \quad (102a)$$

and

$$v_q + jv_d = \sqrt{3}\,\bar{V}\, e^{-j\delta} \quad (102b)$$

where $\bar{I}$ and $\bar{V}$ are RMS positive sequence phasors.

From (102a) and (102b) it follows that (100) can be transformed to the reference frame for the network phasor solution,

$$e_q e^{j\delta} + (X_d - X_q)i_d e^{j\delta} = \bar{V} + R_a\bar{I} + jX_q\bar{I} \quad (103)$$

where the phasors $e_q e^{j\delta}$ and $(X_d - X_q)i_d e^{j\delta}$ lie on the quadrature axis. Equation (103) allows, therefore, the determination of the angle $\delta(0)$, if the phasors $\bar{V}$ and $\bar{I}$ are known. The left hand side of (103) is not important in its value, but its position is that of the quadrature axis.

The rest of the electrical variables can then easily be calculated from the following relationships:

$$i_d = \sqrt{3}\,|\bar{I}|\cdot\sin(\gamma' - \delta) \quad (104a)$$

$$i_q = \sqrt{3}\,|\bar{I}|\cdot\cos(\gamma' - \delta) \quad (104b)$$

and

$$v_d = \sqrt{3}\,|\bar{V}|\,\sin(\alpha' - \delta) \quad (104c)$$

$$v_q = \sqrt{3}\,|\bar{V}|\,\cos(\alpha' - \delta) \quad (104d)$$

Finally, the field current i_f can be found from (98):

$$i_f = \frac{v_q + R_a i_q - X_d i_d}{\omega \sqrt{\frac{3}{2}} M_f} \tag{105}$$

The initial conditions of the electric part of the generator are then fully defined. It remains, therefore, to determine the initial conditions for the mechanical variables of the generator.

The mechanical equations of the generator were defined in section 2.5 ((35)-(39)). However, the equation for mass i is shown again to aid understanding:

$$J_i \frac{d^2\theta_i}{dt^2} + D_{ii} \frac{d\theta_i}{dt} + D_{i-1,i} \frac{d}{dt}(\theta_i - \theta_{i-1}) + D_{i,i+1} \frac{d}{dt}(\theta_i - \theta_{i+1}) +$$

$$K_{i-1,i}(\theta_i - \theta_{i+1}) + K_{i,i+1}(\theta_i - \theta_{i+1}) = T_i \tag{106}$$

For steady-state conditions (106) can be simplified as follows:

$$D_{ii} \frac{d\theta_i}{dt} + K_{i-1,i}(\theta_i - \theta_{i-1}) + K_{i,i+1}(\theta_i - \theta_{i+1}) = T_i \tag{106a}$$

The angular speed $\frac{d\theta_k}{dt}$ is equal for all rotating masses and can be found from the following relationship:

$$\frac{d\theta_k}{dt} = \omega_m = \omega \cdot \frac{2}{n} \qquad \text{for } k = 1, \ldots N \tag{107}$$

where "subscript "m" denotes mechanical variables, where n is the number of poles in the generator, and where ω is the angular frequency of the network.

The initial angular position of the generator rotor can be calculated from the angle $\delta(0)$ as follows:

$$\theta_r = (\delta(0) + \tfrac{\pi}{2}) \cdot \frac{2}{n} \tag{108}$$

where subscript "r" denotes generator rotor variables.

Finally, the angle θ_{i-1} can be found from the angle θ_i:

$$\theta_{i-1} = \theta_i + \frac{\sum_{j=1}^{i-1} Tmj - \sum_{j=1}^{i-1} D_{jj}\omega_m}{K_{i-1,i}} \tag{109}$$

In a similar way, the angle θ_{i+1} can be found from:

$$\theta_{i+1} = \theta_i + \frac{\sum_{j=i+1}^{N} Tmj - \sum_{j=i+1}^{N} D_{jj}\omega_m}{K_{i,i+1}} \tag{110}$$

The sum of the applied mechanical torques Tmj must, of course, equal the sum of electrical and speed self-damping torques, so that there is zero accelerating torque initially:

$$\sum_{j=1}^{N} T_{mj} = \sum_{j=1}^{N} Tej + \sum_{j=1}^{N} D_{jj}\omega_m \tag{111}$$

where subscript "e" denotes electromechanical torque.

Calculation of the initial angular displacement of the masses in the shaft system ends the process of initialization of the generator variables.

5.2 Consistent Per Unit (p.u.) System and Conversion to Physical Units

The choice of a consistent and simple p.u. system is, in general, relatively easy. For rotating machinery, however, the situation gets complicated if more than one reference frame is used. A transformation from one reference frame to another may limit the freedom in the choice of base variables, if symmetry of matrices is to be preserved. This is precisely the case for a synchronous generator when unnormalized transformation matrices are used.

It is common practice in the power industry to describe the generator in Park's d,q,0-coordinates, as explained in section 2.2. The conventional unnormalized transformation does not preserve the symmetry of the inductance matrix [L] of the generator [17]. The resulting asymmetrical matrix $[L_p]$ can be forced back to symmetry with a specific p.u. system in which base power for rotor quantities is $\frac{3}{2}$ times base power for stator quantities [17], [55]. A simpler approach, which does not require complicated scaling procedures to restore the symmetry, is presented in this chapter. As mentioned in section 2.2, the normalized transformation defined in (18) and (19) preserves the symmetry of the inductance matrix [L], i.e., the resulting matrix $[L_p]$ is symmetrical no matter which base values are chosen for stator and rotor circuits [17]. Then the conversion to p.u. values is a simple scaling problem with complete freedom in the choice of base values for each circuit.

Any linear electric network in steady-state operation can be described by one of the following nodal equations:

$$[Y_{phys}] \cdot \underline{V}_{phys} = \underline{I}_{phys} \tag{112}$$

or

$$[Z_{phys}] \cdot \underline{I}_{phys} = \underline{V}_{phys} \tag{113}$$

where the subscript "phys" denotes physical values, and

$$[Z_{phys}] = [Y_{phys}]^{-1} \tag{114}$$

and where $\underline{V}_{phys}$ and $\underline{I}_{phys}$ are vectors of nodal voltages and currents injected into the nodes, in V and A respectively. The nodal impedance matrix $[Z_{phys}]$ is given in its own physical units, Ω.

In general, a system has more than one voltage level, with coupling through transformers. Therefore, different base voltages are normally

chosen for the node voltages, while base power is normally the same for all nodes. It can easily be shown that the following relationship holds between the physical and the p.u. values [56]:

$$[Z_{p.u.}] = [V_b]^{-1}[Z_{phys}][V_b]^{-1}[S_b] \tag{115}$$

or

$$[Z_{phys}] = [V_b][Z_{p.u.}][V_b]\cdot[S_b]^{-1} \tag{116}$$

where:

$[V_b]$ = diagonal matrix of base voltages,

$[S_b]$ = diagonal matrix of base powers.

Equations (115) and (116) are valid for any set of base voltages and powers. However, symmetry of the matrix $[Z_{phys}]$ will be preserved only if there is only one base power, which is the normal practice in power system analysis anyhow.

It is customary to define the data of a synchronous generator in a p.u. system based on its nameplate ratings. For general network studies, where each element has its own nameplate rating, all values must either be converted to the same bases, or to physical quantities. Per unit values offer advantages if a problem is studied on a network analyzer, or on a digital computer with fixed-point arithmetic, because in both cases all values must be of a certain order of magnitude. This problem does not exist in computers with floating-point arithmetic, which is the rule nowadays. Scaling (conversion from p.u. to physical values or vice versa) has no influence on the solution process, except for possible differences in the accumulation of round-off errors. As a consequence, practically identical solutions (except for slight differences in round-off errors) will be obtained with physical quantities

and with p.u. quantities. The influence of scaling on round-off errors is not easy to assess [57]. For a system of linear equations, however, the following statement can be proved [58]: "If scaling is done in such a way that only the exponent changes in floating-point numbers and if the order of elimination is not changed, then the scaled (p.u.) equations will produce precisely the same significants in all answers and in all intermediate numbers". After careful examination of all advantages and disadvantages it was decided to convert the machine data to physical units. Physical quantities are least confusing and assure consistency with the Transients Program. Conversion to physical units is done as follows:

(a) Calculate all the required generator parameters in p.u. from the p.u. data based on nameplate ratings as provided by the manufacturer;

(b) Multiply all elements of the matrices $[L_p]_{p.u.}$ and $[R]_{p.u.}$ by the base impedance of the stator windings, which can be found from the following relationship:

$$Z_{Sb} = \frac{V_{Sb}^2}{S_{Sb}} \tag{117}$$

where:

Z_{Sb} = base impedance of the stator;

S_{Sb} = { three-phase rated power of the stator in MVA, if the stator is onnected in wye. single-phase rated power of the stator in MVA, if the stator is connected in delta.

V_{Sb} = line-to-line rated voltage of the stator in KV (RMS) for both wye and delta connections.

This operation transforms all the stator data to their original physical values. Rotor parameters, as found in step b will be in physical values referred to the stator side of the generator.

(c) Multiply all the parameters related to the rotor circuits which lie on the diagonal of the matrices $[L_p]$ and $[R]$ by n^2, and those on the off-diagonal of $[L_p]$ by n, where:

n = transformer ratio between the stator and the field. This number can be calculated in one of two ways:

(1) from the physical value of the field resistance R_f, if such is known from measurements [22]:

$$\sqrt{\frac{R_f}{R_{fp.u.} \cdot Z_{Sb}}} = n \qquad (118)$$

or:

(2) from the open-circuit characteristic, as schematically shown in Fig. 32.

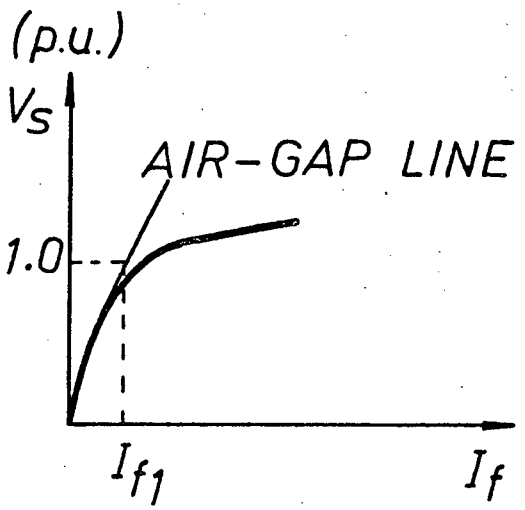

Fig. 32. Typical open-circuit characteristic.

From the generator equations derived in chapter 2.2, it follows that the physical value of the field-to-stator mutual coupling M_f is given by:

$$M_f = \frac{\sqrt{\frac{2}{3}}\, V_{LL}}{I_{f1} \cdot \omega} \tag{119}$$

where V_{LL} = RMS value of line-to-line voltage found on the open-circuit characteristic.

From (119), the transformer ratio n can be defined as follows:

$$n = \frac{M_f}{M_{fp.u.} \cdot Z_{Sb}} \tag{120}$$

The procedure outlined above assumes that the original p.u. data was all based on the same base power, which is normally true for manufacturer's data. Then, the matrix $[S_b]$ is simply a unit matrix premultiplied by a scalar S_{Sb} defined in (117). This procedure also assumes that there are only two base voltages, one for the stator, and the other for the field and damper windings. The latter assumption can be justified as follows:

> Since the damper windings are hypothetical windings, for an interconnected arrangement of many damper bars, any transformer ratio to them can be assumed. It is, therefore, possible to use the same ratio as that from the stator to the field without loss of generality.

This specific conversion procedure is very simple to use and requires only the available standard data. A similar approach based upon different reasoning has been suggested in [59].

5.3 Saturation in the Steady-State Operation of a Synchronous Generator

Saturation may have an impact (sometimes a significant one) on power system transient stability and steady-state stability calculations, as well as on real and reactive power flow calculations [29], [60]. As is well known in practice, it also influences the calculations of electromagnetic transients in power systems [61]. On the other hand, a nonlinear relation between flux and current will, if treated rigorously, complicate the solution process significantly. The solution of large nonlinear systems becomes then very expensive and time consuming. An approximate treatment of saturation effects is, therefore, commonly accepted. The treatment of saturation effects in steady-state operation differs from the approach needed for transient simulations. Before treating the latter case in section 5.4, it seems appropriate to present a short review of the existing approaches used in stability studies, which fall into the category of steady-state phasor solutions.

One of the earliest approaches towards saturation is to be found in [18], [62], where on an empirical basis, it was suggested to calculate the values of the saturated reactances by multiplying the unsaturated values by a constant $F_{st} = 0.88$. This simple approach is clearly not accurate enough, since the saturation effects vary with the type of generator and its loading conditions [63]. More recent approaches can be divided into the following basic groups:

(1) The degree of saturation is a function of the total flux $\psi = \sqrt{\psi_d^2 + \psi_q^2}$. There is, therefore, only one saturation coefficient for the total flux [64-66];

(2) The degree of saturation in each axis is proportional to the components of the voltage source behind Potier (or leakage)

reactance. There are, therefore, two separate saturation coefficients, one for each axis [24], [67].

A number of authors use flux plots to determine the saturation effects [60], [68]. The results published in [68] seem to favour approach 1. It is also worth mentioning that saturation data for a medium-sized generator published in [69] are close to the value of the empirical coefficient F_{st} suggested in [18]. Other authors, however, suggest different saturation characteristics for the d- and q-axes. To sum it up, it is not yet known which procedure is more accurate. The main problem lies in the unavailability of accurate data [29]. A possible solution of this problem could come from measuring the saturation effects directly in phase coordinates [12], [22], but more research is needed [60].

The nonlinear flux-current characteristic caused by saturation implies that it is no longer possible to use, in a straightforward way, phasor solutions in the calculation of the steady-state conditions. To get around this problem, an "equivalent linear machine", which is exactly valid in one particular operating point and approximately valid in the neighbourhood of that point, is introduced [70]. The objective is to linearize the problem by parameter modification. This is achieved by replacing the nonlinear characteristic by a linear curve through the operating point and the origin, as shown in Fig. 33. This approximation is, of course, valid only in the immediate vicinity of the operating point.

The following procedure was developed for the inclusion of saturation effects into the calculation of the initial conditions of a generator:

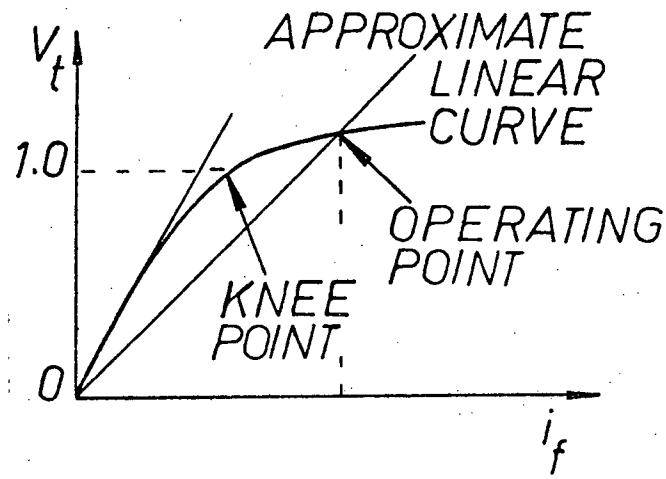

Fig. 33. Linearization through the origin.

(1) Calculate the initial conditions assuming that the generator is unsaturated, as explained in section 5.1.

(2) If the generator operates in the saturated region, the calculations are repeated with the unsaturated parameters replaced by their saturated equivalent values. These values can be found from the slope of the approximate straight line shown in Fig. 33. The process is repeated until it converges.

The steady-state conditions of the network found with phasor solution techniques do not contain harmonics. By simulating the problem in steady-state (no fault applied) as a transient case for a period of a few cycles, starting from the initial conditions with the linearized generator, a new steady-state with harmonics should be reached if saturation in generators and transformers is modelled in the Transients Program [45]. This approach worked quite well in a case where the transformer saturation generated harmonics [71], but it has not yet been tested for generator saturation. A similar approach could be used for

unbalanced cases, since the initial conditions are calculated for positive sequence currents only, as explained in section 5.1.

5.4 Definitions of Saturation in the Simulation of Electromagnetic Transients

The analysis of transient performance of synchronous generators with constant inductances may lead to serious errors both in form and magnitude of currents and voltages [61]. Even the use of the term "inductance" may be misleading, since it is based upon the assumption of linearity, i.e., it is no longer true that $\psi = L \cdot MMF$. It should, rather, be said that ψ is a nonlinear function of MMF. For example, [22] introduces two types of inductances:

(a) secant inductance, defined by total flux per unit current.

(b) incremental inductance, defined by the rate of the change of flux linkage with respect to current.

It is proposed to base the analysis of saturation effects upon the following assumptions:

(1) In any reference frame, the generator fluxes can be represented as follows:

$$\underline{\psi} = \underline{\psi}_l + \underline{\psi}_m \qquad (121)$$

where:

$\underline{\psi}_l$ = vector of fluxes related to leakage inductances, uneffected by saturation;

$\underline{\psi}_m$ = vector of fluxes related to mutual inductances, subjects to saturation effects.

Only the latter fluxes will be considered in the following analysis.

(2) The degree of saturation is a function of the MMF, which in

turn is a function of the total unsaturated flux ψ_u calculated along the airgap line.

(3) The saturation effects are equal on both axes, i.e., there is only one saturation coefficient.

(4) The distortion of any airgap flux waves does not effect the unsaturated inductance values or destroy the sinusoidal variations assumed for rotor and stator inductances.

(5) Hysteresis and eddy current losses are neglected, as is usual in power transformer modelling where it has normally little influence on the results [72].

Assumption 2 implies the knowledge of the dependence between the instantaneous flux and the excitation current. The only available data, however, consists of the open circuit characteristic (terminal voltage as a function of the excitation current) shown schematically in Fig. 32. The converted curve (flux versus current) has the same form as the original curve. A short proof is given in Appendix [7].

The resulting curve can be approximated in a number of ways, e.g., straight-line segments, exponential or quadratic curves. It was decided to adopt a two straight-lines approximation, due to its simplicity, but the actual number of segments does not change the method of analysis. It can be increased, if so required by the shape of the flux-current curve. The total (mutual) flux of the machine may, therefore, be described as follows (subscript "u" denotes an unsaturated value, subscript "m" dropped to simplify notation):

$$\psi = \begin{cases} \psi_u & \text{unsaturated region} \\ m\,\psi_u + a & \text{saturated region} \end{cases} \qquad (122)$$

where:

a and m = constants resulting from the two straight-lines approximation of the saturation curve, or from an approximation with more than two linear segments.

The total unsaturated airgap flux, on the other hand, may be described by the following equation:

$$\psi_u = \sqrt{\psi_{du}^2 + \psi_{qu}^2} \tag{123}$$

where subscripts "d" and "q" denote the direct and quadrature axis values, respectively.

Equations (122) and (123) imply that there is one saturation effect for the total flux, rather than two separate effects, one for each axis. This situation is show schematically in Fig. 34.

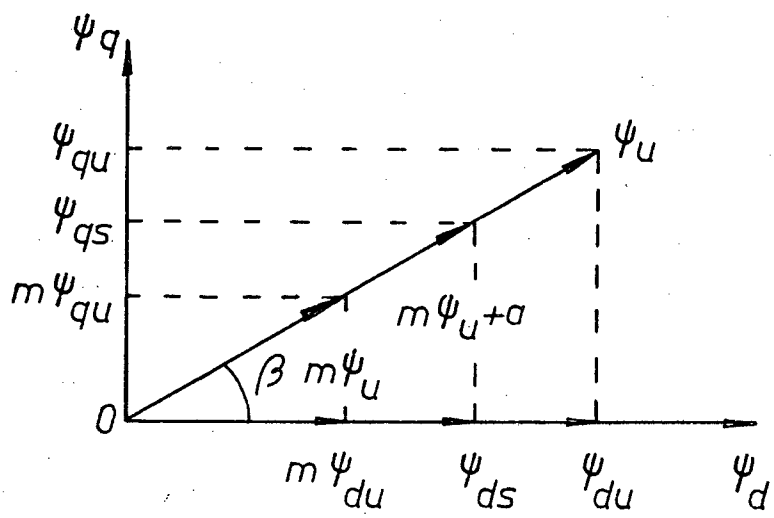

Fig. 34. Schematic representation of saturation effects.

From Fig. 34 and equations (122) and (123) follows that the fluxes in the saturated region can be described as follows (subscript "s" denotes saturated values):

$$\psi_{ds} = m \cdot \psi_{du} + a \cos \beta \tag{124}$$

$$\psi_{qs} = m \cdot \psi_{qu} + a \sin \beta \tag{125}$$

where:

$$\cos \beta = \frac{\psi_{du}}{\psi_u} \tag{126}$$

and

$$\sin \beta = \frac{\psi_{qu}}{\psi_u} \tag{127}$$

As already mentioned, the constants m and a result from the straight-line approximation of the flux-current characteristic. This situation is illustrated schematically in Fig. 35.

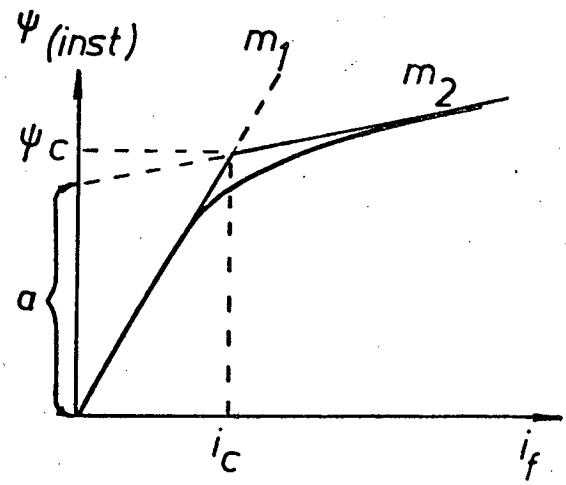

Fig. 35. Straight-line approximation of the flux-current characteristic.

From basic analytic geometry follows that

$$m = \frac{m_2}{m_1} \tag{128}$$

The constant a can be found from the conditions in the "knee-point" (ψ_c, i_c). In this point both fluxes (saturated and unsaturated) must be equal, i.e.,

$$m_1 i_c = m_2 i_c + a \tag{129}$$

From (129) follows that:

$$a = (m_1 - m_2)i_c \tag{130}$$

Equations (124)-(130) describe fully the saturated fluxes in a synchronous generator. They can be easily modified to accommodate additional data, if such is available. It is, for example, possible to create two sets of constants m and a, one for each axis. This would allow each axis to have its own saturation coefficient.

5.5 Implementation in the Transients Program

The generator equations in d,q,0-coordinates can be rewritten into the following form (details were given in section 2.2):

$$\underline{v}_p = -[R]\underline{i}_p - \frac{d}{dt}\underline{\psi}_p - [A]\cdot\underline{\psi}_p \tag{131}$$

where the matrix [A] is defined as follows:

$$[A] = [P]\frac{d}{dt}[P]^{-1} = \begin{bmatrix} 0 & \omega & 0 & | & \\ -\omega & 0 & 0 & | & 0 \\ 0 & 0 & 0 & | & \\ - & - & - & + & - \\ & 0 & & | & 0 \end{bmatrix} \tag{132}$$

Only the two last terms of (131) are subject to saturation influence. Their different physical nature results in two different implementation procedures, one for each of them. Both procedures, however, are based upon the following common assumption:

> The generator does not change its saturation status during one time-step, i.e., if the generator was saturated at the beginning of a time-step, it remains saturated at its end.

The saturable transformer voltages $\frac{d}{dt}\underline{\psi}_{pm}$ are described by the following equation:

$$\underline{v}_{pm} = - \frac{d}{dt} \underline{\psi}_{pm} \tag{133}$$

Equation (133) implies that physically only the incremental fluxes are of importance. Since the generators equations are solved with the trapezoidal rule of integration, (133) is then transformed to the following form (subscript "p" dropped to simplify notation):

$$\underline{\psi}_m(t) = \underline{\psi}_m(t-\Delta t) - \frac{\Delta t}{2}(\underline{v}_m(t) + \underline{v}_m(t-\Delta t)) \tag{134}$$

Substitution of (122) into (134) yields the following expression for the ith component of the vector $\underline{\psi}_m(t)$ (subscript "m" dropped to simplify notation):

$$m\ \psi_{iu}(t) + a = m\ \psi_{iu}(t-\Delta t) + a - \frac{\Delta t}{2}(v_i(t) + v_i(t-\Delta t)) \tag{135}$$

Simple rearrangements yield the following result:

$$v_i(t) = \frac{m \cdot 2}{\Delta t}(\psi_{iu}(t) - \psi_{iu}(t-\Delta t)) - v_i(t-\Delta t) \tag{136}$$

Equation (136) provides the means for including the saturation effects in the transformer voltages of a generator. It is simply enough to multiply all the mutual inductances by the constant m. If the parameters of rotor circuits of the generator are not referred to the stator side, it is necessary to introduce the transformer ratio into the constant m.

The saturable terms related to the speed voltages $[A]\underline{\psi}_p$ appear only in the following two equations:

$$v_{dm} = -\omega\ \psi_{qm} \tag{137}$$

and

$$v_{qm} = +\omega\ \psi_{dm} \tag{138}$$

where subscripts "d" and "q" denote the direct and quadrature axis, respectively, and subscript "m" denotes terms related to mutual inductances. Equations (137) and (138) imply that it is necessary to consider the entire fluxes ψ_{dm} and ψ_{qm}, since (137) and (138) represent

algebraic relationships, rather than differential relationships. If all rotor circuits are converted to the stator side, the following relationships can be obtained for the saturated fluxes (subscript "m" dropped to simplify notation):

$$\psi_{ds} = m M_f(i_d + i_f + i_D) + a \cos \beta \tag{139}$$

and

$$\psi_{qs} = m M_q(i_q + i_g + i_Q) + a \sin \beta \tag{140}$$

It is, therefore, enough to substitute (139) and (140) for the fluxes related to the saturable inductances.

The procedure outlined above is very flexible and can easily accommodate additional data, as it becomes available. It is not tied entirely to the theory outlined in the previous chapter, and it can be adapted to accept any available representation of saturation effects.

6. CONCLUSIONS AND RECOMMENDATIONS FOR FURTHER RESEARCH

A range of problems related to interfacing generator models with an Electromagnetic Transients Program has been described. The main topics covered in this thesis were:

(a) creation of an adequate generator model

(b) development of two alternative interfacing techniques

(c) modelling of saturation effects in the generator.

The validity of the generator model has been verified in a number of test studies, which also included comparisons with field test results. Good agreement was achieved, and the results obtained with the two interfacing methods gave practically identical answers which proves their validity.

The discussion of saturation effects presents only a first attempt in this area. The suggested solution methods should be tested in practice to establish their validity. Similarly, the proposed method II of interfacing generator models with the Transients Program should undergo further tests before completely replacing method I with it. Further possible areas of additional investigations could include such topics as:

(a) inclusion of space harmonics in the field distribution

(b) improvements in the calculation of initial conditions to allow the initialization from unbalanced conditions.

This work should, therefore, be understood as a first step, only, in the modelling of synchronous generators for electromagnetic transient phenomena.

REFERENCES

[1] S. Meyer and H.W. Dommel, "Numerical Modelling of Frequency-Dependent Transmission-Line Parameters in an Electromagnetic Transients Program", IEEE Trans. Power App. Syst., vol. PAS-93, Sept./Oct. 1974, pp. 1401-1409.

[2] V. Brandwajn and H.W. Dommel, "Interfacing Generator Models with an Electromagnetic Transients Program", Paper A 76359-0, presented at the IEEE PES Summer Meeting, Portland, Ore., July 19-23, 1976.

[3] K. Carlson, E.H. Lenfest, and J.J. La Forest, "MANTRAP, Machine and Network Transients Program", Paper V-D, presented at the 9th PICA Conference, New Orleans, La., June 2-4, 1975.

[4] M.C. Hall, "Machine Model for Transients Program", Internal Memorandum, Southern California Edison Company, Rosemead, Ca., 1975.

[5] IEEE Subsynchronous Resonance Task Force Report, "First Benchmark Model for Computer Simulation of Subsynchronous Resonance", Paper F 77102-7, presented at the IEEE PES Winter Meeting, New York, N.Y., Jan. 30-Feb. 4, 1977.

[6] P. Eykhoff, "System Identification, Parameter and State Estimation", Wiley-Interscience, N.Y., 1974.

[7] R.H. Park, "Two Reaction Theory of Synchronous Machines", AIEE Trans., vol. 48, pt. I, July 1929, pp. 716-730.

[8] G. Müller, "Theorie der rotierenden Maschine", Leipzig, 1968.

[9] B. Adkins and R.G. Harley, "The General Theory of Alternating Current Machines: Application to Practical Problems", Chapman and Hall, London, 1975.

[10] IEEE Committee Report, "Recommended Phasor Diagram for Synchronous Machines", IEEE Trans. Power App. Syst., vol. PAS-88, Nov. 1969, pp. 1593-1610.

[11] B. Adkins, "Transient Theory of Synchronous Generators Connected to Power Systems", Proc. IEE, vol. 98, No. 2, 1951, pp. 510-523.

[12] M. Rafian and M.A. Laughton, "Determination of Synchronous-Machine Phase-Co-Ordinate Parameters", Proc. IEE, vol. 123(8), Aug. 1976, pp. 818-824.

[13] Y. Takeda and B. Adkins, "Determination of Synchronous-Machine Parameters Allowing for Unequal Mutual Inductances", Proc. IEE, vol. 121(12), Dec. 1974, pp. 1501-1504.

[14] I.M. Canay, "Causes of Discrepancies on Calculation of Rotor Quantities and Exact Equivalent Diagrams of the Synchronous Machine", IEEE Trans. Power App. Syst., vol. PAS-88, July 1969, pp. 1114-1120.

[15] H. Späth, "Der Einfluss von Kopplungen zwischen dem Nullsystem und der d- order q-Achse auf das Betrieb von Synchron-Schenkelpolmaschinen", ETZ-A, Bd 93, 1972, pp. 712-714.

[16] E.W. Kimbark, "Power System Stability: Synchronous Machines", New York: Dover, 1968 (reprint of 1956 ed.).

[17] M.R. Harris, P.J. Lawrenson, and J.M. Stevenson, "Per-Unit Systems with Special Reference to Electrical Machines", Cambridge University Press, Cambridge, 1970.

[18] L.A. Kilgore, "Calculation of Synchronous Machine Constants", Trans. AIEE, vol. 50, 1931, pp. 1201-1214.

[19] C. Concordia, "Synchronous Machines: Theory and Performance", John Wiley and Sons, New York, 1951.

[20] Y. Yu and H.A.M. Moussa, "Experimental Determination of Exact Equivalent Circuit Parameters of Synchronous Machines", IEEE Trans. Power App. Syst., vol. PAS-90, Nov./Dec. 1971, pp. 2555-2560.

[21] G. Shackshaft, "New Approach for the Determination of Synchronous-Machine Parameters from Tests", Proc. IEE, vol. 121(11), Nov. 1974, pp. 1385-1392.

[22] L.A. Snider and I.R. Smith, "Measurement of Inductance Coefficients of Saturated Synchronous Machine", Proc. IEE, vol. 119(5), May 1972, pp. 597-601.

[23] G. Manchur et al., "Generator Models Established by Frequency Response Tests on a 555 MVA Machine", Stability of Large Electric Power Systems, IEEE Press, New York, 1974, pp. 37-44.

[24] P. Dandeno, R.L. Hauth, and R.P. Schulz, "Effects of Synchronous Machine Modelling in Large Systems Studies", ibid, pp. 28-36.

[25] V. Gourishankar, "Electromagnetical Energy Conversion", International Textbook Company, Seranton, 1975.

[26] L.A. Soderquist, "Fundamentals of System Stability", The Role of Prime Movers in Systems Stability, IEEE Tutorial Course, New York, N.Y., 1970, pp. 7-15.

[27] R.T. Byerly, "Power Systems Stability - Effects of Control System Performance", ibid, pp. 57-66.

[28] P. Subramian and P. Malik, "Digital Simulation of a Synchronous Generator in Direct-Phase Quantities", Proc. IEE, vol. 118(1), Jan. 1971, pp. 153-160.

[29] C. Concordia, Discussion to G. Shackshaft and R. Neilson, "Results of Stability Tests on an Underexcited 120 MW Generator", Proc. IEE, vol. 119, 1972, pp. 1487-1494.

[30] F.H. Branin, Jr., "Computer Methods of Network Analysis", Proc. IEEE, vol. 55, Nov. 1967, pp. 1787-1801.

[31] C.W. Gear, "Numerical Initial Value Problems in Ordinary Differential Equations", Prentice-Hall, Englewood Cliffs, N.J., 1971.

[32] G. Gross and A.R. Bergen, "A Class of New Multistep Integration Algorithms for the Computation of Power System Dynamical Response", IEEE Trans. Power App. Syst., vol. PAS-91, Jan./Feb. 1977, pp. 293-306.

[33] C.W. Gear, "The Automatic Integration of Large Systems of Ordinary Differential Equations", The Digest Record of the Joint Conference on Mathematical and Computer Aids to Design, Anaheim, Ca., Oct. 27-31, 1969, pp. 27-58.

[34] H.W. Dommel and W.S. Meyer, "Computation of Electromagnetic Transients", Proc. IEEE, vol. 62, July 1974, pp. 983-993.

[35] G.G. Dahlquist, "A Special Stability Problem for Linear Multistep Methods", Nordisk Tidskrift for Informations-Behandling, BIT (3), 1963, pp. 27-43.

[36] S.N. Talukdar, "Iterative Multistep Methods for Transient Stability Studies", IEEE Trans. Power App. Syst., vol. PAS-90, Jan./Feb. 1971, pp. 96-102.

[37] A. Semlyen and A. Dabuleanu, "A System Approach to Accurate Switching Transient Calculations Based on State Variable Component Modelling", IEEE Trans. Power App. Syst., vol. PAS-94, March/April 1975, pp. 572-578.

[38] S.C. Tripathy and N.D. Rao, "A-Stable Numerical Integration Method for Transmission System Transients", Paper F 77 062-3 presented at the IEEE PES Winter Meeting, New York, N.Y., Jan. 30-Feb. 4, 1977.

[39] E.J. Davison, "A High-order Crank-Nicholson Technique for Solving Differential Equations", The Computer Journal, vol. 10(2), Aug. 1967, pp. 195-197.

[40] H.W. Dommel, "Digital Computer Solutions of Electromagnetic Transients in Single- and Multiphase Networks", IEEE Trans. Power App. Syst., vol. PAS-88, Apr. 1969, pp. 388-399.

[41] O.I. Elgerd, "Electric Energy Systems Theory: An Introduction", McGraw-Hill, New York, N.Y., 1971.

[42] R.W. Hamming, "Numerical Methods for Scientists and Engineers", International Student Edition, McGraw-Hill, Tokyo, 1962.

[43] C.W. Gear, "The Automatic Integration of Stiff Ordinary Differential Equations", Proceeding IFIPS Conference, Edinburgh, 1968, pp. 187-193.

[44] W.S. Meyer, Transients Program Memorandum, vol. UJV, March 1974.

[45] H.W. Dommel, "Nonlinear and Time-Varying Elements in Digital Simulation of Electromagnetic Transients", IEEE Trans. Power App. Syst., vol. PAS-90, Nov./Dec. 1971, pp. 2561-2567.

[46] H.J. Carlin and A.B. Giordano, "Network Theory: An Introduction to Reciprocal and Nonreciprocal Circuits", Prentice-Hall, Englewood Cliffs, N.J., 1964.

[47] D.A. Calahan, "Numerical Considerations for Implementation of Nonlinear Transient Circuit Analysis Program", IEEE Trans. on Circuit Theory, vol. CT-18(1), Jan. 1971, pp. 66-73.

[48] H.W. Dommel, "A Method for Solving Transient Phenomena in Multiphase Systems", Report 5.8, presented at 2nd Power System Computation Conference, Stockholm, 1966. See also Electric Research Council, Transmission Line Reference Book: 345 KV and Above, Electric Power Research Institute, Palo Alto, Ca., 1975, pp. 292-293.

[49] L. Dube and H.W. Dommel, "Simulation of Control Systems in an Electromagnetic Transients Program with TACS", Paper submitted for PICA Conference, Toronto, Ont., May 24-27, 1977.

[50] E. Bodewig, "Matrix Calculus", 2nd edition, North-Holland, 1959.

[51] S.N. Talukdar, "METAP - A Modular and Expandable Program for Simulating Power System Transients", IEEE Trans. Power App. Syst., vol. PAS-95(6), Nov./Dec. 1976, pp. 1882-1891.

[52] H.W. Dommel and N. Sato, "Fast Transient Stability Solutions", IEEE Trans. Power App. Syst., vol. PAS-91, July/Aug. 1972, pp. 1643-1650.

[53] A. Charlton and G. Shackshaft, "Comparison of Accuracy of Methods for Studying Stability, Northfleet Exercise", Electra, No. 23, July 1972, pp. 9-49.

[54] G. Shackshaft and R. Neilson, "Results of Stability Tests on an Under-excited 120 MW Generator", Central Electricity Generating Board, July 1971.

[55] A.W. Rankin, "Per-Unit Impedances of Synchronous Machines", AIEE Transactions, vol. 64, Aug. 1945, pp. 569-572 and pp. 839-841.

[56] H.W. Dommel, "Notes on Power System Analysis", University of British Columbia, Vancouver, B.C., 1974.

[57] S.H. Crandall, "Engineering Analysis - A Survey of Numerical Procedures", McGraw-Hill, New York, N.Y., 1956, p. 37.

[58] G.E. Forsythe and C.B. Moler, "Computer Solution of Linear Algebraic Systems", Prentice-Hall, Englewood Cliffs, N.J., 1967, p. 39.

[59] D.C. White and H.H. Woodson, "Electromechanical Energy Conversion", J. Wiley, New York, N.Y., 1959, p. 518.

[60] N.H. Demerdash and H.B. Hamilton, "A Simplified Approach to Determination of Saturated Synchronous Reactances of Large Turbogenerators under Load", IEEE Trans. Power App. Syst., vol. PAS-95(2), March/April 1976, pp. 560-569.

[61] R. Rüdenberg, "Transient Performance of Electric Power Systems, Phenomena in Lumped Networks", MIT Press, Cambridge, Mass., 1970.

[62] S.H. Wright, "Determination of Synchronous Machine Constants by Test", Trans. AIEE, vol. 50, Dec. 1931, pp. 1331.

[63] B. Adkins, Discussion to [60].

[64] G. Shackshaft, "General-Purpose Turbo-Alternator Model", Proc. IEE, vol. 110(4), April 1963, pp. 703-713.

[65] W.D. Humpage and T.N. Saha, "Digital-Computer Methods in Dynamic-Response Analyses of Turbogenerator Units", Proc. IEE, vol. 114(8), Aug. 1967, pp. 1115-1130.

[66] J.D. Schulz, W.D. Jones and D.N. Ewart, "Dynamic Models of Turbine Generators Derived from Solid Rotor Equivalent Circuits", IEEE Trans. Power App. Syst., vol. 92(3), May/June 1973, pp. 926-933.

[67] D.W. Olive, "New Techniques for the Calculation of Dynamic Stability", IEEE Trans. Power App. Syst., vol. PAS-85, July 1966, pp. 767-777.

[68] E.F. Fuchs and E.A. Erdelyi, "Determination of Waterwheel Alternator Steady State Reactances from Flux Plots", IEEE Trans. Power App. Syst., vol. PAS-91, 1972, pp. 1795-1802.

[69] E.F. Fuchs, Discussion to [60].

[70] B. Adkins, Discussion to [60].

[71] H.W. Dommel and W.S. Meyer, "Computation of Electromagnetic Transients", Proc. IEEE, vol. 62, July 1974, pp. 983-993.

[72] Cigre Working Group 13.05, "Modelling of saturable Elements for Transient Overvoltages Studies", to be published in Electra.

[73] "Test Procedures for Synchronous Machines", IEEE Publication No. 115, 1965.

[74] B.C. Kuo, "Discrete-Data Control Systems", Prentice-Hall, Englewood Cliffs, N.J., 1970, pp. 336-344.

[75] B. Noble, "Applied Linear Algebra", Prentice-Hall, Englewood Cliff, N.J., 1969.

APPENDIX 1

DEFINITIONS OF L'_d, L''_d, T'_{do}, T''_{do} AND L'_q, L''_q, T'_{qo}, AND T''_{go}

Only the definitions of direct axis quantities will be derived. The quadrature axis quantities can be obtained from the definitions of the direct axis by replacing the subscripts "d", "f", and "D" with "q", "g", and "Q", and by replacing the voltage v_f with 0, i.e., $v_g = 0$, since the g-winding is permanently short-circuited.

The quantities L'_d, L''_d, T'_{do} and T''_{do} are equivalent parameters which are only defined for transient conditions following a disturbance. According to the IEEE (ANSI) standards [73] in the U.S.A. and similar standards elsewhere, a simultaneous three-phase short-circuit is used to measure these quantities. It can be simulated with (21)-(23) by applying voltages to the generator terminals which are equal in magnitude and of opposite sign to those existing in the balanced steady-state at rated speed prior to the fault.

1. Subtransient Inductance and Open-Circuit Time Constants

Immediately after the disturbance (first few cycles), there will be currents flowing in the damper windings. The following assumptions can be made during that short period:

(a) no voltage regulator action yet, i.e.,

$$v_f = \text{const} \tag{1-1}$$

(b) constant flux linkages in the rotor circuits, i.e.,

$$\psi_f = \text{const} \tag{1-2}$$

$$\psi_D = \text{const} \tag{1-3}$$

The last assumption is equivalent to neglecting the resistances in the field and damper windings, which cause a slow decay in

the fluxes. Immediately after the disturbance, this decay is negligible.

Equations (22) can be used to express the currents i_f and i_D as functions of these constant flux linkages:

$$\begin{bmatrix} i_f \\ i_D \end{bmatrix} = \frac{1}{L_f L_D - M_f^2} \begin{bmatrix} L_D & -M_f \\ -M_f & L_f \end{bmatrix} \cdot \begin{bmatrix} \psi_f - \sqrt{\frac{3}{2}} M_f i_d \\ \psi_D - \sqrt{\frac{3}{2}} M_f i_d \end{bmatrix} \tag{1-4}$$

Substitution of the above expressions into the equation for the flux in the d-axis yields:

$$\psi_d = (L_d - \frac{3}{2} M_f^2 \frac{L_f + L_D - 2M_f}{L_f L_D - M_f^2}) \, i_d + K_1 \psi_f + K_2 \psi_D \tag{1-5}$$

where

$$K_1 = \frac{\sqrt{\frac{3}{2}} M_f (L_D - M_f)}{L_f L_D - M_f^2} \tag{1-6}$$

and

$$K_2 = \frac{\sqrt{\frac{3}{2}} M_f (L_f - M_f)}{L_f L_D - M_f^2} \tag{1-7}$$

The subtransient inductance L_d'' relates stator flux ψ_d to stator currents i_d. It is, therefore, defined as follows:

$$L_d'' = L_d = \frac{3}{2} M_f^2 \frac{L_f + L_D - 2M_f}{L_f L_D - M_f^2} \tag{1-8}$$

The open-circuit time constants define the decay of the rotor fluxes after the disturbance. They can be found from the two differential equations for rotor fluxes. From (21) follows that

$$-\begin{bmatrix} \frac{d\psi_f}{dt} \\ \frac{d\psi_D}{dt} \end{bmatrix} = \begin{bmatrix} R_f & 0 \\ 0 & R_D \end{bmatrix} \cdot \begin{bmatrix} i_f \\ i_D \end{bmatrix} + \begin{bmatrix} -v_f \\ 0 \end{bmatrix} \tag{1-9}$$

Substitution of (1-4) into (1-9) with $i_d = 0$ (open-circuit) yields:

$$-\begin{bmatrix} \frac{d\psi_f}{dt} \\ \frac{d\psi_D}{dt} \end{bmatrix} = \frac{1}{L_f L_D - M_f^2} \begin{bmatrix} R_f L_D & -R_f M_f \\ -R_D M_f & R_D L_f \end{bmatrix} \cdot \begin{bmatrix} \psi_f \\ \psi_D \end{bmatrix} + \begin{bmatrix} -v_f \\ 0 \end{bmatrix} \qquad (1\text{-}10)$$

The open-circuit time constants are the reciprocals of the eigenvalues of the matrix in (1-10) and they can be found from the following equation:

$$\left(\frac{R_f L_D}{a} - \frac{1}{T}\right)\left(\frac{R_D L_f}{a} - \frac{1}{T}\right) - \frac{R_f R_D M_f^2}{a} = 0 \qquad (1\text{-}11)$$

where

$$a = L_f L_D - M_f^2 \qquad (1\text{-}12)$$

Solving (1-11) for T yields the following result:

$$\left.\begin{matrix} T'_{do} \\ T''_{do} \end{matrix}\right\} = \frac{1}{2}\left(\frac{L_f}{R_f} + \frac{L_D}{R_D}\right) \pm \frac{1}{2}\sqrt{\left(\frac{L_f}{R_f} - \frac{L_D}{R_D}\right)^2 + 4\,\frac{M_f^2}{R_f R_D}} \qquad (1\text{-}13)$$

with the positive sign of the root for T'_{do}, and the negative sign for T''_{do}.

2. Transient Inductance L'_d

After elapse of a few cycles, it can be assumed that the damper winding current has already died out, i.e.,

$$i_D = 0 \qquad (1\text{-}14)$$

Therefore, only the field winding with an unchanged flux ψ_f has to be considered. From (22) it follows that under these conditions the field current is given as:

$$i_f = \psi_f - \frac{\sqrt{\frac{3}{2}}\, M_f}{L_f} \qquad (1\text{-}15)$$

Substitution of (1-15) into the flux equation for the direct axis yields:

$$\psi_d = (L_d - \frac{3}{2}\frac{M_f^2}{L_f})\, i_d + \sqrt{\frac{3}{2}}\, M_f\, \psi_f \qquad (1\text{-}16)$$

The transient inductance L'_d is, therefore, defined as follows:

$$L'_d = L_d - \frac{3}{2}\frac{M_f^2}{L_f} \qquad (1\text{-}17)$$

The quadrature axis quantities are defined in an analogous way with the necessary changes in subscripts mentioned earlier.

3. Special Case of One Damper Winding on the Q-Axis

The definitions have to be changed in this case. The absence of the g-winding can be expressed by assuming that:

$$R_g = 0 \qquad (1\text{-}18)$$

and

$$L_g = \infty \qquad (1\text{-}19)$$

Substitution of (1-18) and (1-19) into (1-11) yields the following result:

$$T''_{qo} = \frac{L_Q}{R_Q} \qquad (1\text{-}20)$$

The substransient inductance L''_q then becomes:

$$L''_q = L_q - \frac{3}{2}\frac{M_q^2}{L_Q} \qquad (1\text{-}21)$$

No transient quantities can be defined in this case.

APPENDIX 2

TRANSFORMATION OF THE EQUATIONS OF THE ELECTRIC PART

The voltage equations of a synchronous generator in d,q,0-coordinates have the following, well known form:

$$\underline{v}_p = -[R]\underline{i} - [L'_p]\underline{i}_p - [L_p]\frac{d}{dt}\underline{i}_p \qquad (2\text{-}1)$$

Application of the trapezoidal rule of integration yields:

$$\frac{2}{\Delta t}\underline{i}_p(t) = \frac{2}{\Delta t}\underline{i}_p(t-\Delta t) - [L_p]^{-1}\underline{v}_p(t) - [L_p]^{-1}[R]\underline{i}_p(t) - [L_p]^{-1}[L'_p(t)]\underline{i}_p(t) -$$

$$[L_p]^{-1}\underline{v}_p(t-\Delta t) - [L_p]^{-1}[R]\underline{i}_p(t-\Delta t) - [L_p]^{-1}[L'_p(t-\Delta t)]\underline{i}_p(t-\Delta t) \qquad (2\text{-}2)$$

Simple rearrangements allow rewriting of (2-2) into the following form:

$$\underline{v}_p(t) = [R^{comp}]\underline{i}_p(t) + \underline{hist}_p(t-\Delta t) \qquad (2\text{-}3)$$

where the companion resistance matrix is:

$$[R^{comp}] = -[\frac{2}{\Delta t}[L_p] + [R] + [L'_p(t)]] \qquad (2\text{-}4)$$

and the past-history terms are:

$$\underline{hist}_p(t-\Delta t) = [\frac{2}{\Delta t}[L_p] - [R] - [L'_p(t-\Delta t)]]\cdot\underline{i}(t) - \underline{v}_p(t-\Delta t) \qquad (2\text{-}5)$$

Equation (2-3) has the form of a resistive companion model. This form is preserved if the equations are transformed from Park's coordinates to phase coordinates. The resulting equations can be written in the following way [2]:

$$\underline{v}(t) = [R^{comp}_{a,b,c}]i(t) + \underline{hist}(t-\Delta t) \qquad (2\text{-}6)$$

where the subscript "a,b,c" denotes phase a,b,c-coordinates.
The matrices $[R^{comp}]$ and $[R^{comp}_{a,b,c}]$ are not constant, and they have to be recalculated at each time step. The amount of calculations is, however, significantly smaller for the matrix $[R^{comp}]$ than for the matrix $[R^{comp}_{a,b,c}]$,

if the matrix $[L_p]$ is constant. This affects the numerical efficiency of the solution. Because of this, d,q,0-coordinates were chosen for the final algorithm.

APPENDIX 3

MULTIPHASE THEVENIN EQUIVALENT CIRCUIT OF A TRANSMISSION NETWORK

It is assumed that all network parameters are linear. This is the only assumption necessary to permit the calculation of the Thevenin equivalent circuit of a system shown schematically in Fig. 3.1.

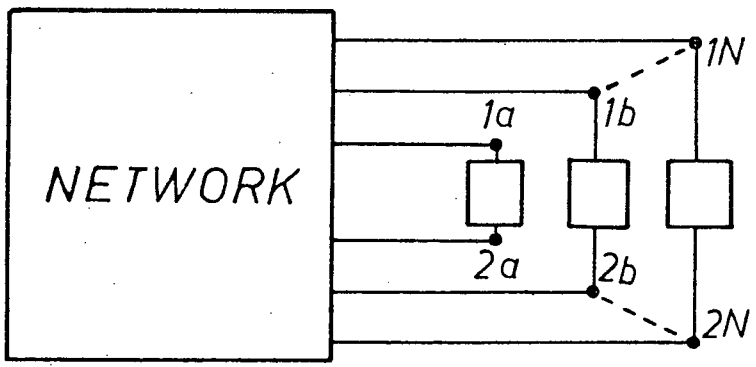

Fig. 3.1. Schematic representation of the network.

The object is to calculate the Thevenin equivalent circuit of the network seen from the terminals 1a-2a, 1b-2b, ..., 1N-2N.

The network is described by the following nodal equation:

$$[G]\cdot\underline{v} = \underline{i} \tag{3.1}$$

where [G] is a conductance matrix created by application of the trapezoidal rule of integration to differential equations of the network. The Thevenin equivalent circuit can be obtained as follows:

(1) Short-circuit all voltage sources and cancel all current sources in the network,

(2) Connect a current source of +1.0 p.u. to terminal 1i and of -1.0 p.u. to terminal 2i, and solve Eq. (3.1) for $\underline{v}$. This

produces a column vector $\underline{v}_{Ti}$ which is, in effect, the difference of the 1i-th and 2i-th columns of $[G]^{-1}$, i.e.

$$[G]\underline{v} = \underline{0} \text{ except } \begin{matrix} +1.0 \text{ in 1i-th component} \\ -1.0 \text{ in 2i-th component} \end{matrix} \tag{3.2}$$

produces a vector:

$$\underline{v}_{Ti} = \underline{v}_{1i} - \underline{v}_{2i} \tag{3.3}$$

The vector $\underline{v}_{Ti}$ is the i-th column of the Thevenin resistive matrix $[R_N^{terminal}]$ in Eq. (83).

(3) Repeat step 2 for all other terminal pairs of interest, i = 2, ... N. This ends the calculation of the Thevenin resistive matrix $[R_N^{terminal}]$. The open circuit voltages $\underline{v}_{NO}(t)$ are calculated by the Transients Program as described in [45].

APPENDIX 4

RESISTIVE COMPANION MODEL

The general property of implicit integration methods to create resistive companion models will be demonstrated for the electric part of a synchronous generator. The procedure for other network components is very similar.

The differential equations of a generator in d,q,0-coordinates can be rewritten into the general form of:

$$\frac{d}{dt}\underline{i}_p = [C_1]\underline{i}_p + [C_2]\underline{v}_p \tag{4-1}$$

where:

$$[C_1] = -[L_p]^{-1}([R_p] + [L_p']) \tag{4-2}$$

and

$$[C_2] = -[L_p]^{-1} \tag{4-3}$$

As is well known, the exact solution of (4-1) has the following general form [74]:

$$\underline{i}_p(t) = [e^{[C_1]\Delta t}]\cdot\underline{i}_p(t-\Delta t) + \int_{t-\Delta t}^{t} [e^{[C_1](t-\tau)}][C_2]\underline{v}_p(\tau)\, d\tau \tag{4-4}$$

After application of any implicit integration technique, (4-1) can be rewritten into the following form:

$$\underline{i}_p(t) = [C_3]\underline{i}_p(t-\Delta t) + [C_4]\underline{v}_p(t) + \underline{u} \tag{4-5}$$

where $\underline{u}$ represents the remaining part of the integral from (4-4) which contains only known "past history" values at $t-\Delta t$, $t-2\Delta t$, etc. The definition of the matrix $[C_3]$ depends on the type of implicit integration technique used in the solution of (4-1). For the trapezoidal rule of integration, it is given as follows:

$$[C_3] = ([I] - \frac{\Delta t}{2}[C_1])^{-1}\cdot([I] + \frac{\Delta t}{2}[C_1]) \tag{4-6}$$

Simple rearrangements of (4-5) result in the following relationship:

$$\underline{v}_p(t) = [C_4]^{-1}\underline{i}_p(t) - [C_4]^{-1}[C_3]\underline{i}_p(t-\Delta t) - [C_4]^{-1}\cdot\underline{u} \qquad (4\text{-}7)$$

or in a shorter form:

$$\underline{v}_p(t) = [C_5]\underline{i}_p(t) + \underline{hist}(t-\Delta t) \qquad (4\text{-}8)$$

Equation (4-8) has the desired form of a resistive companion model and it has been obtained without specifying the type of implicit integration method. Therefore, the resistive companion model can be calculated for any system of equations of the form of (4-1) independent of the type of implicit integration technique used in the solution of (4-1). The calculation of the matrix $[C_5]$ and the vector $\underline{hist}(t-\Delta t)$ is very simple when the trapezoidal rule of integration is applied.

APPENDIX 5

REDUCTION OF THE GENERATOR EQUATIONS

The reduced resistive matrix $[R_{ss}^{red}]$ is defined as follows:

$$[R_{ss}^{red}] = [R_{ss}] - [R_{sr}][R_{rr}]^{-1}[R_{rs}] \tag{5-1}$$

where matrix $[R_{ss}]$ has the following, well known form (in d,q,0-coordinates) [8], [9]:

$$[R_{ss}] = \begin{bmatrix} a_{11} & a_{12} & 0 \\ a_{21} & a_{22} & 0 \\ 0 & 0 & a_{33} \end{bmatrix} \tag{5-2}$$

The elements a_{11}, a_{22}, and a_{33} are functions of the stepsize Δt only. The elements a_{12} and a_{21} are functions of both ω and Δt, with a linear dependence on ω.

Proof

The matrix $[R_{rr}]$ has the following form:

$$[R_{rr}] = \left[\begin{array}{c|c} B_1 & 0 \\ \hline 0 & B_2 \end{array}\right] \tag{5-3}$$

where all the nonzero elements are functions of Δt only. The inverse matrix $[R_{rr}]^{-1}$ is simply [75]:

$$[R_{rr}]^{-1} = \left[\begin{array}{c|c} B_1^{-1} & 0 \\ \hline 0 & B_2^{-1} \end{array}\right] \tag{5-4}$$

The matrices $[R_{rs}]$ and $[R_{sr}]$ are defined as follows:

$$[R_{rs}] = \begin{bmatrix} a_{41} & 0 & 0 \\ a_{51} & 0 & 0 \\ 0 & a_{62} & 0 \\ 0 & a_{72} & 0 \end{bmatrix} \tag{5-5}$$

with all the nonzero elements being functions of Δt only;

$$[R_{sr}] = \begin{bmatrix} a_{14} & a_{15} & a_{16} & a_{17} \\ a_{24} & a_{25} & a_{26} & a_{27} \\ 0 & 0 & 0 & 0 \end{bmatrix} \tag{5-6}$$

with the elements a_{14}, a_{15}, a_{26}, and a_{27} being functions of Δt only and the elements a_{16}, a_{17}, a_{24}, and a_{25} being functions of both ω and Δt with linear dependence on ω.

Simple matrix multiplication yields:

$$[R_{rr}]^{-1}[R_{rs}] = \begin{bmatrix} b_{11} & 0 & 0 \\ b_{12} & 0 & 0 \\ 0 & b_{32} & 0 \\ 0 & b_{42} & 0 \end{bmatrix} \tag{5-7}$$

where all the nonzero elements are obviously functions of Δt only.

Finally, the product $[R_{sr}][R_{rr}]^{-1}[R_{rs}]$ is given as:

$$[R_{sr}][R_{rr}]^{-1}[R_{rs}] = \begin{bmatrix} a_{14}\, b_{11} + a_{15}\, b_{12} & a_{16}\, b_{32} + a_{17}\, b_{42} & 0 \\ a_{24}\, b_{11} + a_{25}\, b_{12} & a_{26}\, b_{32} + a_{27}\, b_{42} & 0 \\ 0 & 0 & 0 \end{bmatrix}$$

$$= \begin{bmatrix} c_{11} & c_{12} & 0 \\ c_{21} & c_{22} & 0 \\ 0 & 0 & 0 \end{bmatrix} \tag{5-8}$$

Since only the elements a_{16}, a_{17}, a_{24}, and a_{25} depend (linearly) on ω, the elements c_{12} and c_{21} in the resulting matrix will have the same type of dependence.

Substitution of (5-8) into (5-1) yields the desired result:

$$[R_{ss}^{red}] = \begin{bmatrix} d_{11} & d_{12} & 0 \\ d_{21} & d_{22} & 0 \\ 0 & 0 & d_{33} \end{bmatrix} \tag{5-9}$$

which has the form of (81).

The matrix $[R_{ss}^{red}]$ has to be calculated only once as the constant of a simulation run if Δt does not change and if saturation is not considered. The elements d_{12} and d_{21} depend linearly on ω, and their updating for changes in ω is then obviously quite simple.

Similar procedures can be used for the four-phase equivalent circuit of the generator mentioned in chapter 3.5. The resistive matrix $[R_{ss}^{red}]$ will then be given as:

$$[R_{ss}^{red}] = \begin{bmatrix} e_{11} & e_{12} & 0 & e_{14} \\ e_{21} & e_{22} & 0 & e_{24} \\ 0 & 0 & e_{33} & 0 \\ e & 0 & 0 & e_{44} \end{bmatrix} \qquad (5\text{-}10)$$

where the elements e_{11}, e_{14}, e_{22}, e_{33}, e_{41}, and e_{44} are functions of Δt only. The elements e_{12}, e_{21}, and e_{24} are functions of both ω and Δt with linear dependence on ω. It can also be shown that the following entries of (5-10) are equal to the corresponding entries of (5-9):

$$e_{12} = d_{12} \qquad (5\text{-}11)$$

$$e_{22} = d_{22} \qquad (5\text{-}12)$$

$$e_{33} = d_{33} \,. \qquad (5\text{-}13)$$

APPENDIX 6

PRACTICAL CALCULATION OF THE MATRIX $[R_{ss}^{red}]$

The Gauss-Jordan elimination process, which has been chosen, as the most efficient method, produces not only the reduced matrix $[R_{ss}^{red}]$, but also the distribution factor matrices $[D_{12}] = [R_{sr}] \cdot [R_{rr}]^{-1}$ and $[D_{21}] = -[R_{rr}]^{-1}[R_{rs}]$. The matrix $[D_{12}]$ is needed for the calculation of the right-hand side of (80), and the matrix $[D_{21}]$ is necessary in the solution of the equations of the concealed terminals, once the retained variables have been found. A short description of the algorithm is followed by a flowchart of a computer program based on this algorithm.

Consider a system of linear algebraic equations:

$$[C]\underline{x} = \underline{b} \tag{6-1}$$

where:

$[C]$ = n x n matrix of coefficients,

and $\underline{x}$, $\underline{b}$ = vectors with n components.

The objective is to arrive at a reduced system of equations for subset 1 in (6-2):

$$\left[\begin{array}{c|c} C_{11} & C_{12} \\ \hline C_{21} & C_{22} \end{array}\right] \cdot \begin{bmatrix} \underline{x}_1 \\ \underline{x}_2 \end{bmatrix} = \begin{bmatrix} \underline{b}_1 \\ \underline{b}_2 \end{bmatrix} \tag{6-2}$$

where $[C_{11}]$ and $[C_{22}]$ are matrices of order m x m and (n-m) x (n-m), respectively, and $\underline{x}_1$, $\underline{b}_1$ are vectors with m components and $\underline{x}_2$, $\underline{b}_2$ vectors with (n-m) components.

Elimination of variables $\underline{x}_2$ from subset 1 results in the following system of equation:

$$\begin{bmatrix} C_{11}^{red} & \vdots & C_{12}C_{22}^{-1} \\ \cdots & \vdots & \cdots \\ -C_{22}^{-1}C_{21} & \vdots & C_{22}^{-1} \end{bmatrix} \cdot \begin{bmatrix} \underline{x}_1 \\ \underline{b}_2 \end{bmatrix} = \begin{bmatrix} \underline{b}_1 \\ \underline{x}_2 \end{bmatrix} \qquad (6\text{-}3)$$

Equation (6-3) has the desired form allowing the calculation of variables $\underline{x}_1$ without the need to calculate the variables $\underline{x}_2$, provided b_2 is known. The transformation of the matrix of (6-2) into the matrix of (6-3) is carried out by exchanging - one at a time - the variables x_j, b_j for $m+1 \leq j \leq n$. This is the Gauss-Jordan elimination process. For example, if the variables x_j, b_j are to be exchanged (variables x_{j+1}, b_{j+1}, etc. have already been exchanged) and the coefficients from the last exchange are $c_{ik}^{(old)}$, then the j-th row of (6-2) may be written down as follows:

$$c_{j1}^{(old)}x_1 + c_{j2}^{(old)}x_2 + \ldots + c_{jj}^{(old)}x_j + c_{j(j+1)}b_{j+1} + \ldots + c_{jn}b_n = b_j \qquad (6\text{-}4)$$

Exchange of x_j, b_j yields:

$$-\frac{c_{j1}^{(old)}}{c_j}x_1 - \ldots - \frac{c_{j(j-1)}^{(old)}}{c_j}x_{j-1} + \frac{1}{c_j}b_j - \frac{c_{j(j+1)}^{(old)}}{c_j}b_{j+1} - \ldots \frac{c_{jn}^{(old)}}{c_j}b_n = x_j \qquad (6\text{-}5)$$

where $c_j = c_{jj}^{(old)}$

If (6-5) is rewritten with the coefficients;

$$c_{j1}^{(new)}x_1 + \ldots c_{j(j-1)}^{(new)}x_{j-1} + c_{jj}^{(new)}b_j + \ldots + c_{jn}^{(new)}b_n = x_j \qquad (6\text{-}6)$$

then it is obvious that the following relationships hold for the eliminated row:

$$c_{jk}^{(new)} = -\frac{c_{jk}^{(old)}}{c_{jj}^{(old)}} \qquad \text{for} \quad j \neq k \qquad (6\text{-}7a)$$

and

$$c_{jj}^{(new)} = \frac{1}{c_{jj}^{(old)}} \qquad \text{otherwise} \qquad (6\text{-}7b)$$

Insertion of (6-6) into the remaining equations results in the following relationships:

$$c_{ik}^{(new)} = c_{ik}^{(old)} - c_{ij}^{(old)} \frac{c_{jk}^{(old)}}{c_{jj}^{(old)}} \qquad \text{for } k \neq j \qquad (6\text{-}8a)$$

and

$$c_{ij}^{(new)} = \frac{c_{ij}^{(old)}}{c_{jj}^{(old)}} \qquad \text{otherwise} \qquad (6\text{-}8b)$$

A flow chart of a computer program executing the algorithm described above is presented on the next page.

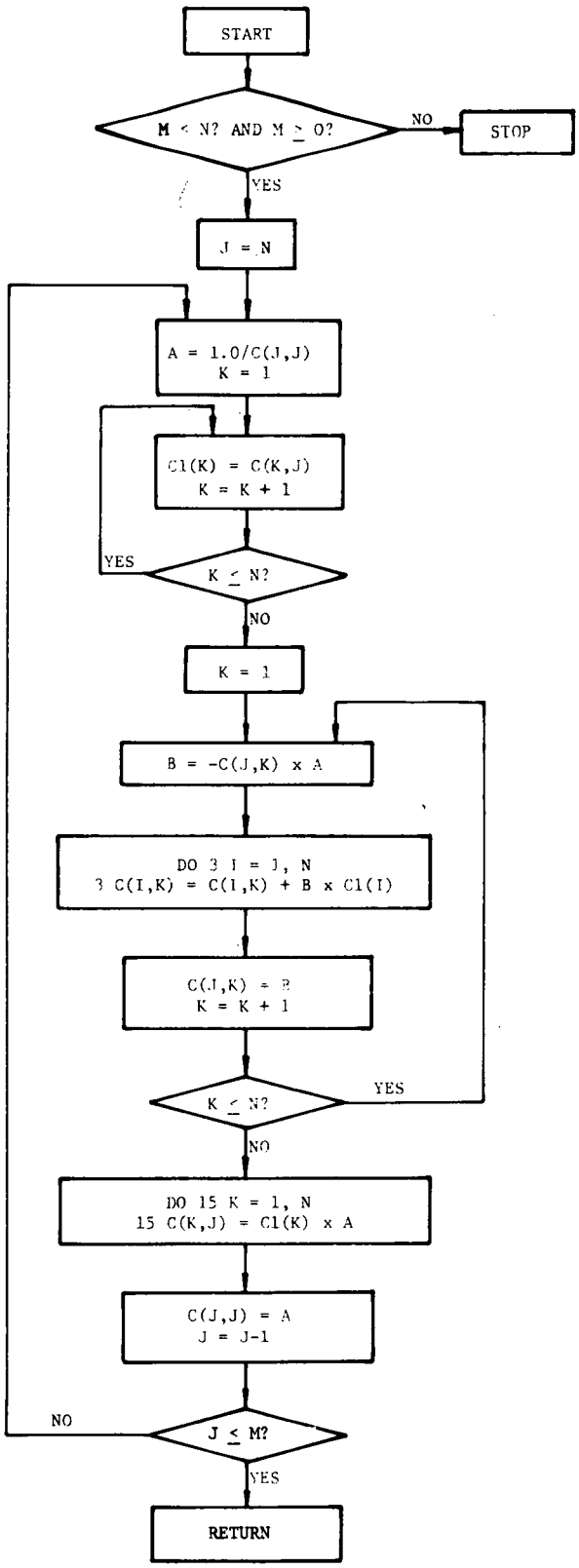

Fig. 6-1. Flow chart of computer program for matrix reduction.

APPENDIX 7

CONVERSION OF THE OPEN CIRCUIT CHARACTERISTIC TO A FLUX-CURRENT CHARACTERISTIC

The open-circuit characteristic $V_{(RMS)} = f(i_f)$ is measured under balanced no-load conditions, i.e.,

$$i_a = i_b = i_c = i_D = i_Q = i_g = 0 \tag{7-1}$$

The voltage equations (in phase coordinates) for these conditions are as follows:

$$v_a = \omega M_f \sin \beta_1 \, i_f \tag{7-2}$$

$$v_b = \omega M_f \sin \beta_2 \, i_f \tag{7-3}$$

$$v_c = \omega M_f \sin \beta_3 \, i_f \tag{7-4}$$

from which follows that sinusoidal changes in flux are followed by sinusoidal changes in voltages, since

$$\underline{v} = - \frac{d\psi}{dt} \tag{7-5}$$

if hysteresis and eddy current losses are neglected, as per assumption 5, chapter 5.4. Therefore, the RMS value of voltage difference between any two phases is given as follows:

$$V_{(rms)} = \frac{\omega \cdot M_f \cdot i_f \sqrt{3}}{\sqrt{2}} = \frac{\omega \cdot \psi}{\sqrt{2}} \tag{7-6}$$

From (7-6) follows that the conversion of $V_{(RMS)}$ values to the instantaneous flux values becomes a simple rescaling:

$$\psi = \frac{V_{(RMS)} \cdot \sqrt{2}}{\omega} \tag{7-7}$$

The excitation current i_f does not have to be converted. Consider the voltage equation for v_q, the only nonzero voltage under balanced no-load conditions:

$$v_q = \omega \cdot \sqrt{\frac{3}{2}} M_f \cdot i_f = \omega \, \psi_d \qquad (7\text{-}8)$$

Equation (7-8) can be visualized a system of coils placed in a rotating field created by a permanent magnet. This situation is shown schematically in Fig. 7-1.

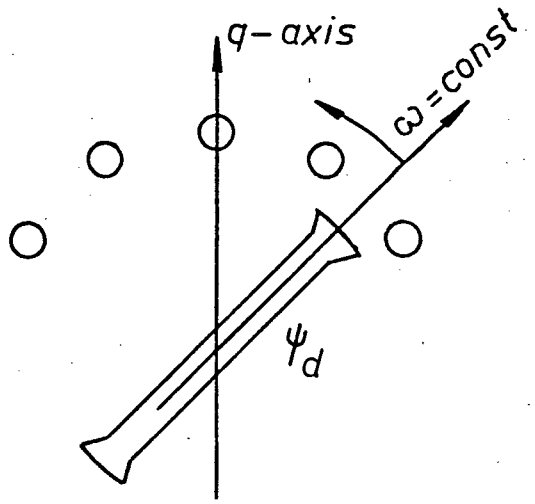

Fig. 7-1. Schematic representation of an unloaded generator.

The decrease in the value of M_f (due to saturation) results in a decreased value of the flux linkage ψ_d, and therefore in a decreased voltage v_q. However, since no a.c.-components are present, there are no harmonics generated in the field distribution, i.e., the voltage v_q is still described by a linear equation of the form of (7-8). Therefore, the converted open circuit characteristichas the same form, as the original curve.

APPENDIX 8

EXAMPLE FOR A MULTI-MASS SYSTEM

The case presented here is a standard IEEE benchmark test case for the simulation of subsynchronous resonance phenomena [5]. The effects of a simultaneous three-phase short-circuit in a system as shown in Fig. 8.1 and 8.2 are simulated.

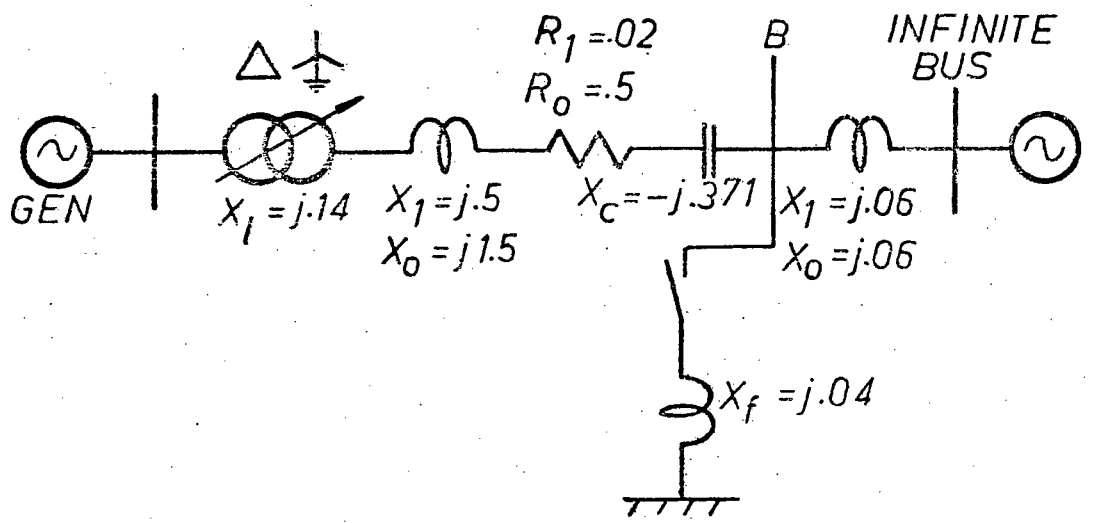

Fig. 8.1. System diagram.

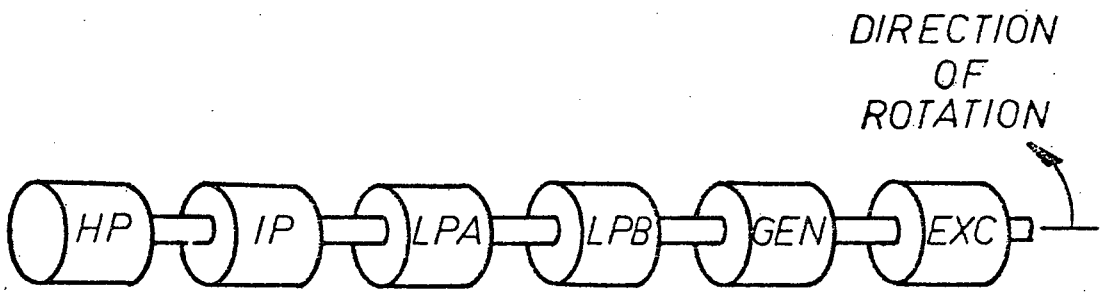

Fig. 8.2. Model of the shaft system.

The three-phase fault was applied at bus B at time t = 0 and then removed after time 0.075 sec, as soon as the current in each phase crossed zero.

The results presented here were obtained with method I with a time step of 100 μsec. Fig. 8.3 shows the simulated electromagnetic torque of the generator, Fig. 8.4 shows the simulated mechanical speed of the generator rotor, and Fig. 8.5 shows the torque on the shaft between the generator rotor and the exciter. The increasing oscillations of this torque point out the reason for shaft damage which occurred in a real case from which the data of Fig. 8.1 and 8.2 were derived.

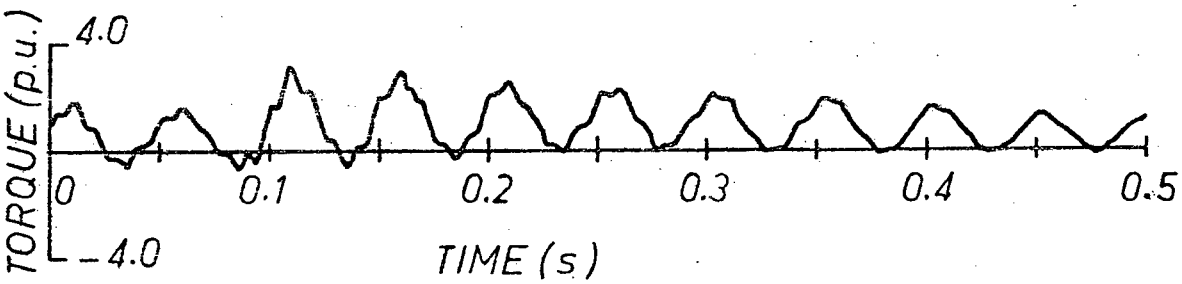

Fig. 8.3. Simulated electromagnetic torque of the generator.

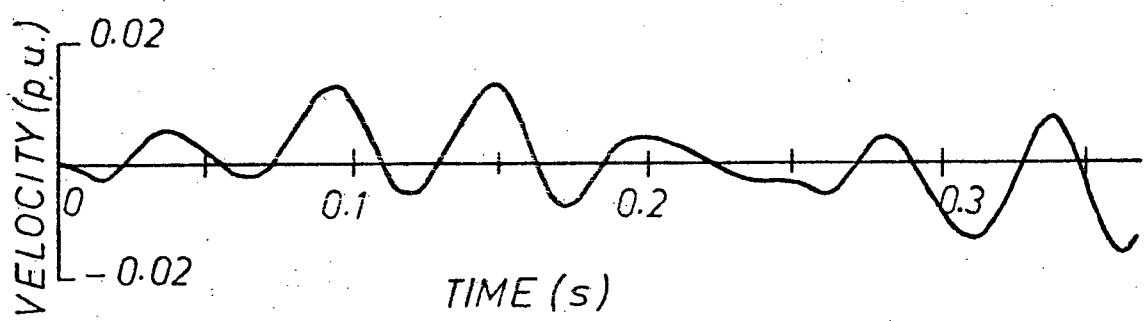

Fig. 8.4. Simulated mechanical speed of the generator rotor.

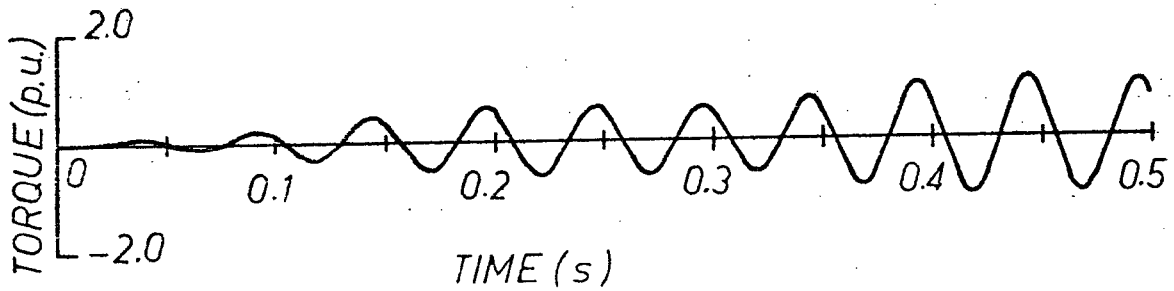

Fig. 8.5. Simulated torque on the shaft between the generator rotor and the exciter.

The results presented here are practically indistinguishable from those in [5], which were obtained with a program developed in industry.